PRODUCTION AND CONSUMPTION OF ORGANIC CARBON AND OXYGEN IN SECHELT INLET, BRITISH COLUMBIA

By

David Andrew Timothy

B.Sc. Environmental Engineering, M.I.T., 1989

A THESIS SUBMITTED IN PARTIAL FULFILLMENT OF

THE REQUIREMENTS FOR THE DEGREE OF

MASTER OF SCIENCE

in

THE FACULTY OF GRADUATE STUDIES

DEPARTMENT OF OCEANOGRAPHY

We accept this thesis as conforming

to the required standard

THE UNIVERSITY OF BRITISH COLUMBIA

July, 1994

© David Andrew Timothy, 1994

In presenting this thesis in partial fulfilment of the requirements for an advanced degree at the University of British Columbia, I agree that the Library shall make it freely available for reference and study. I further agree that permission for extensive copying of this thesis for scholarly purposes may be granted by the head of my department or by his or her representatives. It is understood that copying or publication of this thesis for financial gain shall not be allowed without my written permission.

(Signature)

Department of Oceanography

The University of British Columbia
Vancouver, Canada

Date July 15, 1994

DE-6 (2/88)

Abstract

In an effort to better understand the relationships of hydrodynamic, biological and chemical processes in British Columbia fjords, multi-disciplinary oceanographic data were collected from Sechelt Inlet between the end of January and the end of June, 1991. The purpose of this thesis is to provide depth dependent rates of oxygen production and consumption. Oxygen dynamics are inferred from changes in organic carbon content.

Autotrophic ^{14}C uptake is normalized to estimates of the daily average irradiance to which phytoplankton had been exposed before being collected for incubation. The normalized ^{14}C assimilation values are used to estimate daily rates of oxygen production in the euphotic zone and they are correlated with chlorophyll *a* concentration. The relationship between ^{14}C uptake and chl*a* is not directly used for estimates of oxygen production during the five month study period, but may be applied where chl*a* but not photosynthetic carbon assimilation data exist.

Oxygen consumption in the water column below the euphotic zone and in the sediments is estimated from analyses of sediment trap data collected monthly at three stations. Water column oxygen consumption is determined using an algorithm which estimates the rate of decay with depth of the organic carbon flux, despite measured increases in flux with depth. The algorithm also provides estimates of the composition of the material caught in lower but not upper sediment traps. Following a discussion of possible causes of measured flux increases with depth, it is concluded that changes in trapping efficiency were largely responsible for the pattern of flux observed in Sechelt Inlet during the experiment. Benthic oxygen demand is estimated by degrading a constant fraction of the trap-measured flux of organic carbon to the sediments. The estimates of sediment

oxygen demand are found to agree with direct measurements of benthic oxygen demand in other temperate fjords.

This work is concluded by comparing predicted and trap measured fluxes of organic carbon, where predicted fluxes are estimated from primary production and an estimate of the f-ratio (= new production/total production) during the experiment. A method is described in which $f_{NO_3^-}$ (= nitrate uptake/total nitrogen uptake) can be used to predict the export flux of organic carbon during ecologically and hydrographically dynamic periods. A large discrepancy is found between predicted and measured fluxes of organic carbon during the study period in Sechelt Inlet. It is suggested that this discrepancy was caused by dissolved and/or fine organic matter that was not caught by the sediment traps and was eventually consumed in the water column, probably by free-living, motile bacteria.

Table of Contents

List of Tables

List of Figures

Acknowledgements

Most of the work of this thesis is derived from conversations with individuals who have occasionally shown some interest and always a great deal of patience with my questions. The greatest patience and support has been given by Dr. Pond. His ability to interpret and simplify oceanographic information and his diligence during the writing of this thesis have been remarkable. With Dr. Pond, Debby Ianson must be thanked for what has probably accumulated into days of mathematical consulting.

I thank Dr. Taylor for giving me the flexibility to study outside of his field of expertise and providing helpful comments throughout this exercise; and I am sincerely grateful to Dr. Calvert who has shared his experience and given me encouragement to explore in oceanography.

The data used for this thesis were collected before I arrived to U.B.C. Thanks to Maureen Soon for superb care in collecting, analyzing and recording data. Thanks also to Terri Sutherland, Kedong Yin, Peter Thompson, A. Ramnarine, Hugh MacLean and the officers and crew of the *C.S.S. Vector* for their roles in the collection and analysis of data.

Many thanks to Rowan Haigh for help with species identification and to others in the Taylor lab for putting-up with my badgering; to Dr. Lewis and his laboratory for the use of computer and printer; to Dr. Ric Taylor and Dr. Kozak for trying to direct me towards the proper use of statistical packages; to Drs. Pedersen, Harrison and Orians for discussion; to Cynthia and Raj for doing most of the silica measurements; to Scott T. for sharing data and figures; to Jesse for sharing the blame; and to Phillip B., Rob G., Allen M., Greg C., John C., John B., David M. and everybody in the 'annex' for their help

and suggestions. A very special thank you goes to Dr. Dymond and to the serendipity of his sabbatical at U.B.C; and thanks to others at O.S.U. and U.W. who have shared ideas. This research was supported by the Natural Sciences and Engineering Research Council of Canada. I am grateful for funds that were provided to me during my studies.

Despite our studies, the oceans will always remain a mystery to us. They will always be beautiful. Take, for example, the sea bass:

"Of all the fishes in the sea,
my favorite is the bass.
He climbs upon the seaweed trees
and slides down on his hands and knees."
(P. Bogdanovich)

If there is anything we must pass on, it is the mystery of the bass.

Chapter 1

Introduction

1.1 Determining rates of biological oxygen production and consumption

The oxygen content of water in equilibrium with the atmosphere is a function of pressure, temperature and salinity. Thus, the exposure of sea water to the atmosphere would cause the oxygen content of the oceans to vary with temperature and salinity were it not for biota in the sea. During photosynthesis, photo-autotrophic organisms strip electrons from water molecules and use them to convert low energy carbon dioxide to higher energy but less stable organic compounds. Oxygen is a product of this reaction and can accumulate in the euphotic zone when photosynthesis is significant. Oxygen is also the thermodynamically preferable electron acceptor for the degradation of organic material and heterotrophic organisms will consume labile organic carbon and oxygen throughout the water column and in the sediments if both are available.

The goal of this work is to determine rates of biologically-mediated reactions with oxygen in a British Columbia fjord. It is theoretically possible to measure these rates from spatial and temporal changes in oxygen concentration. However, the oxygen content of water is influenced by advection and eddy diffusion as well as biological activity. Separating fluxes of oxygen caused by advection and diffusion from *in situ* oxygen production and consumption using a purely physical approach requires detailed descriptions of the fluid dynamics that influence a region. Creating such a description for a water body contained by an intricate topography and with currents caused by a number of

forces, including density gradients, tides and winds, is complicated. It is also possible to trace the formation and degradation of organic matter and to stoichiometrically translate organic carbon dynamics to rates of biological oxygen production and consumption. The later approach has been chosen in this thesis and is applied to data collected over a five-month period inclusive of the 1991 spring bloom in Sechelt Inlet.

The sampling program and data analyses are described in chapter 2. In chapter 3, estimates of daily rates of photosynthesis from ^{14}C incubation experiments are made and in chapter 4 those estimates are converted to rates of oxygen production in the euphotic zone.

In chapter 5, measurements of flux from sediment trap deployments are used to estimate the decay of organic carbon below the depth of 50 m. For many of the depth intervals and deployment periods, an increase in flux with depth was recorded by the sediment traps. Particle decay was determined using an algorithm designed for use with data from vertically-separated pairs of sediment traps. The algorithm simultaneously describes the decay of the material representatively caught in both traps and the composition of the material caught only by the lower trap. In chapter 6, the source and sinking rate of the organic material caught by the sediment traps is discussed and the amount of organic carbon decay determined in chapter 5 is stoichiometrically translated to water column oxygen demand. Comparisons of trap-measured flux of organic carbon to the sediments with the rate of permanent burial of organic carbon made in other coastal inlets are used to estimate organic carbon diagenesis and sediment oxygen demand. The chemical oxygen demand of oxygenated waters that surround and/or mix with anoxic waters and sediments is also discussed in chapter 6.

The organic carbon created in the euphotic zone is coupled with the organic carbon flux into deeper waters in chapter 7. It is found that a large fraction of the organic matter leaving surface waters during the experiment may not have been caught in the

sediment traps. A profile of biologically-mediated oxygen production and consumption is presented. The profile does not account for organic carbon that might have been missed by the sediment traps. Possible influences of this material on estimates of oxygen production and consumption are discussed.

The rates of biological oxygen production and consumption suggested in this work will be used with hydrodynamic models in a larger effort to better understand differences between fjords along the B.C. coast. One question specifically addressed with this information will be: 'what causes anoxia in some inlets but not in others?' It is hoped that, in turn, the hydrodynamic models now being developed can help to answer some of the questions raised in this work.

1.2 Description of Sechelt Inlet

Sechelt Inlet (figure 1.1) is a fjord on the British Columbia coast about 40 km northwest of the city of Vancouver. The drainage basin of Sechelt Inlet is small relative to other inlets in B.C.; terrestrial run-off into the system is about 110 m^3/s (Pickard, 1961). The majority of the fresh water input to the system is at the head of Salmon Inlet through the Clowhom River, which is dammed by B.C. Hydro. Although the flow of water is controlled to satisfy power needs, water is released as the storage capacity of the reservoir is reached. Because of the small drainage basin of Sechelt Inlet, the spring freshet caused by seasonal snow melt is not significant.

The fresh water input at the head of Salmon Inlet drives estuarine circulation (Lazier, 1963). A barotropic pressure gradient forces a seaward flow of low-salinity water in the upper 5 m of Sechelt Inlet. This outflow entrains saltier water upwards so that surface waters are denser at the mouth of the inlet than at its head. A baroclinic pressure gradient results, driving an inward flow between the depths of about 5 and 65 m.

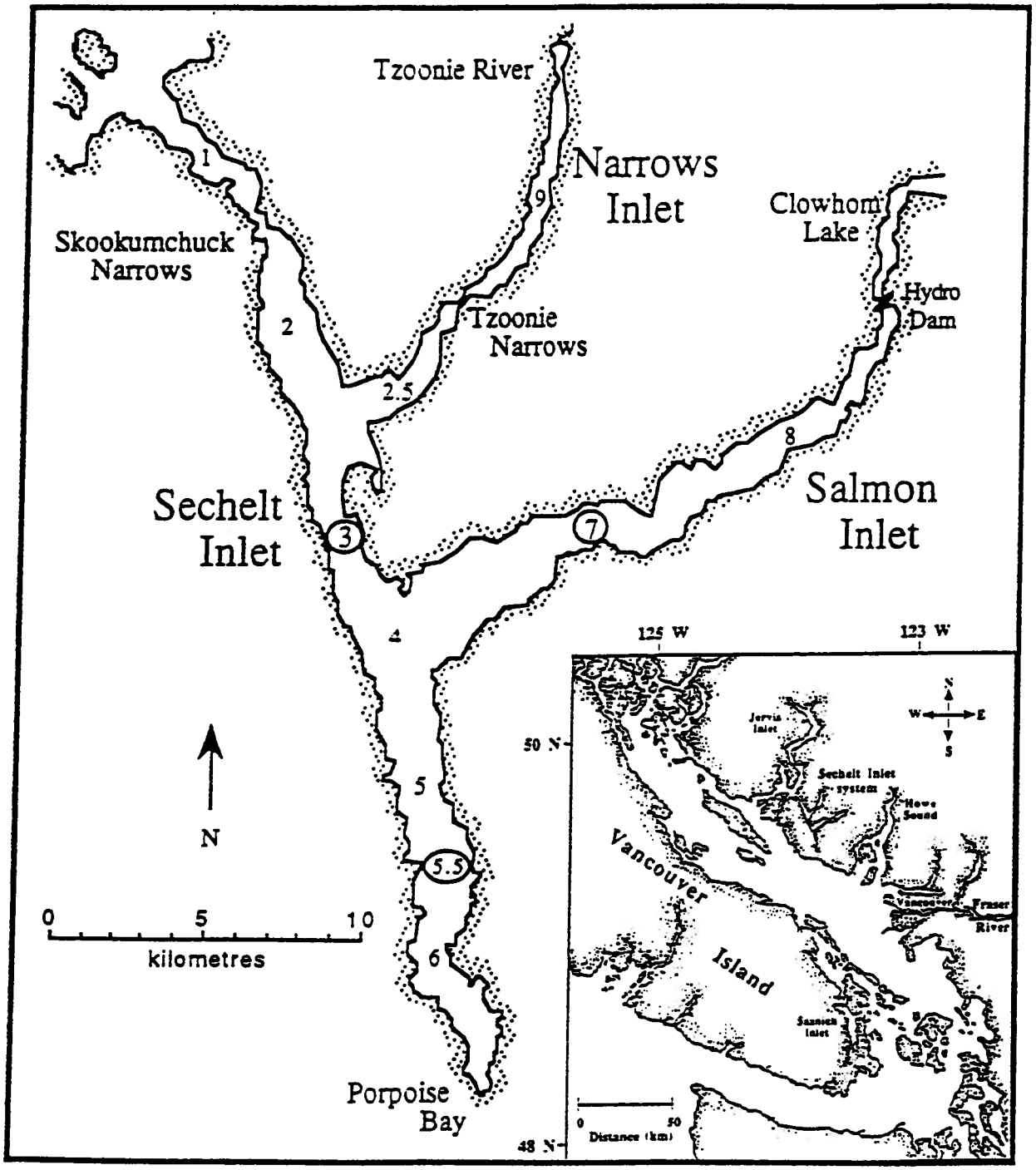

Figure 1.1: Sechelt Inlet and the stations visited during the study period. The locations of the sediment trap moorings and the ^{14}C uptake experiments are circled.

Sechelt Inlet is about 40 km long from the head of Salmon Inlet to the mouth at Skookumchuck Narrows. The 200 m isobath along this axis is approximately 29 km in length and the deepest point in the Sechelt Inlet system is 287 m at station SC-3. The extension from the mouth of Salmon Inlet to the head of Porpoise Bay is about 14 km long and Narrows Inlet is approximately 16 km in length. The channel at Skookumchuck Narrows separating Sechelt Inlet from Jervis Inlet is approximately 8 km long and its maximum water depth is 75 m. The tightest constriction through Skookumchuck Narrows is Sechelt Rapids and is 14 m deep at mid-channel and 400 m wide. Tidal currents through Skookumchuck Narrows become turbulent and reach 30 km/hr through Sechelt Rapids. The turbulent jet entering Sechelt Inlet was described by Lazier (1963). Tinnis (in progress) is addressing the loss of tidal energy caused by turbulence and the flow restriction at Skookumchuck Narrows, and is describing the propagation of internal waves that are created at this dynamic region of Sechelt Inlet.

Narrows Inlet is separated from Sechelt Inlet by a 14 m sill at Tzoonie Narrows and the greatest depth for the inner basin of Narrows Inlet is about 84 m. Estuarine circulation in Narrows Inlet is set-up by the Tzoonie River, which is free-flowing but releases only about 10 m^3/s of fresh water (estimated by eye in May, 1992). The deepest waters in Narrows Inlet are generally lower in oxygen concentration than in Sechelt Inlet (Lazier, 1963). During the 1991 sampling program, oxygen concentrations of zero were recorded at 80 m depth at station SC-9 in Narrows Inlet in January and February. Diffusive mixing and nutrient regeneration for Narrows Inlet have been described by Smethie (1981; 1987).

An intensive program designed to study phytoplankton ecology within Sechelt Inlet occurred between 1988 and 1990. Currently, there are three completed works that have resulted from that study (Sutherland, 1991; Haigh *et al.*, 1992; Taylor *et al.*, 1994).

Chapter 2

Data acquisition, analysis and results

2.1 Sampling protocol

The data used for this thesis were collected by an interdisciplinary group that visited Sechelt Inlet on a monthly basis from December, 1990 to June, 1991 on the *C.S.S. Vector*. Sampling dates and the data collected during each cruise are presented in table 2.1 and the station locations are shown in figure 1.1. Not all parameters measured in Sechelt Inlet were collected at every station; the sample locations and depths where each parameter was recorded are described in this chapter. Because the sediment traps were first deployed on January 22 and 23 and the ^{14}C incubation experiments began on those dates, the sampling period relevant to this thesis is considered to have lasted five months.

This chapter is broken into three sections. The first describes the measurements of parameters used to estimate daily rates of primary production and gives the data in tabular form. The second describes the sediment traps and their mooring configurations, and it describes the chemical analyses performed on the trap samples as well as compiles the chemical analysis data. The third section discusses data that were collected during the study period that have not been used directly in the quantification of carbon and oxygen production and consumption, but are supplemental to the interactions considered in this thesis.

DATE 1990-1991	T, sal, O_2 1 2 3 4 5 6 7 8 9	^{14}C uptake 3 5.5 7	chl*a*, sp. enum. 2 3 5 6 8 9	surf nutr 2 3 5 5.5 6 7 8 9	deep nutr 2 3 5 6 7 8 9	trap retrieval 3 5.5 7
Dec 11-12	x		9	5.5	3 5 7	
Jan 22-23	x	5.5	x	x	x	
Feb 19-20	x	x	3 5 8 9	x	x	5.5
Mar 26-27	x	x	x	x	x	x
Apr 23-25	x	7	x	x	x	3
May 22-23	x	x	x	x	x	x
Jun 22-23	x	x	x	x	x	x

Table 2.1: Sampling dates, stations and the data retrieved. Column headings are data sets and the stations from which those data may have been collected. 'x' denotes that the entire data were collected at each station. Station numbers within the table indicate that the data were collected from all but those stations for that month. Where there are no entries, that data set was not collected. In February, species enumeration was made at each station, but the chl*a* data are missing from the stations indicated. Surface nutrients are from the upper 20 m. Sediment trap deployment periods were the month preceding their retrieval.

2.2 Primary production data

2.2.1 Measures of irradiance

Prior to each ^{14}C incubation, photosynthetically available radiation (PAR; ~400-700 nm) was measured with a LI-COR 185B Quantum/Radiometer/Photometer from the surface to approximately the 3% light level. The LI-COR 185B Quantum/Radiometer/Photometer has a number of ranges from which PAR readings can be made. The smallest range is 0-3 $\mu E/m^2/s$ and the largest is 0-3x$10^4 \mu E/m^2/s$. The accuracy of the instrument is 1% of the full scale in use. Measurements of irradiance made during the study are presented in tables 2.2 and 2.3.

2.2.2 ^{14}C incubations

Estimates of photosynthetic carbon assimilation were made from ^{14}C uptake measurements. During each monthly cruise, samples for ^{14}C incubations were collected from the 56, 32, 22, 13 and 7% light levels at stations SC-3, SC-5.5, and SC-7.

$NaH^{14}CO_3$ (ICN; 4.5 mCi/mmol) was prepared following Strickland and Parsons (1968) and refrigerated before use. Disposable polypropylene pipette tips used for ^{14}C incubations were soaked in 10% HCl and thoroughly rinsed with distilled deionized water prior to use so that trace metal contamination would be reduced (Fitzwater *et al.*, 1982).

Carbon assimilation rates were determined by adding 2.0 μCi $NaH^{14}CO_3$ to duplicate 200 ml bottles in transparent borosilicate glass tubes. After thorough mixing, the bottles were incubated for about 2 hrs in ship-board incubators. *In situ* light levels were mimicked with the use of neutral density screening around each bottle. Samples were cooled with flowing surface seawater. At the end of the incubation period, cells were collected by filtration onto Whatman GF/F glass-fibre filters with applied pressures of less than 100 mm Hg. Filters were placed so that they laid flat on the bottom of glass scintillation vials

containing 10ml Aquasol II scintillation fluor. Zero-time blanks were used to correct for cell and bottle adsorption of ^{14}C.

Total ^{14}C activity of the stock solution was determined by mixing equal amounts of 20-25 μl $H^{14}CO_3^-$ stock solution (nominal activity of 0.4-0.5 μCi) with an equal volume of 1 N NaOH in scintillation vials and then adding 10 ml of scintillation fluor (Iverson, *et al.*, 1976). Samples were counted on an Isocap 300 liquid scintillation counter, and quench correction was by the channels-ratio method. Carbon uptake rates were calculated according to the method of Parsons *et al.* (1984a).

This technique of measuring carbon assimilation has virtually no upper limit and the lower limit is 0.05 mg $C/m^3/hr$ (Parsons *et al.*, 1984a). Measurements are accurate to ± 3 mg $C/m^3/hr$ at 30 mg $C/m^3/hr$ (Parsons *et al.*, 1984a) and are presented in tables 2.2 and 2.3.

Photosynthetic carbon assimilation per m^2 is calculated by averaging the measured ^{14}C assimilation at two depths and multiplying that average by the corresponding depth interval. The measurement of carbon assimilation at the most shallow sampling depth is allowed to represent carbon assimilation from the surface to that depth. The carbon assimilation per depth interval values are summed to obtain g $C/m^2/hr$.

depth m	I $\frac{\mu E}{m^2 s}$	^{14}C $\frac{mg\ C}{m^3 hr}$	depth m	I $\frac{\mu E}{m^2 s}$	^{14}C $\frac{mg\ C}{m^3 hr}$	depth m	I $\frac{\mu E}{m^2 s}$	^{14}C $\frac{mg\ C}{m^3 hr}$
SC-3: Jan 23			**SC-5.5: Jan**			**SC-7: Jan 23**		
surface	100					surface	14	
1	51	0.63				1	7.2	1.4
2	32	0.35	no data			3	4.2	0.88
4	18	0.043	collected			4	2.7	0.75
6	12	0.25				6	1.7	0.35
9	6.5	0.14				8	1.1	0.23
12	4.0					10	0.80	
SC-3: Feb 19			**SC-5.5: Feb 19**			**SC-7: Feb 19**		
surface	500		surface	46		surface	68	
1	250	2.2	1	29	0.60	2	35	0.88
2	150	1.2	2	14	0.60	3	21	0.45
3	100	0.19	3	8.1	0.53	5	13	0.023
5	47	0.075	4	5.1	0.078	7	9.0	0.18
6	39	0.28	5	3.4	0.18	9	5.0	0.19
7	30		6	2.8		11	3.6	
SC-3: Mar 26			**SC-5.5: Mar 26**			**SC-7: Mar 27**		
surface	850		surface	900		surface	890	
1	140	170	1	190	110	1	353	220
2	55	130	2	63	83	2	75	200
4	10	73	4	13	85	3	30	190
6	3.0	12	6	3.4	28	4	16	130
8	1.4	0.63	8	1.1	12	6	1.6	53
10	1.0		10	0.70		9	0.35	

Table 2.2: Irradiance and ^{14}C uptake as collected: Jan $\rightarrow$ Mar.

depth m	I $\frac{\mu E}{m^2 s}$	^{14}C $\frac{mg\ C}{m^3\ hr}$	depth m	I $\frac{\mu E}{m^2 s}$	^{14}C $\frac{mg\ C}{m^3\ hr}$	depth m	I $\frac{\mu E}{m^2 s}$	^{14}C $\frac{mg\ C}{m^3\ hr}$
SC-3: Apr 23			**SC-5.5: Apr 24**			**SC-7: Apr 25**		
surface	12		surface	400		surface	91	
2	6.5	6.3	1	250	7.8	2	29	-
4	3.4	3.8	3	130	6.8	4	14	-
6	2.1	1.5	4	72	2.8	6	8.4	0.24
8	1.4	0.018	6	41	2.5	8	5.6	0.88
13	0.83	-	8	25	1.6	13	2.4	0.28
18	0.58		10	16		18	1.2	
SC-3: May 22			**SC-5.5: May 23**			**SC-7: May 22**		
surface	230		surface	570		surface	1000	
2	120	23	1	370	18	2	510	5.5
3	63	70	2	170	58	3	280	3.3
5	36	58	3	100	48	4	190	3.0
6	23	6.3	4	61	28	6	130	1.8
8	17	1.9	5	39	20	9	74	4.3
9	11		6	26		12	36	
SC-3: Jun 22			**SC-5.5: Jun 22**			**SC-7: Jun 23**		
surface	300		surface	270		surface	370	
1	180	22	1	160	25	2	210	16
3	87	12	3	75	8.8	4	110	11
4	45	3.8	4	48	6.0	6	78	2.5
5	30	2.1	5	29	1.5	10	59	0.53
7	19	0.65	7	16	0.95	15	53	0.11
8	13		9	9.9		20	51	

Table 2.3: Irradiance and ^{14}C uptake as collected: Apr $\rightarrow$ Jun. Negative recordings are marked with a dash.

Converting ^{14}C incubations to units of (day^{-1})

Multiplying the ratio (daily integrated PAR)/(total PAR during a ^{14}C incubation) by carbon assimilation with units of g C/m^2/incubation provides an estimate of carbon assimilation per day (Clifford *et al.*, 1992). However, there are no time series of PAR from the cruises into Sechelt Inlet. Therefore, this ratio is estimated by assuming that daily irradiance follows the sine function. For the sine function formulation of daily irradiance, θ is the angle of the sun and y is solar irradiance relative to that at noon so that (θ, y) is (0, 0) at sunrise, ($\pi/2$, 1) at noon and (π, 0) at sunset. If the time at the beginning and the end of each experiment is converted to radians, then

$$\frac{1}{2}\int_{\theta_1}^{\theta_2} \sin\theta \, d\theta = -\frac{1}{2}(\cos\theta_2 - \cos\theta_1) = \frac{1}{D} \tag{2.1}$$

θ_1 and θ_2 are the beginning and the end of an incubation period and D is the ratio (daily integrated PAR)/(total PAR during a ^{14}C incubation). The fraction 1/2 is needed because $\int_0^{\pi} \sin\theta = 2$, so for the sine function scheme daily integrated PAR is equal to 2. Multiplication of carbon assimilation with units of g C/m^3/incubation or g C/m^2/incubation by D provides an estimate of photosynthesis with the units g C/m^3/day or g C/m^2/day.

The primary assumptions in the computation of D are that daily solar irradiance can be approximated with the sine function and that atmospheric light attenuation due to clouds during the incubation period and for the entire day are the same. D for each ^{14}C incubation during the experiment is presented in table 2.4.

Correcting ^{14}C measurements for day to day variability in sunlight

On the day of a ^{14}C incubation, daily integrated PAR may not be representative of the average daily integrated PAR for the growth period of the phytoplankton being sampled. The importance of considering daily average PAR to which a phytoplankton population has been exposed is shown with a simple example: a phytoplankton population may grow

	D		
DATE	**SC-3**	**SC-5.5**	**SC-7**
Jan 23	5.1	-	4.6
Feb 19	3.4	10.6	4.7
Mar 26	4.3	10.5	-
Mar 27	-	-	3.5
Apr 23	7.0	-	-
Apr 24	-	5.1	-
Apr 25	-	-	4.9
May 22	4.8	-	10.8
May 23	-	5.8	-
Jun 22	5.3	6.1	-
Jun 23	-	-	4.9

Table 2.4: The factor D used to convert carbon assimilation per incubation period into carbon assimilation per day. D is determined from equation 2.1 and is unique for each incubation.

to abundance during a period of sunshine, but on the day of a ^{14}C incubation it might be cloudy. Records from that cloudy day will produce confusing data if one is trying to relate measured carbon assimilation with an estimate of photosynthetic capacity (chl*a* concentration). The goal of this section is to determine the ratio (average irradiance during phytoplankton growth)/(irradiance on day of ^{14}C incubation) = M.

Environment Canada uses Campbell-Stokes Sunshine Recorders to measure cloud opacity. The instruments record the number of hours per day that light intensity is above a thresh-hold value. (The thresh-hold is set such that recordings are a function of cloud cover.) Measurements from the Campbell-Stokes Sunshine Recorders are in the units 'actual sunlight hours' (ASH, with units of hrs) and for a given day can range from 0 to the number of hours between sunrise and sunset. Although these units cannot be converted to PAR, it is suggested that

$$\frac{\mathrm{ASH}_1}{\mathrm{ASH}_2} \approx \frac{\mathrm{PAR}_1}{\mathrm{PAR}_2} \tag{2.2}$$

DATE	daylength hrs	<ASH/day>	ASH/day	M
Jan 23	9.00	2.0	0.20	10
Feb 19	10.42	2.5	0.60	4.2
Mar 26	12.52	4.5	9.7	0.46
Mar 27	12.60	4.5	11	0.41
Apr 23	14.17	7.1	0.50	14
Apr 24	14.22	7.1	5.7	1.2
Apr 25	14.32	7.1	7.9	0.90
May 22	15.62	5.8	9.2	0.63
May 23	15.63	5.8	7.1	0.82
Jun 22	16.23	5.5	0.0	2.1*
Jun 23	16.23	5.5	3.1	1.8

Table 2.5: Hours of sunshine as recorded by Campbell-Stokes Sunshine Recorders at Powell River and Vancouver Airport. The average of the two locations is used. The dates given are those on which ^{14}C incubations were performed. <ASH/day> is the average ASH per day for a given month. ASH/day is the 'actual sunshine hours' on the day of an experiment. M is determined from equation 2.3. The value of M for June 22 (*) is determined by comparing the light profiles of that experiment day with the ones from June 23.

where 1 and 2 are two different periods of light intensity. ASH is measured daily at the Vancouver Airport and in Powell River. Sechelt Inlet is mid-way between these locations. Therefore, ASH is averaged between the Vancouver Airport and Powell River to represent ASH in Sechelt Inlet.

The data obtained from Environment Canada includes ASH/month for each month of the study period. Dividing ASH/month by the number of days in a month provides <ASH/day>, the average number of 'actual sunlight hours' per day during a month. ASH/day for each day ^{14}C incubations occurred has also been received from Environment Canada. In this way,

$$\frac{< \text{ASH/day} >}{\text{ASH/day}} = M \tag{2.3}$$

Because cruises into Sechelt Inlet were carried out towards the end of each month, the

days from which <ASH/day> is determined are dominated by days preceding ^{14}C incubations. Photosynthetic carbon assimilation with units of g $C/m^3/day$ or g $C/m^2/day$ are multiplied by M to estimate g $C/m^3/\overline{day}$ or g $C/m^2/\overline{day}$ where the unit $1/\overline{day}$ represents a period of time for which total irradiance is equal to the average total irradiance per day during a month.

Campbell-Stokes Sunshine Recorders are not designed to measure PAR, so M is applied to Sechelt Inlet cautiously. Nevertheless, a cloudy day in a month of sunshine or vise versa should be indicated by M. Table 2.5 shows the relevant data collected from Environment Canada and M for each day that ^{14}C incubations were performed.

2.2.3 Chlorophyll *a* and phaeopigment measurements

Samples for chl*a* and phaeopigment measurements were collected during the monthly cruises from December to June at stations SC-2, SC-3, SC-5, SC-6, SC-8 and SC-9. A segmented integrating pipe sampler (SIPS; Sutherland *et al.*, 1992) was used to collect water from the depth intervals of 0-1.5, 1.5-3, 3-6, 9-12 and 18-21 m. The contents from each depth interval were mixed on board and 100 ml of seawater were filtered through pre-combusted 2.5 cm glass fiber filters (GF/F, 0.7 μm) and the filters were frozen. In the laboratory the filters were placed in 90% acetone, sonicated in ice water for 20 min, and extracted in the dark at 5^0 C. Chl*a* and phaeopigment concentrations of the acetone solution were measured fluorometrically using a Turner Designs Model 10 fluorometer. Fluorescence was converted to chl*a* and phaeopigment concentrations using the equations of Parsons *et al.* (1984a).

Parsons *et al.* (1984a) report that at low concentrations (0.5 mg/m^3) the precision for chl*a* replicates should be better than 10%. All chl*a* and phaeopigment data collected during the study period are presented in tables 2.6 through 2.9.

date	depth range m	SC-2 chl*a* mg/m^3	SC-2 phaeo mg/m^3	SC-3 chl*a* mg/m^3	SC-3 phaeo mg/m^3	SC-5 chl*a* mg/m^3	SC-5 phaeo mg/m^3
	0-1.5	0.16	0.82	0.63	1.0	0.22	0.50
Dec	1.5-3	0.15	0.49	0.18	0.37	0.21	0.43
11-12	3-6	0.23	0.48	0.16	0.42	0.17	0.42
	9-12	0.13	0.52	0.082	0.26	0.12	0.29
	18-21	0.088	0.27	0.059	0.29	0.040	0.28
	0-1.5	0.68	1.6	0.60	1.7	0.48	1.0
Jan	1.5-3	0.71	1.3	0.61	1.2	0.78	1.5
22-23	3-6	0.88	1.4	0.66	1.0	0.77	1.5
	9-12	0.37	0.64	0.17	0.50	0.49	0.73
	18-21	0.21	0.41	0.025	0.23	0.059	0.23
	0-1.5	0.43	0.99				
Feb	1.5-3	0.38	0.74	no data		no data	
19-20	3-6	0.39	0.68	collected		collected	
	9-12	0.37	0.75				
	18-21	0.25	0.63				

Table 2.6: Chl*a* and phaeopigments at stations SC-2, SC-3 and SC-5 for December → February.

date	depth range m	SC-6 chl*a* mg/m^3	SC-6 phaeo mg/m^3	SC-8 chl*a* mg/m^3	SC-8 phaeo mg/m^3	SC-9 chl*a* mg/m^3	SC-9 phaeo mg/m^3
	0-1.5	0.040	0.17	0.15	0.36		
Dec	1.5-3	0.26	0.60	0.084	0.26	no data	
11-12	3-6	0.26	0.73	0.29	0.44	collected	
	9-12	0.00	0.078	0.16	0.47		
	18-21	0.055	0.26	0.050	0.23		
	0-1.5	0.68	1.2	0.62	1.2	0.62	0.93
Jan	1.5-3	0.94	1.4	0.79	1.6	0.62	0.92
22-23	3-6	0.69	1.0	1.1	1.8	0.55	0.89
	9-12	0.22	0.31	0.24	0.32	0.20	0.35
	18-21	0.10	0.29	0.31	0.00	0.034	0.13
	0-1.5	0.11	0.26				
Feb	1.5-3	0.39	0.56	no data		no data	
19-20	3-6	0.34	0.60	collected		collected	
	9-12	0.12	0.36				
	18-21	0.044	0.40				

Table 2.7: Chl*a* and phaeopigments at stations SC-6, SC-8 and SC-9 for December → February.

date	depth range m	SC-2 chl*a* mg/m^3	SC-2 phaeo mg/m^3	SC-3 chl*a* mg/m^3	SC-3 phaeo mg/m^3	SC-5 chl*a* mg/m^3	SC-5 phaeo mg/m^3
	0-1.5	69	20	63	19	61	19
Mar	1.5-3	63	23	47	17	44	14
26-27	3-6	51	14	46	14	37	13
	9-12	12	5.6	50	15	32	8.5
	18-21	1.8	1.8	3.2	1.2	1.6	1.4
	0-1.5	6.2	3.7	5.0	3.2	0.55	0.47
Apr	1.5-3	1.4	1.4	5.2	2.7	0.73	0.70
23-25	3-6	3.6	2.1	8.0	6.1	0.56	0.52
	9-12	1.7	1.8	2.8	2.2	0.26	0.63
	18-21	1.2	1.7	1.7	4.0	3.2	3.4
	0-1.5	3.1	1.8	1.5	1.3	5.7	1.8
May	1.5-3	1.8	1.6	2.2	2.3	2.8	1.3
22-23	3-6	11	16	6.7	2.8	9.5	6.3
	9-12	19	16	3.1	2.3	1.9	2.6
	18-21	2.1	2.3	0.86	2.2	0.42	1.6
	0-1.5	21	11	14	7.5	6.6	3.0
Jun	1.5-3	17	10	11	6.2	8.1	3.1
22-23	3-6	15	8.1	7.4	2.4	5.6	2.8
	9-12	6.2	2.1	2.2	2.0	1.4	1.8
	18-21	5.8	2.0	2.1	1.6	1.1	1.5

Table 2.8: Chl*a* and phaeopigments at stations SC-2, SC-3 and SC-5 for March → June.

date	depth range m	SC-6		SC-8		SC-9	
		chl*a* mg/m^3	phaeo mg/m^3	chl*a* mg/m^3	phaeo mg/m^3	chl*a* mg/m^3	phaeo mg/m^3
	0-1.5	34	12	70	17	36	12
Mar	1.5-3	14	7.7	57	14	16	6.8
26-27	3-6	12	6.6	48	12	7.8	1.4
	9-12	45	14	44	11	16	6.8
	18-21	3.4	0.51	5.2	0.99	1.4	0.89
	0-1.5	3.2	1.6	0.92	0.99	6.3	3.3
Apr	1.5-3	0.31	0.28	2.9	1.7	4.7	2.8
23-25	3-6	1.8	1.5	1.5	1.2	7.5	6.9
	9-12	2.1	1.9	0.11	0.21	1.8	2.0
	18-21	1.4	1.4	1.6	3.0	0.60	1.0
	0-1.5	3.8	2.3	0.41	0.56	0.60	0.70
May	1.5-3	2.5	2.2	0.77	0.99	3.8	3.3
22-23	3-6	3.8	2.1	2.0	1.9	9.3	7.1
	9-12	1.7	2.8	1.7	1.5	8.8	6.8
	18-21	0.14	1.0	0.30	0.99	4.7	1.8
	0-1.5	7.4	3.4	1.6	1.8	21	9.3
Jun	1.5-3	7.1	3.7	1.9	2.1	12	7.3
22-23	3-6	6.3	4.3	2.3	2.5	6.8	3.2
	9-12	3.7	3.6	1.8	2.2	1.6	1.4
	18-21	2.6	3.0	-	-	0.50	0.82

Table 2.9: Chl*a* and phaeopigments at stations SC-6, SC-8 and SC-9 for March → June.

2.3 Sediment trap data

The particle flux component of the interdisciplinary study in Sechelt Inlet employed sediment trap arrays at stations SC-3 (depth=280 m), SC-5.5 (depth=180 m), and SC-7 (depth=265 m). Station locations are shown in figure 1.1. For each array a pair of sediment traps was placed 50 m from the surface, 50 m from the bottom and at mid-depth. Initial deployments at stations SC-3 and SC-7 were on January 23, 1991 and the sediment trap mooring at station SC-5.5 was deployed on February 19, 1991. The traps were serviced monthly and they were last recovered on June 23 and 24, 1991. No sediment trap data were collected from station SC-3 in April.

Organic carbon, $CaCO_3$ carbon, nitrogen and biogenic silica measurements were made on the sediment trap samples. Sediment trap design and servicing technique, and chemical analyses were similar to work done earlier in Saanich Inlet and Jervis Inlet and described by Francois (1987).

2.3.1 Trap design

The design of the sediment traps was developed by K. Iseki, F. Whitney and C.S. Wong at the Institute of Ocean Science (unpublished). At each depth were two PVC cylinders with an internal diameter of 12.5 cm, an outer diameter of 14 cm and a height of 48 cm. Baffle grids (1.5 cm square x 5 cm deep) were placed in the opening of the traps and in the sampling chambers. Their purpose was to decrease the effects of turbulent mixing within the traps, especially during deployment and recovery (Gardner, 1980b).

2.3.2 Preservatives

Sediment traps were always in pairs. At the bottom of each trap was 500 ml of 30% NaCl solution; the gradient created with ambient sea water was meant to reduce turbulent

mixing. In one trap of each pair, the NaCl solution also contained 0.5% sodium azide as a bactericide. NaN_3 inhibits aerobic but not anaerobic bacterial decomposition. Through comparison with the trap lacking a bactericide, the effectiveness of NaN_3 as an inhibitor to *in situ* degradation of sediment trap material can be evaluated. Effectively, there are two sets of data from each depth and paired t-tests were conducted to establish the significance of the difference between the two treatments.

It was found that organic carbon, nitrogen and silica were not significantly different between sample environments for α=0.2. Total dry weight and lithogenous matter were not significantly different for α=0.1. Therefore, the average of the two preservative treatments at each depth was used for these constituents.

The mean flux of $CaCO_3$ was 25% greater for the NaN_3 treated sediment traps than for the traps without NaN_3 and statistically the two fluxes are not considered to have been similar until α=0.001. However, $CaCO_3$ was averaged as the other constituents in this work for two reasons. First, the cause of the systematic difference in $CaCO_3$ flux for the two treatments is uncertain. Second, $CaCO_3$ makes up approximately 1% of the total flux. Errors in its measurement will have little consequence on the results of the algorithm presented in chapter 5.

(The algorithm described in chapter 5 has been applied to a much larger sediment trap data set from Jervis Inlet, which was collected and processed in much the same way as that from Sechelt Inlet. Values for the two sample treatments were not averaged. The solutions of the algorithm applied to Jervis Inlet for both treatments are within 20% of each other in the worst case and there does not appear to be a systematic difference for algorithm solutions between sample treatments.)

2.3.3 Total dry weight

Upon retrieval, the sediment trap samples were filtered through 0.47 mm Nitex monofilament bolting cloth to remove large zooplankton and other swimmers. A measured quantity of distilled deionized water was used to ensure that all fine particles passed through the cloth. In the laboratory, samples were centrifuged at 3000 rpm in pre-weighed centrifuge tubes and repetitively rinsed with distilled deionized water in order to remove most of the salt from the samples. At the end of centrifugation, the supernatant volume was determined and its solid phase freeze-dried, weighed and ground to a fine powder in an agate mortar and pestle.

2.3.4 Organic carbon and nitrogen measurements

Total carbon and nitrogen were determined by gas-chromatography on a model 1106 Carlo-Erba CHN analyzer, calibrated with acetanalide ($CH_3CONH_6H_5$). Between five and ten mg of freeze-dried sample were placed into small tin cups and precisely weighed with a model M3 Mettler microbalance. The cups were then loaded into the sample changer of the CHN analyzer and combusted at approximately 1020^0 C in a stream of He and O_2. The combustion gases were quantitatively oxidized by passing through a Cr_2O_3 column and over copper heated to 650^0 C. (Contact with copper removes excess O_2 and reduces nitrogen oxides that are produced during the initial combustion.) CO_2, H_2O, and N_2 were separated on a Porapak QS chromatographic column and measured by thermal conductivity. The analytical precision as measured by one standard deviation for this technique has been estimated to be $\pm 1.3\%$ for carbon and $\pm 2\%$ for nitrogen.

Organic carbon was determined by subtracting $CaCO_3$ carbon from total carbon. (No corrections need be made when converting total to organic nitrogen because nitrogen is

rare in any inorganic forms.) $CaCO_3$ was measured on a Coulometrics Inc. CO_2 coulometer. Samples were reacted with 3 ml of 2.4 N HCl to liberate CO_2 which was swepted into a cell containing ethanolamine and a colorimetric indicator. The cell is between a light source and a photodetector. The CO_2 is quantitatively absorbed and reacts with the ethanolamine to form a strong, titratable acid which causes the indicator color to fade. A photodetector causes base to be electronically added to the coulometer cell until the original color returns. The total amount of current required for the titration is electrically integrated and the CO_2 coulometer displays the analysis result as micrograms of carbon. Using this technique, Huffman (1977) reported a standard deviation of 2% for 11 measurements of samples with a fixed $CaCO_3$ content.

2.3.5 Biogenic silica and estimates of the lithogenous flux

Biogenic silica was measured in the sediment trap samples following the method and equations of Mortlock and Froelich (1989). The procedure involves extracting amorphous silica from a sediment sample with an alkaline solution and then measuring the dissolved silicon concentration in the extract by molybdate-blue spectrophotometry. This technique directly yields a measure of mM Si or %Si, which is converted to $\%SiO_2 \cdot nH_2O$ by assuming that biogenic silica is 10% water by weight, so that $\%SiO_2 \cdot nH_2O = 2.4 \times \%Si$. The precision of this technique ranges from 4% for samples containing $> 50\%$ biogenic silica to 8% for samples with $< 15\%$ biogenic silica (Mortlock and Froelich; 1989).

There is no measurement of any lithogenous material for the sediment trap samples from Sechelt Inlet. However, the lithogenous flux may be estimated by recognizing that the total dry weight will be dominated by organic matter, SiO_2nH_2O, $CaCO_3$ and lithogenous material. Of these components, the lithogenous fraction of the total dry weight is the only unknown and so can be determined by difference. In order to do so,

organic carbon must be converted to total organic matter. The average organic carbon to nitrogen (C:N) ratio in Sechelt Inlet during the study period was 8.7 by weight (table 5.2) or 10 by atoms. Assuming a ratio for organic carbon to phosphorus of 106:1 (Redfield *et al.*, 1963), the C:N:P ratio of a model organic molecule in Sechelt Inlet during the study period was 106:10:1 and can be written as $(CH_2O)_{106}(NH_3)_{10}(H_3PO_4)$. Carbon makes up 37% of this molecule by weight, so that multiplying measurements of the weight of organic carbon by the factor of 2.7 provides an estimate of the total weight of organic matter.

Results of the trap sample analyses are presented in tables 2.10 through 2.12.

SC-3							
deploy period	**constituent**	**NaCl**			**NaCl+NaN_3**		
		50 m	**140 m**	**230 m**	**50 m**	**140 m**	**230 m**
Jan 23 to Feb 19	dry weight	2190	2380	3180	2170	2380	3090
	organic carbon	200	220	260	190	220	240
	nitrogen	17	21	26	16	20	23
	$CaCO_3$	22	23	19	30	34	36
	biogenic silica	100	190	550	100	170	540
	lithogenous	1580	1620	1970	1570	1610	1920
Feb 19 to Mar 26	dry weight	1350	2440	3010	1290	2730	3180
	organic carbon	140	210	220	130	250	240
	nitrogen	17	27	29	16	31	34
	$CaCO_3$	30	21	14	35	27	26
	biogenic silica	510	970	1140	500	1110	1220
	lithogenous	460	920	1300	430	980	1330
Mar 26 to Apr 23		no data collected					
Apr 23 to May 22	dry weight	3090	3510	3120	3380	3820	3330
	organic carbon	240	380	200	260	330	220
	nitrogen	28	38	26	29	37	28
	$CaCO_3$	36	38	34	56	48	48
	biogenic silica	1630	1410	1260	1760	1420	1390
	lithogenous	830	1100	1330	920	1530	1350
May 22 to Jun 22	dry weight	3560	4410	2440	3030	3410	3670
	organic carbon	320	330	150	260	250	230
	nitrogen	41	43	19	33	30	30
	$CaCO_3$	55	52	22	42	35	55
	biogenic silica	1940	2610	1250	1810	1860	1810
	lithogenous	750	930	800	530	900	1230

Table 2.10: Total and compositional fluxes in $mg/m^2/day$ at station SC-3 during the study period. Although preservative treatments are separated here and in tables 2.11 and 2.12, all data analyses average the two treatments. The lithogenous flux is not measured directly; its determination is described in the text.

SC-5.5							
deploy period	**constituent**	**NaCl**			**NaCl+NaN_3**		
		50 m	**90 m**	**130 m**	**50 m**	**90 m**	**130 m**
Jan 22 to Feb 19		no data collected					
Feb 19 to Mar 26	dry weight	490	750	1420	520	690	1380
	organic carbon	55	82	140	55	65	130
	nitrogen	6.9	9.7	16	6.3	7.2	14
	$CaCO_3$	0.11	1.9	2.7	2.6	2.4	3.2
	biogenic silica	-	200	350	-	180	340
	lithogenous	-	340	740	-	340	710
Mar 26 to Apr 24	dry weight	2650	3870	4330	2570	3280	2740
	organic carbon	250	270	310	220	230	210
	nitrogen	29	31	37	25	26	24
	$CaCO_3$	0.75	3.5	4.1	5.3	6.4	1.5
	biogenic silica	1190	1610	1700	1130	1200	1150
	lithogenous	840	1570	1870	900	1510	1080
Apr 24 to May 23	dry weight	2100	2100	3450	1910	1850	3280
	organic carbon	160	160	270	180	150	270
	nitrogen	18	19	30	20	17	31
	$CaCO_3$	3.0	4.9	15	11	7.6	18
	biogenic silica	560	780	1420	670	800	1350
	lithogenous	1150	910	1340	790	660	1240
May 23 to Jun 22	dry weight	3100	3740	5210	3080	5250	3440
	organic carbon	260	280	440	260	430	280
	nitrogen	32	35	53	33	50	34
	$CaCO_3$	50	66	28	250	48	71
	biogenic silica	1560	1770	2510	1550	2420	1850
	lithogenous	830	1190	1560	630	1710	830

Table 2.11: Total and compositional fluxes in $mg/m^2/day$ at station SC-5.5.

SC-7							
deploy period	**constituent**	**NaCl**			**NaCl+NaN_3**		
		50 m	**130 m**	**215 m**	**50 m**	**130 m**	**215 m**
Jan 23 to Feb 19	dry weight	2090	2020	2570	2050	1940	2540
	organic carbon	160	170	190	150	170	200
	nitrogen	13	15	18	11	14	18
	$CaCO_3$	5.6	2.3	3.9	12	10	10
	biogenic silica	60	120	350	56	100	260
	lithogenous	1610	1480	1750	1600	1400	1770
Feb 19 to Mar 27	dry weight	490	590	1120	440	590	1070
	organic carbon	63	59	90	53	67	82
	nitrogen	8.1	6.8	9.9	6.1	7.3	8.4
	$CaCO_3$	1.9	2.5	1.4	4.9	6.2	3.2
	biogenic silica	-	-	280	150	120	230
	lithogenous	-	-	620	150	300	640
Mar 27 to Apr 23	dry weight	2610	3300	3490	2630	2300	2860
	organic carbon	210	220	210	220	200	190
	nitrogen	25	27	26	27	24	25
	$CaCO_3$	1.5	4.2	1.1	3.2	3.8	2.5
	biogenic silica	1010	1550	1390	1140	1370	1500
	lithogenous	1080	1180	1570	940	420	880
Apr 23 to May 22	dry weight	1140	1360	1190	1180	1320	730
	organic carbon	140	110	93	150	130	59
	nitrogen	16	13	11	17	15	6.8
	$CaCO_3$	5.6	2.9	1.2	15	8.2	6.3
	biogenic silica	440	600	500	490	570	310
	lithogenous	350	490	450	300	420	270
May 22 to Jun 23	dry weight	1860	2020	2010	1760	1920	1840
	organic carbon	200	190	160	190	190	140
	nitrogen	25	23	19	24	23	17
	$CaCO_3$	21	12	8.1	37	28	12
	biogenic silica	950	990	1050	920	1040	890
	lithogenous	390	540	560	340	380	580

Table 2.12: Total and compositional fluxes in $mg/m^2/day$ at station SC-7.

2.4 Other data

2.4.1 Phytoplankton species analyses

Samples for phytoplankton analysis were taken from the water collected for measurements of chl*a* and phaeopigment. On board, 125 ml were preserved with acidic Lugol's solution and later proportionate volumes from each depth interval were mixed to produce an 'integrated' sample. The integrated sample was analyzed for phytoplankton species using the Utermöhl technique (Hasle, 1978). 10-50 ml were settled in a counting chamber for at least 12 hr. Nanoplankton were counted at 500x along a 10-20 mm transect across the diameter of the settling chamber; the more common microplankton species were viewed at 240x along 1-6 transects (depending on the concentration of particular species); and the entire chamber bottom was scanned at 95x for large and/or rare species. Results of the phytoplankton species analyses are presented in appendix A.

2.4.2 Temperature, salinity, dissolved oxygen and nutrients

At stations SC-1 through SC-9 and excluding station SC-5.5, temperature and salinity were obtained from a Guildline CTD in conjunction with a rosette sampler containing Niskin bottles. In general, the Niskin bottles sampled at 2, 5, 10, 20, 30, 50, 75, 100, 150, 200 and 250 m. The shallower stations (SC-1, SC-6 and SC-9) were sampled at 10 to 25 m intervals below 50 m. Small variations from this scheme did occur between stations and from month to month. Salinity was determined in the laboratory and for the deeper samples agreed with the CTD to about 0.01 in S on average. On board, dissolved oxygen was measured for samples from the Niskin bottles using the method of Carpenter (1965). The accuracy of this method is reportedly better than 1% at the concentration of 10 mg/l (Parsons *et al.*, 1984a).

Nutrient sampling was done under two regimes. Near-surface nutrient samples were

collected simultaneously with both chl*a* samples obtained by SIPS and ^{14}C incubation samples obtained by Niskin bottle. Nutrient samples from 30m and deeper were taken with the rosette sampler at all the depths and stations described above for T, S and dissolved O_2 excluding stations SC-1 and SC-4. Nutrient samples were taken from the depths of 0, 2, 5, 10 and 20 m by Niskin bottle at stations SC-3 and SC-7 as well.

Nitrate (+ nitrite), ammonium, phosphate and dissolved silicon were measured for both sets of surface samples and for the hydrographic samples. All samples were filtered through pre-combusted 2.5 cm glass fiber filters (GF/F, 0.7 μm) into 30 ml acid-washed Nalgene polypropylene bottles, immediately frozen and transferred to a freezer that was kept below -20^0 C. Nutrient analyses were carried out on a Technicon Autoanalyzer following the spectrophotometric method described by Parsons *et al.* (1984a). The precision of these measurements (Parsons *et al.*, 1984a) are 3% for nitrate at 20 μM and for dissolved silicon at 10 μM; 1% for phosphate at 3 μM; and is better than 0.1 μM for ammonium concentrations less than 10 μM. Extended periods of freezing tend to increase the variance in ammonium measurements (Parsons *et al.*, 1984a). Temperature, salinity, dissolved oxygen and nutrient data are presented in Appendix B.

Chapter 3

Estimation of Carbon Assimilation due to Photosynthesis

3.1 Introduction: Modeling photosynthetic carbon assimilation

Many oceanographic models of primary production are empirical or semi-empirical relationships that correlate carbon assimilation with chl*a* and light (Ryther and Yentsch, 1957; Eppley et. al., 1985; Platt, 1986; Sathyendranath *et al.*, 1989). These models successfully predict carbon assimilation for some field scenarios (Platt *et al.*, 1988), but are not yet general enough to describe phytoplankton growth over a wide range of environmental conditions (Campbell and O'Reilly, 1988; Falkowski, 1992).

Laboratory-based studies have produced a number of mechanistic models of phytoplankton growth (Shuter, 1979; Laws and Bannister, 1980; Kiefer and Mitchell, 1983; Cullen, 1990 and references therein). They are generally based on photosynthetic theory, and consider phytoplankton adaptation to variations in nutrients and light. Although these models typically make similar predictions of primary production given specific conditions, the lack of a systematic approach for determining rates of photosynthesis from physiological and environmental parameters makes their comparison complicated (Cullen, 1990). Furthermore, mechanistic models rely on a description of nutrient and light history for single species cultures grown in the laboratory under steady state (Laws and Bannister, 1980; Kiefer and Mitchell, 1983; Sakshaug *et al.*, 1989). Extrapolating these models to natural populations is difficult because phytoplankton populations are rarely monospecific and steady state is usually not applicable to phytoplankton ecology

where environmental conditions change rapidly (Cullen *et al.*, 1991).

In this chapter, a relationship is derived to predict carbon assimilation from chl*a* concentration alone.

3.2 The data from Sechelt Inlet used to estimate carbon assimilation

Throughout this chapter, a number of terms are used to discuss photosynthesis and phytoplankton growth. The following terms are rates and have units of mass/volume/time.

- carbon assimilation = carbon uptake, photosynthesis, primary production.
- P_g = gross carbon assimilation, gross primary production.
- $P_n = P_g - R$ = net carbon assimilation, net primary production.
- R = phytoplankton dark- and photo- respiration, and extra-cellular excretion of organic carbon.
- P_c = net community production = P_n minus the respiration of all heterotrophs.

In order to lay a foundation for discussing phytoplankton growth during the study period, vertical profiles of biologically-relevant properties in the upper water column of Sechelt Inlet are presented in figures 3.1 through 3.6. These figures show profiles of P_n and parameters that affect P_n; light, nitrate concentration, salinity (to provide an indication of vertical mixing) and chl*a* for the upper 20 m of the water column.

Each light profile in figures 3.1 through 3.6 is chosen from either SC-3, SC-5.5 or SC-7 and represents the extinction of light with depth for the cruise of that month. The light attenuation coefficients K_L and K_{int} specific to each light profile are given. Their computation is described in section 3.2.3. These light profiles have been chosen to best represent the average attenuation coefficients at the three stations for each month.

Nitrate and salinity profiles are shown together in figures 3.1 through 3.6. Nitrate is often the limiting nutrient in Sechelt Inlet (Haigh *et al.*, 1992). Its consumption throughout the study period is noted as it decreases in concentration in the upper 20 m of the water column from January to June. Gradients in the salinity profiles are qualitative measures of vertical mixing, and estuarine entrainment of deeper water is considered the primary source of nutrients into the euphotic zone of Sechelt Inlet (Haigh *et al.*, 1992). However, mixing can also carry phytoplankton away from light. Thus, mixing-nutrient dynamics have a great effect on primary production.

Chl*a* is included in these profiles as phytoplankton growth will affect changes in its concentration. Therefore, chl*a* can be viewed as a relative measure of phytoplankton biomass (Cullen, 1982). More importantly for this work, chl*a* and light determine *in situ* carbon assimilation (Ryther, 1956a; Kiefer and Mitchell, 1983; Sakshaug *et al.*, 1989; Cullen, 1990).

Because the nitrate, salinity, chl*a* and ^{14}C uptake profiles were similar at SC-3, SC-5.5 and SC-7 for each month, these parameters are averaged over those stations for figures 3.1 through 3.6.

3.2.1 ^{14}C uptake measurements

Although long ^{14}C uptake incubations (2-4 hrs) are reported to measure P_n rather than P_g (Eppley and Sloan, 1965; Ryther and Mentzel, 1965), there is concern that this is not truly the case (Peterson, 1980; Carpenter and Lively, 1980), and that in fact ^{14}C uptake experiments give a value somewhere between gross and net carbon assimilation. This work presumes that ^{14}C incubations measure P_n.

As described in chapter 2, two hour ^{14}C incubations were performed monthly at stations SC-3, SC-5.5 and SC-7. Incubations were done at five depths for each experiment, representing approximately the 56, 32, 22, 13 and 7% light levels.

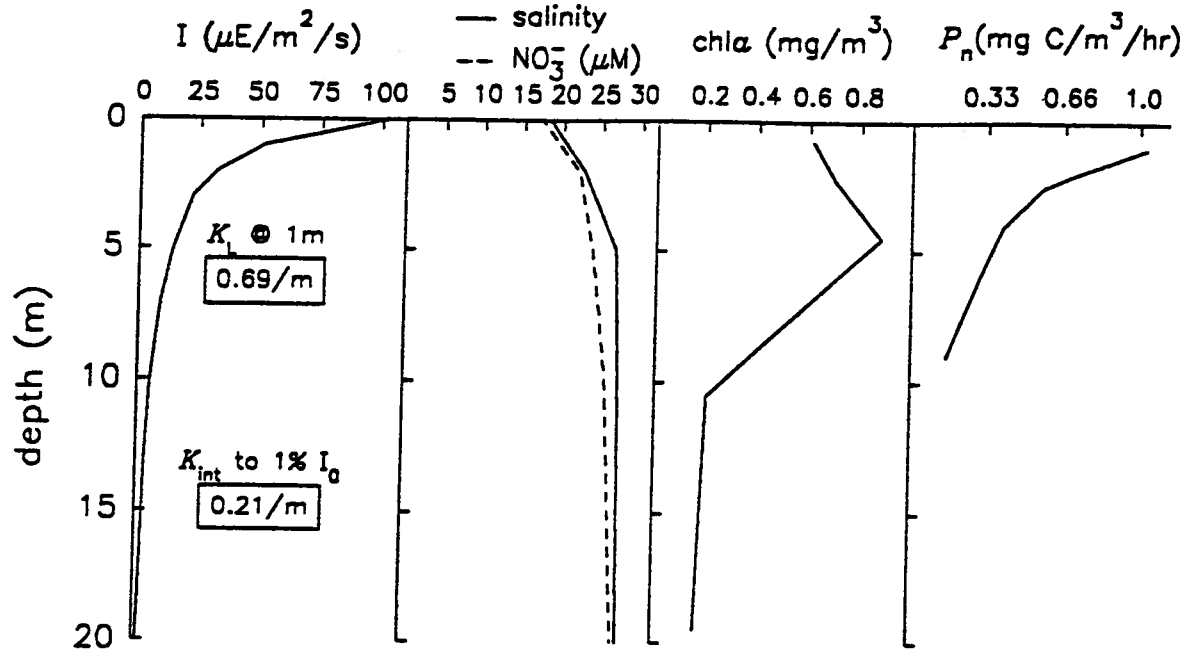

Figure 3.1: Vertical profiles of biologically relevant parameters: January 22-23.

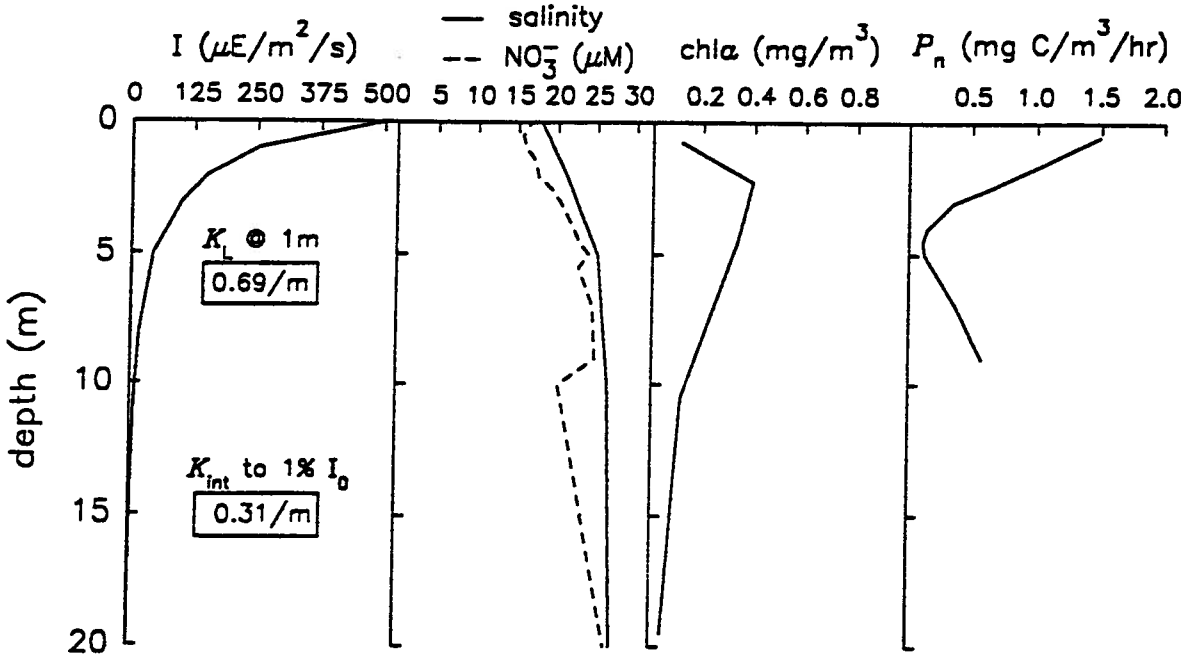

Figure 3.2: Vertical profiles of biologically relevant parameters: February 19-20.

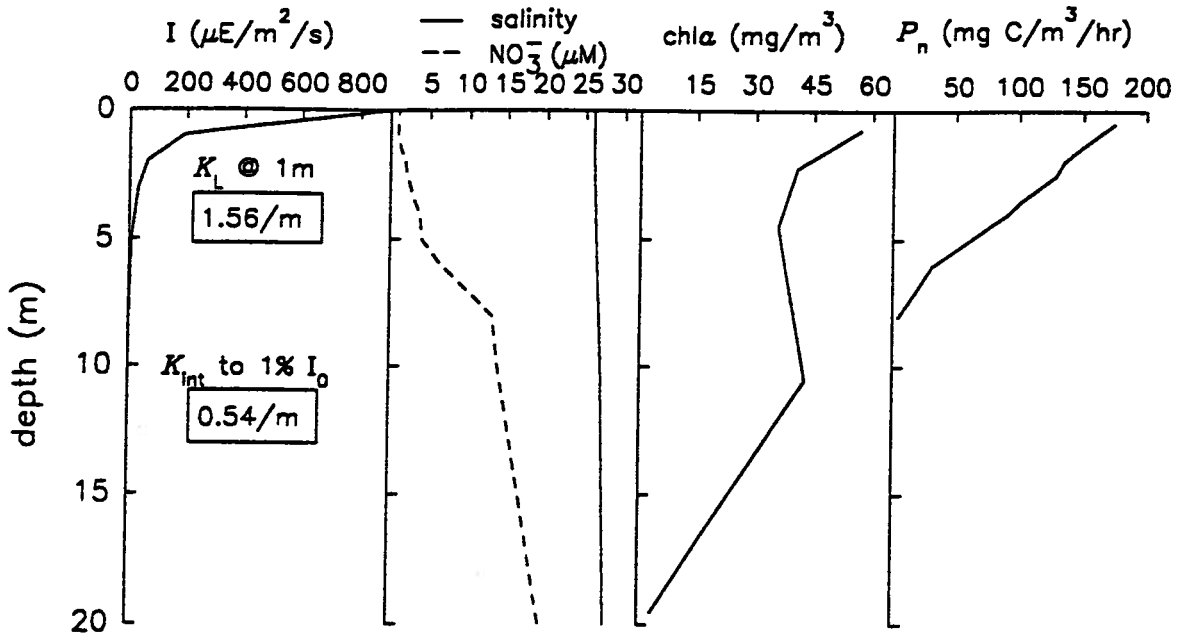

Figure 3.3: Vertical profiles of biologically relevant parameters: March 26-27.

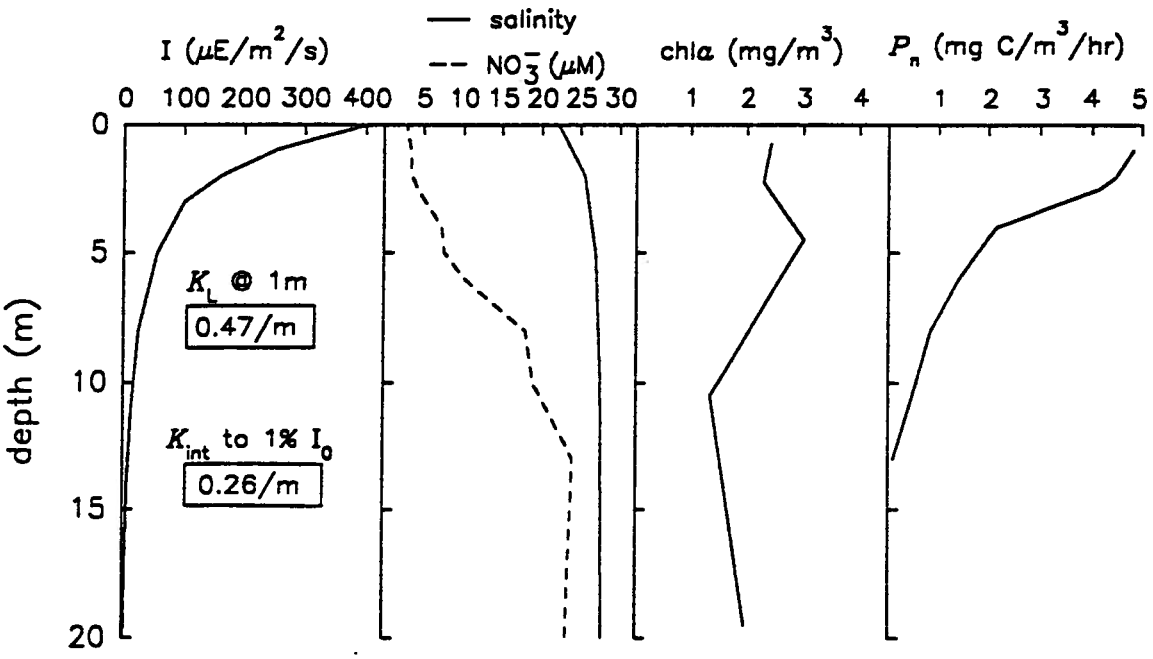

Figure 3.4: Vertical profiles of biologically relevant parameters: April 23-25.

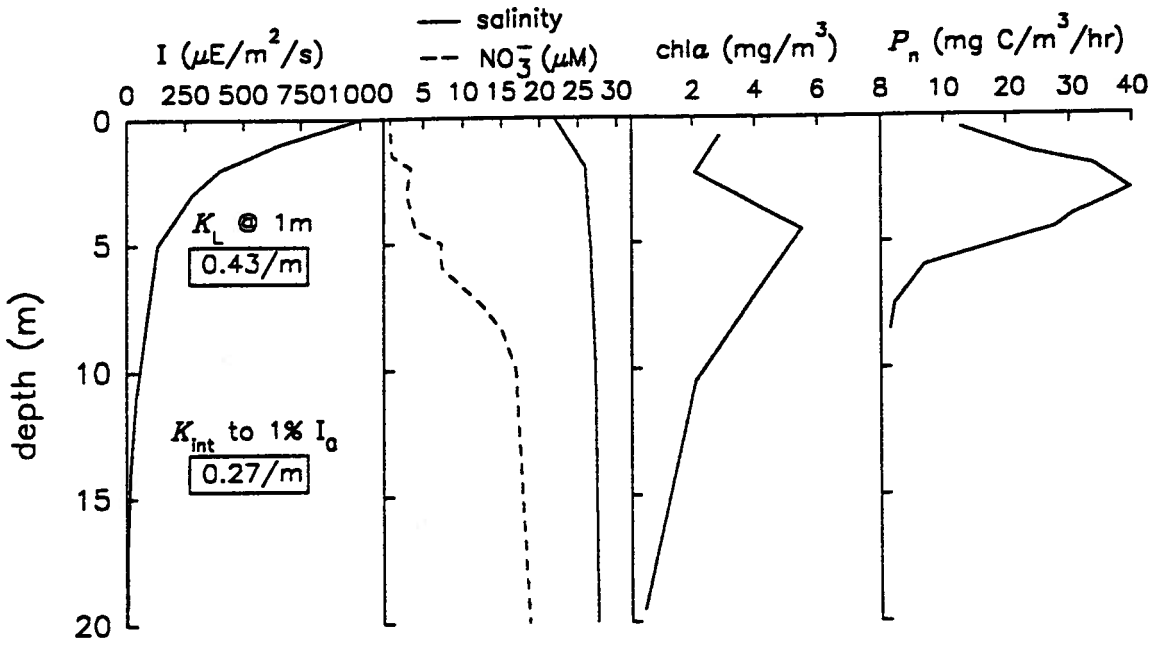

Figure 3.5: Vertical profiles of biologically relevant parameters: May 22-23.

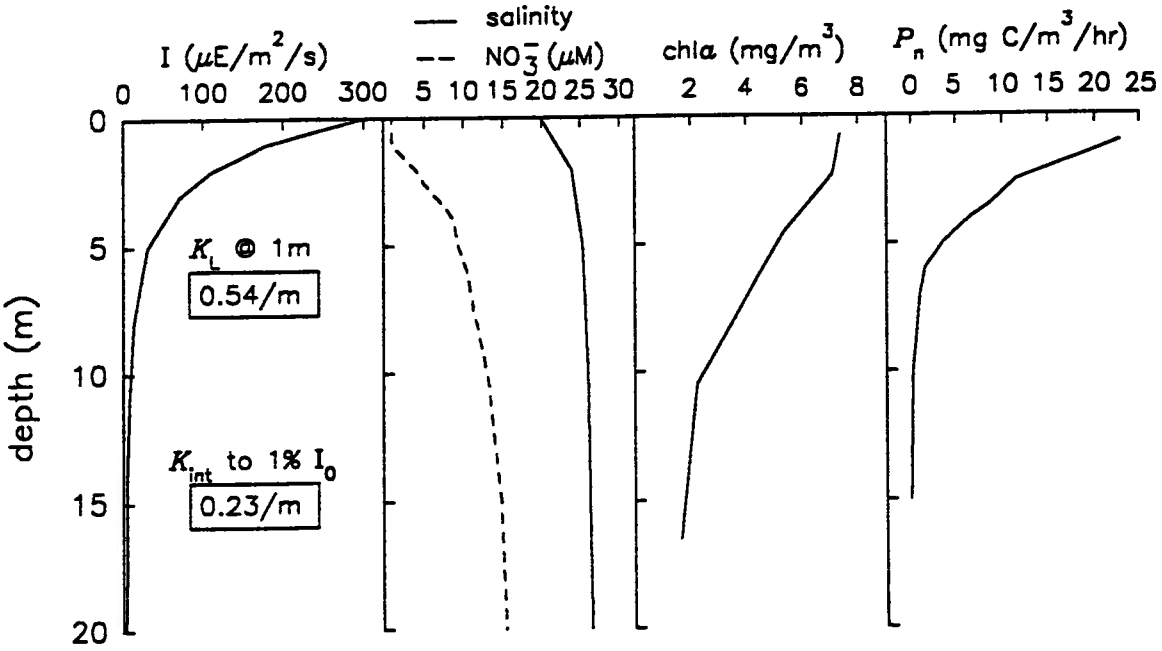

Figure 3.6: Vertical profiles of biologically relevant parameters: June 22-23.

There are two problems with the data set from Sechelt Inlet if one is to correlate carbon assimilation with chl*a* concentration. The first is that chl*a* measurements and ^{14}C uptake experiments were not performed simultaneously, but nearby on the same day. The second is that light data were only collected to learn the relative light intensity with depth and no data from the monthly cruises into Sechelt Inltet exist to describe irradiance throughout the day of each experiment or over the five month duration of the experiment. This information is important so as to be able to translate values of carbon assimilation from g/(incubation period) to g/day and g/$\overline{day}$. The methods used to circumvent this lack of irradiance data are described in section 2.2.2.

3.2.2 Chl*a* measurements

In order to compare the chl*a* and ^{14}C data, the chl*a* measurements have been transposed to the locations of the ^{14}C and irradiance experiments instead of vice versa. The distance between the locations where the chl*a* and ^{14}C uptake data were collected was approximately 500 m at SC-3. The chl*a* measurements from SC-5 and SC-6 have been averaged to represent chl*a* concentrations at SC-5.5 where ^{14}C incubations were performed. Chl*a* concentrations from station SC-8 have been translated about 14 km to SC-7 so that these data could be used in comparing chl*a* and ^{14}C data. Also, most of the chl*a* data from February are missing. For that month, chl*a* concentrations at SC-2 and SC-6 are used to represent those at SC-3 and SC-5.5, respectively. Chl*a* concentrations averaged between SC-2 and SC-6 have been used for correlations with P_n at SC-7. The translations made in February should be considered less severe than those at other times because both P_n and chl*a* concentrations were relatively low for that month, thus having little weight on final correlations.

These spatial translations clearly raise doubts when comparing ^{14}C uptake with chl*a* data. However, the exercise presented in this chapter has produced some useful insights.

The final relationship found between chl*a* concentration and P_n in this chapter is used in chapter 4, while the discussion of photosynthetic oxygen production in chapter 7 relies on ^{14}C incubations at SC-3, SC-5.5 and SC-7. Therefore, final estimates of carbon assimilation and oxygen production in Sechelt Inlet during the five month study period do not use correlations between chl*a* concentration and P_n. It is emphasised that any hypotheses made in this chapter are tentative and require further investigation.

In making the best of these data, two points should be made. First, horizontal variations in Sechelt Inlet are reasonably small, suggesting that the chl*a* concentration at two locations may be similar (Haigh *et al.*, 1992). During this study the chl*a* concentrations throughout the entire inlet (away from SC-2 and SC-9 where the physical dynamics are quite different from the rest of the inlet system) vary by only a factor of two or less in January, February and March. Horizontal variability increases after the spring bloom, suggesting that the lack of coincidence for the chl*a* and ^{14}C uptake data sets may be more important in the second half of the study period than in the first.

Second, vertical fluctuations in phytoplankton biomass are large because light, nutrients, and water column stability change rapidly in that dimension. However, integration of phytoplankton biomass over depth will tend to average vertical variability when comparing measurements from different stations. Therefore, a vertically integrated chl*a* concentration (g/m^2) is translated to a nearby station with more confidence than the chl*a* concentration at a specific depth (g/m^3).

3.2.3 Light extinction with depth

Recognizing that algae in shallow waters might absorb light to a degree that is detrimental to phytoplankton in deeper waters, the light and chl*a* profiles have been used to separate light attenuation caused by phytoplankton from the light attenuation by water and suspended material. Equation 3.1 describes the light intensity at any depth (I_z)

as a function of surface irradiance (I_0) and of the light attenuation coefficients of water (k_w), of suspended particulate material (k_s) and phytoplankton (k_p) (Platt *et al.*, 1977). Depth (z) is positive downward.

$$I_z = I_0 \, e^{K \, \Delta z} \tag{3.1}$$

$$K = k_w + k_s + k_p \tag{3.2}$$

There are two general depth ranges over which K can be solved. The first is from the surface to depth z and produces depth integrated values of K (K_{int}). The second is over a smaller depth range within the water column and yields local values of K (K_L). Direct measurements of irradiance (section 2.2.1) were made at approximately the depths from which samples were collected for ^{14}C incubations (56, 32 22, 13 and 7% light levels, with additional readings at the surface and at the 3% light level). K_L has been determined for the depth ranges between direct readings of irradiance and the calculated values of K_L are assigned to the mid-depth of each depth range. Linear extrapolation between mid-depths has been used to estimate K_L throughout the water column. Assuming that k_w is constant, K_L will vary with phytoplankton biomass and with the presence of suspended particles. K_L can be compared to depth-matched chl*a* concentrations in order try to separate k_p from k_s.

Figure 3.7 is a plot of K_L against chl*a*. It shows that the phytoplankton biomass can be a strong influence on light attenuation at high chl*a* concentrations. However, figure 3.8 shows that below values of approximately 0.020 g/m^3, K_L is independent of chl*a* concentration. The values of K_L for chl*a* < 0.020 g/m^3 are therefore interpreted to be $k_w + k_s$, where variability is dominated by differing amounts of suspended particles.

A high degree of light attenuation will restrict photosynthesis in deeper waters regardless of chl*a* concentrations and nutrient availability. To evaluate the relative availability of light to phytoplankton on the day of each light profile, total water column integrated

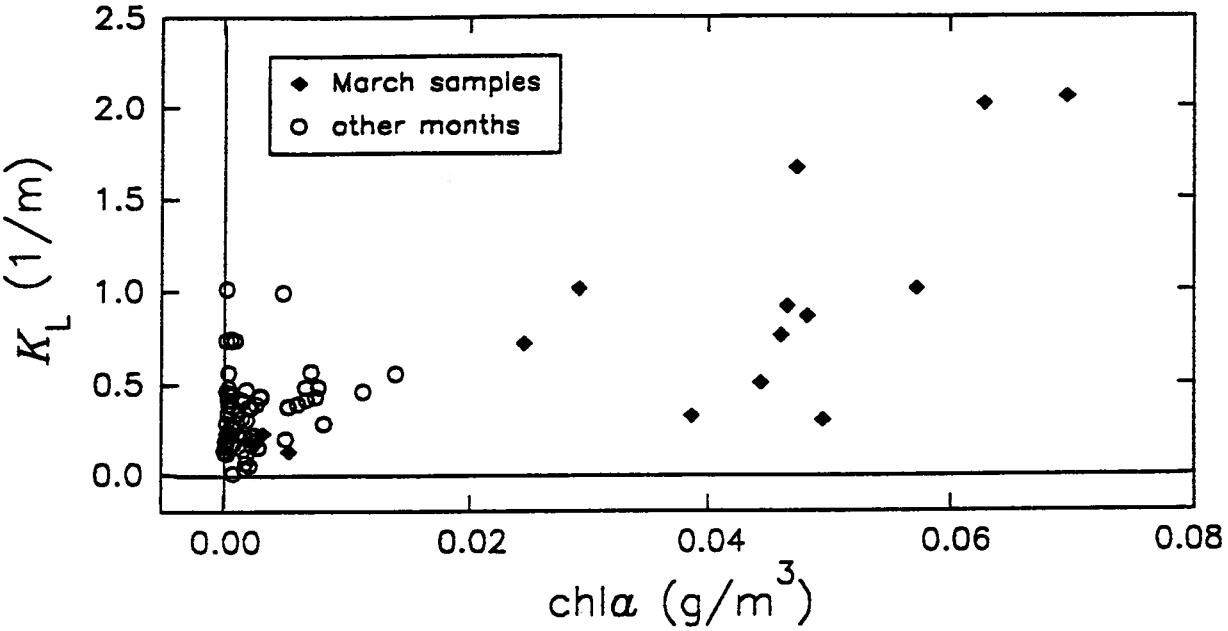

Figure 3.7: K_L vs. chl$a$ concentration.

irradiance has been compared to surface irradiance (figure 3.9). Integrated irradiance is calculated by integrating equation 3.1 from the surface to the depth of approximately the 1% light level. K_L over respective depth intervals is used for this integration. Figure 3.9 shows that relative light availability was much lower in March than for the rest of the study period.

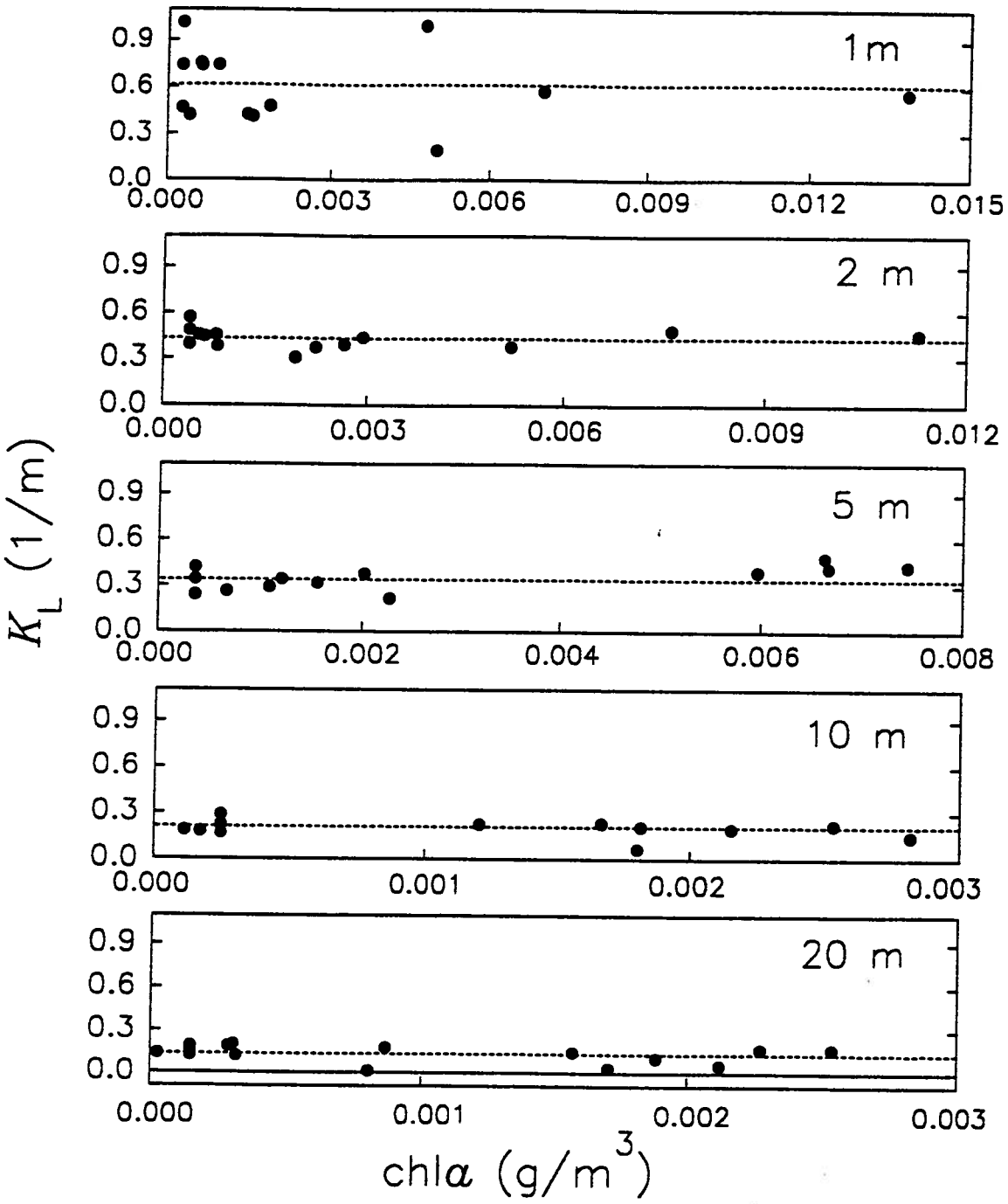

Figure 3.8: K_L vs. chl$a$ concentration at 1, 2, 5, 10 and 20m. Data from March are excluded from these plots to emphasize the lack of a correlation between K_L and chl$a$ for chl$a$ concentrations < 0.020 g/m^3.

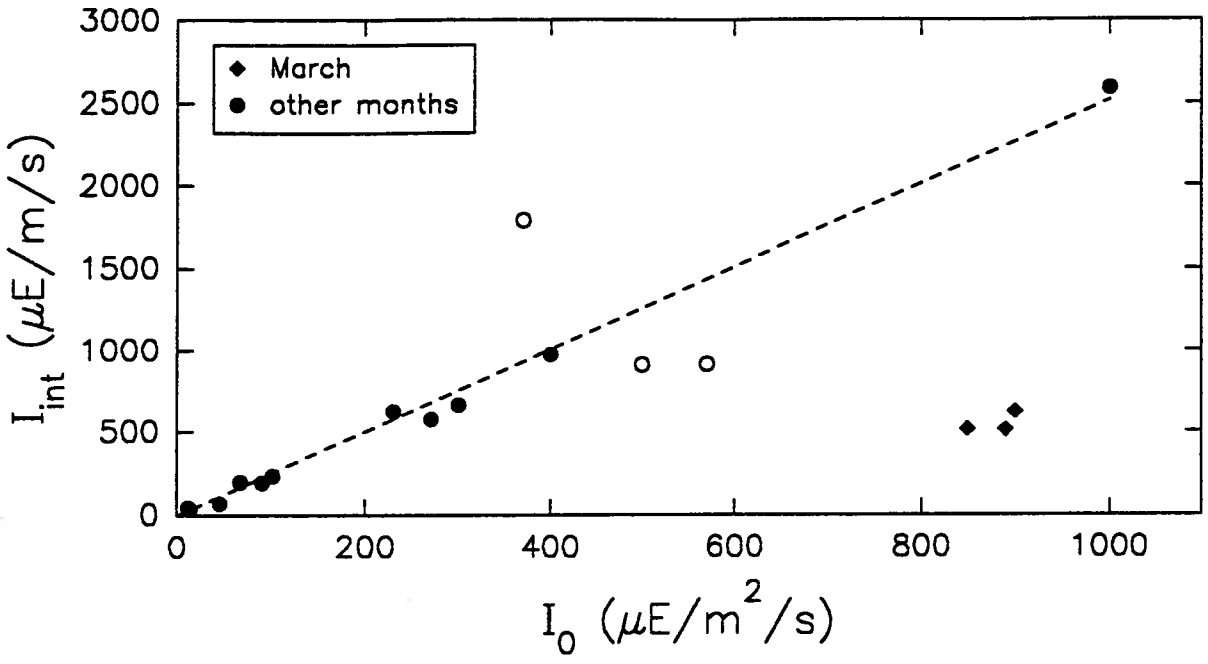

Figure 3.9: Integrated vs. surface irradiance in Sechelt Inlet. I_0 is surface irradiance. I_{int} is the amount of light in the water column to the 1% light level and is calculated using the appropriate K_L for each depth interval between light measurements. The dashed line is a regression of the data represented by the filled circles; it has a slope of 2.5 m. I_{int}/I_0 for March is approximately 4× less than that for the rest of the study period. Open circles are data from different stations and months that fall off the regression line for unknown reasons.

3.3 A model of P_n and its application to Sechelt Inlet

Assuming that phytoplankton growth is constant over time (t), net growth rate (μ with units t^{-1}) can be calculated by quantifying changes in cellular carbon.

$$C = C_0 e^{\mu t} \tag{3.3}$$

Differentiating with respect to time,

$$\frac{dC}{dt} = \mu\, C \tag{3.4}$$

where dC/dt is carbon assimilation. The goal of this work is to determine the dependence of dC/dt on chl$a$ concentration. Equation 3.4 is rewritten.

$$\frac{dC}{dt} = (\mu \ \text{C:chl}a)\ \text{chl}a \tag{3.5}$$

C:chl$a$ is the cellular ratio of carbon to chl$a$ in living phytoplankton. From equation 3.5, the minimum information required to predict carbon assimilation is chl$a$ concentration and (μ C:chl$a$). (μ C:chl$a$) will be referred to as Υ for the remainder of the text. The nature of Υ as chl$a$ concentrations change can be evaluated by plotting dC/dt against chl$a$. Figure 3.10 depicts P_n from the ^{14}C incubations vs. chl$a$ concentration interpolated to the location of P_n measurements. There appears to be no relationship between these variables.

The rate of photosynthetic carbon assimilation changes with light intensity and therefore throughout the day. To ensure that measurements from similar photoperiods are being compared, the carbon assimilation data are converted from units of (g C/m^3/hr) to units of (g C/m^3/day) using equation 2.1. Despite this manipulation, figure 3.11 shows that any relationship between chl$a$ and P_n is still unclear.

Phytoplankton may be mixed across vertical gradients in light faster than they can photoacclimate to a particular light intensity. Therefore, the phytoplankton assemblage

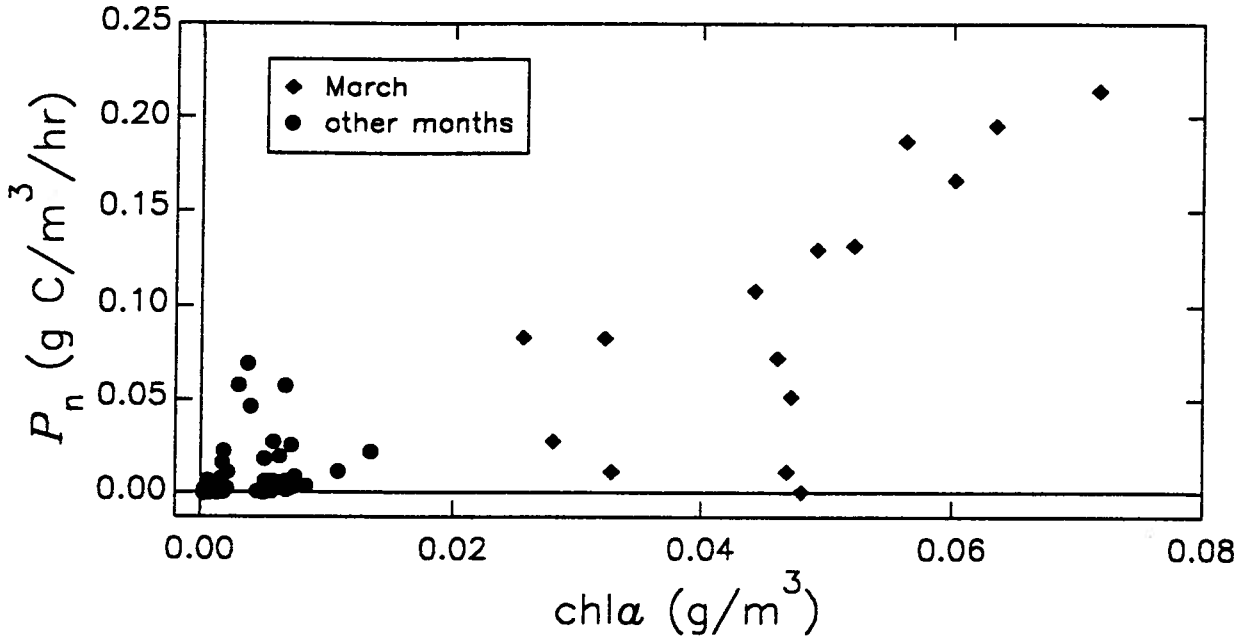

Figure 3.10: Hourly estimates of P_n vs. chl$a$ concentration.

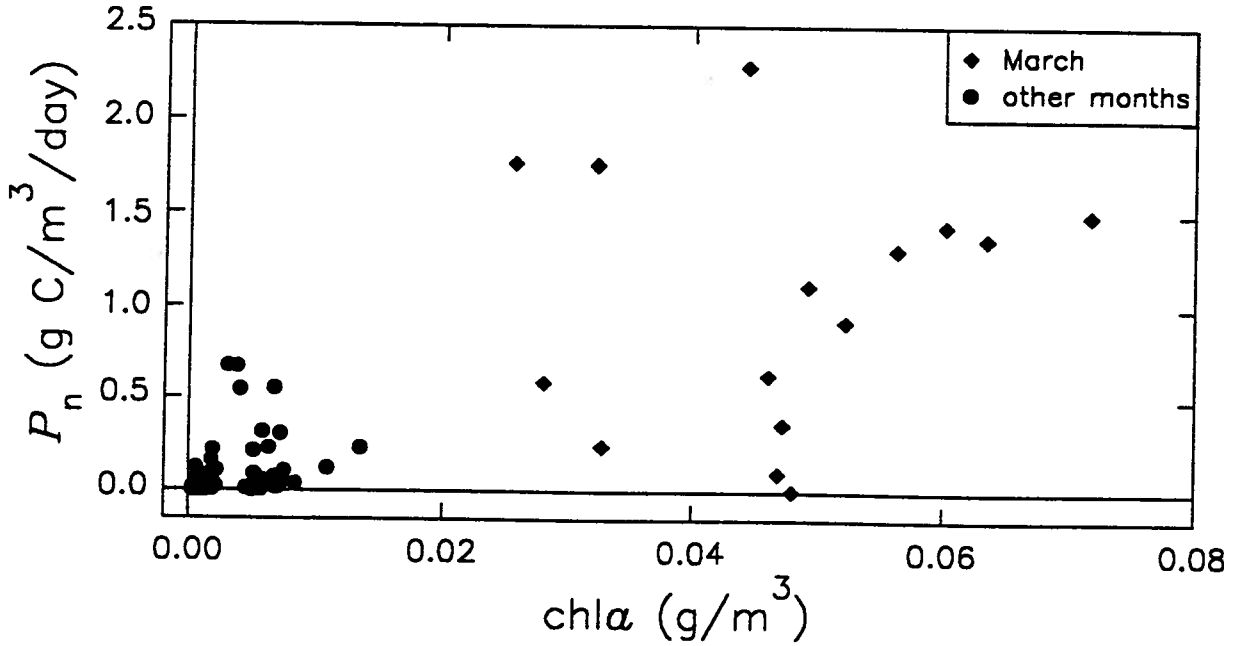

Figure 3.11: Daily estimates of P_n vs. chl$a$ concentration.

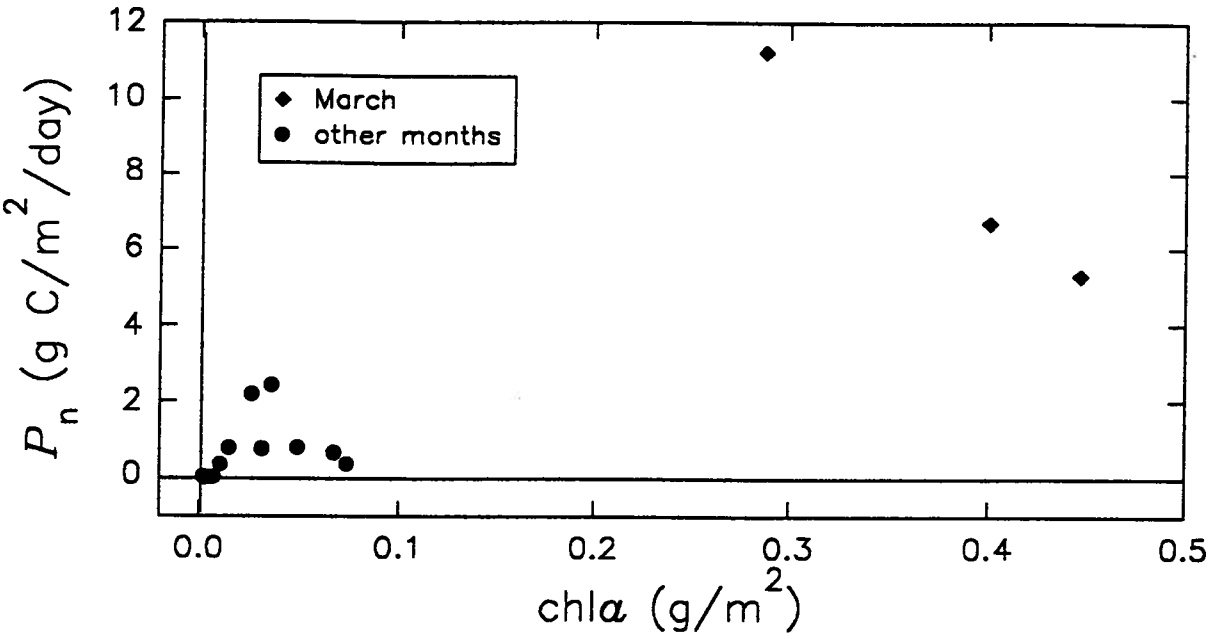

Figure 3.12: Depth integrated daily estimates P_n vs. chl$a$ concentration.

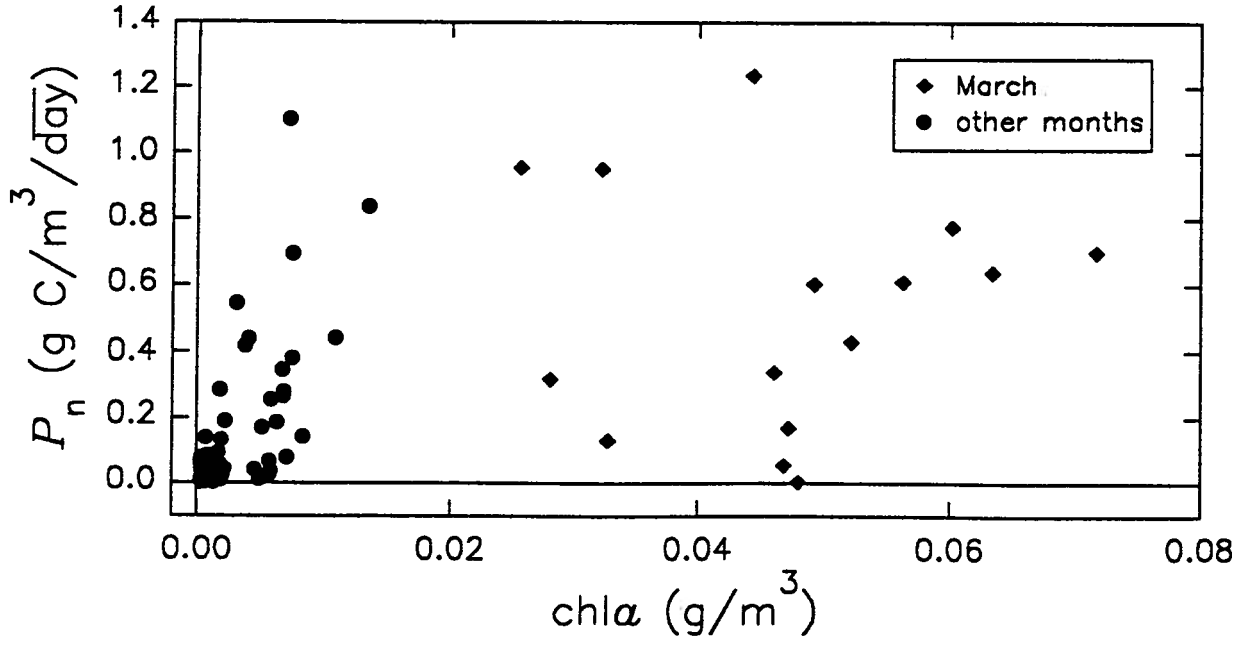

Figure 3.13: P_n adjusted to average daily irradiance vs. chl$a$ concentration.

of a ^{14}C incubation may not be acclimated to *in situ* light but instead to the average light field through which it has recently been mixed. Furthermore, total water column integrated chl*a* concentration may be expected to respond to total water column integrated irradiance. Both chl*a* and P_n have been integrated over the depth of the euphotic zone and plotted in figure 3.12. However, this consideration does little to improve upon the correlation between chl*a* and P_n as presented in figures 3.10 and 3.11. Worthy of note in figure 3.12 are the very high rates of primary productivity measured in March.

Despite the uncertainties caused by mixing and the fact that chl*a* was not taken at the location of the ^{14}C experiments, a relationship between P_n and chl*a* at depth is sought for the Sechelt Inlet data set. The data of figure 3.11 are multiplied by the appropriate M value from table 2.5 to allow for sampling on days that were not representative of the average irradiance seen by a phytoplankton population. P_n adjusted to average daily radiation is plotted in figure 3.13. If the data from March are disregarded, then a linear relationship between chl*a* and P_n is observed in figure 3.13. Figures 3.7 and 3.9 suggest that on March 26 and 27, chl*a* concentrations in Sechelt Inlet were high enough to significantly attenuate light. Perhaps P_n was low relative to chl*a* concentrations because phytoplankton below the upper portion of the euphotic zone did not receive the proportional amount of light that was delivered to similar depths but on different sampling dates.

To reduce the scatter in figure 3.13, which may in part be due to vertical mixing of phytoplankton and to the translation of the chl*a* data to the P_n positions, chl*a* and P_n are integrated over the water column and plotted against each other in figure 3.14. Although the data are sparse, a fit is hypothesized that relies on the interpretation that the inlet was 'saturated' with chl*a* relative to light availability during the sampling period in March. The maximum capacity of photosynthesis (P_n^{max}) in Sechelt Inlet during the experiment of 5.3 g $C/m^2/\overline{day}$ is taken as the average of the two P_n values greater than

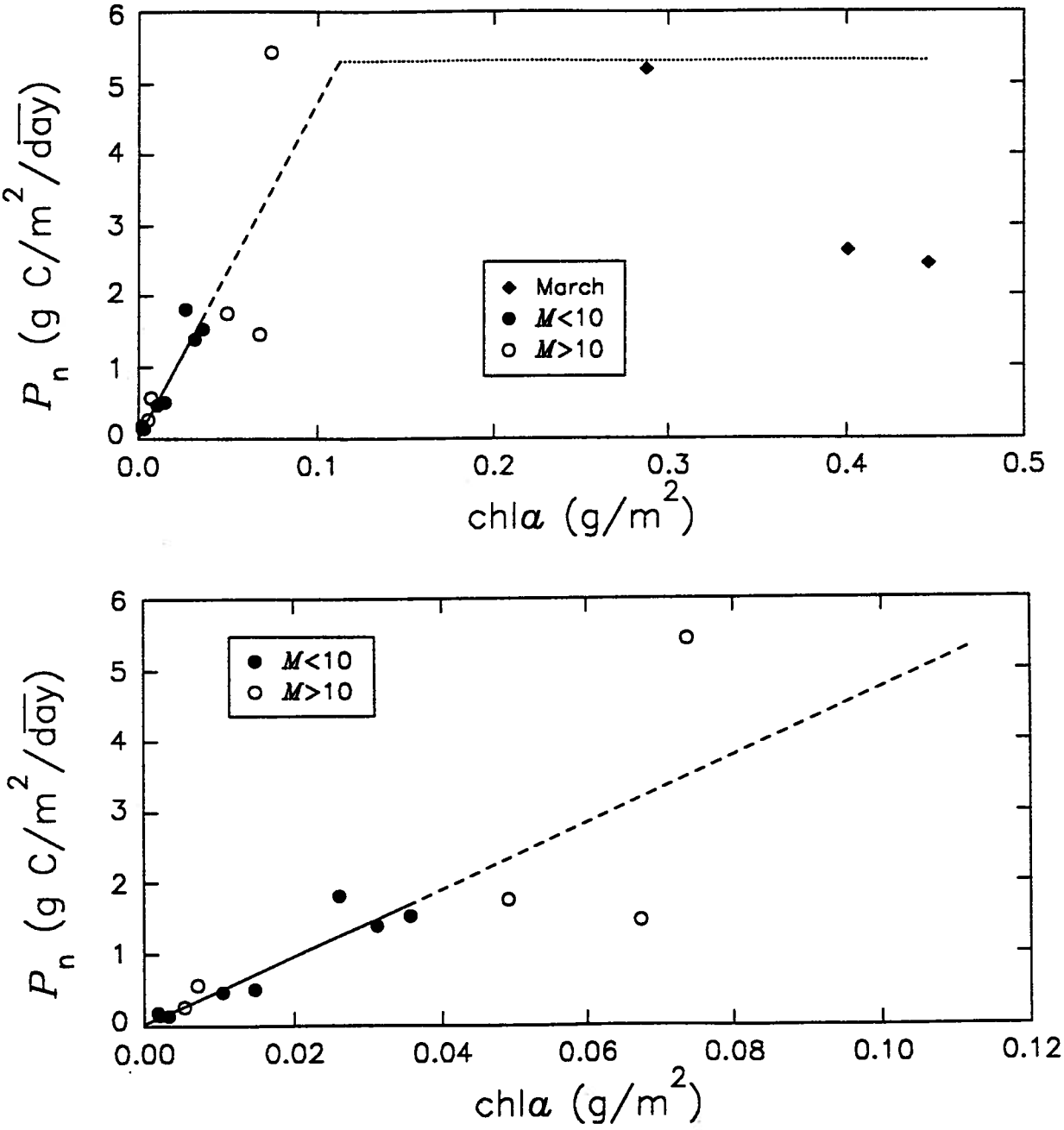

Figure 3.14: P_n with units (g C/m^2/$\overline{day}$) vs. chl$a$ concentration. The upper graph includes the entire data set while the lower graph depicts only its linear portion. The regression line, the determination of P_n^{max} and the differentiation between $M < 10$ and $M \geq 10$ are described in the text.

regressed data	Υ day^{-1}	SE of Υ day^{-1}	SE of P_n g $C/m^2/day$	y-int g $C/m^2/day$	n	r^2
all data	48	9.5	0.85	0.01	13	0.69
M < 10	48	7.0	0.26	0.06	8	0.88

Table 3.1: Solutions of regressions performed on the linear portion of figure 3.14 with and without the data for which $M \geq 10$. The values for Υ are the same for both regressions. SE is the standard error, y-int is the intercept, n is the number of data and r^2 is the degree of fit for the regression.

5 g $C/m^2/\overline{day}$. The initial slope of the relationship between net primary production and chl*a* is determined by a regression through the data set excluding the March samples (table 3.1).

The Campbell-Stokes Sunshine Recorder is insensitive to PAR and particularly so on cloudy days (e.g. on June 22, zero 'actual sunlight hours' were recorded). As 'actual sunlight hours' approach zero for a given day, M unrealistically approaches ∞. The data in figure 3.14 representing samples from 'dark' days may be over-corrected, so data for which $M \geq 10$ are separated from those for which $M < 10$. This threshold for M is chosen by examining table 2.5, where $4 > M < 1/4$ except for several values of $M \geq 10$. (Two ^{14}C incubations from June 22, for which zero 'actual sunshine hours' were recorded, are included with the set of data for which $M \geq 10$. The value of $M = 2.1$ for June 22 was obtained by comparison of its total integrated light {using equation 2.1 and irradiance values from table 2.3} with that from June 23, which recorded 3.1 'actual sunlight hours'.) Table 3.1 gives the results of regressions performed with and without the data for which $M \geq 10$.

Despite the limitations of the data used to create figure 3.14, its similarity with saturation curves is striking. The x-axis of most saturation curves in phytoplankton ecology is substrate, while the y-axis is a measure of growth normalized to biomass.

It is hypothesized that the relationship of figure 3.14 is a saturation curve for the phytoplankton population of Sechelt Inlet. The population's substrate was chl*a* and was saturating at concentrations of about 0.11 g/m^2 during the experiment (figure 3.14).

3.4 Discussion: Predicted changes in Υ

If Υ is a constant, C:chl*a* and μ must covary in an inverse linear manner (equation 3.5). Sakshaug *et al.* (1989) presented a large data set that describes the response of *Skeletonema costatum* at steady state growth to variations in light and nutrients. Those data are presented in table 3.2. The data are organized into groups with identical light regimes, but within each group nitrate concentrations vary. Relative degrees of nitrate availability are represented by the C:N ratio of each culture. C:N increases as nitrate availability decrease. The light regimes differ in both daylength (D_s = {hrs light}/{24 hrs}) and light intensity. For the first entry in each light regime (nutrient replete cultures), Sakshaug *et al.* (1989) calculated μ from equations for growth (Sakshaug and Andersen, 1986) instead of reporting measured values of μ. Υ for the data where μ is calculated instead of measured is systematically higher than other data in each light regime and is not included. The boldface entry in the heading of each group is the average of the Υ values reported for that group. The original table by Sakshaug *et al.* (1989) reports μ (day^{-1}), chl*a*, carbon and nitrogen per cell (pg) and the chl*a*:C ratio, as well as the light condition of each group. Those data used to calculate C:N, C:chl*a* and Υ are given in table 3.2.

Sakshaug *et al.* (1989) recognized that if the light regime is held constant, C:chl*a* linearly increases while μ linearly decreases with decreasing nitrate availability. In the context of this work, table 3.2 shows that Υ is rather constant within each light regime, and therefore independent of nitrate availability. Sakshaug *et al.* (1989) also observed

μ day^{-1}	chl*a* $\frac{pg}{cell}$	C $\frac{pg}{cell}$	C:N $\frac{pg}{pg}$	C:chl*a* $\frac{pg}{pg}$	Υ day^{-1}	μ day^{-1}	chl*a* $\frac{pg}{cell}$	C $\frac{pg}{cell}$	C:N $\frac{pg}{pg}$	C:chl*a* $\frac{pg}{pg}$	Υ day^{-1}
(i)	I = 1200 $\mu E/m^2/s$, $D_s = 1$				**170**	(ii)	I = 100 $\mu E/m^2/s$, $D_s = 1$				**58**
1.4	0.19	21	6.4	110		1.4	0.57	28	6.4	48	
1.1	0.12	17	8.9	140	160	1.1	.26	11	9.2	42	46
0.96	0.078	12	11	160	160	0.96	0.26	13	9.3	50	49
0.72	0.051	12	12	230	170	0.71	0.11	9.6	15	91	65
0.56	0.027	9.0	13	330	190	0.55	0.11	12	16	120	64
0.39	0.028	11	14	370	140	0.39	0.084	11	15	130	49
0.22	0.014	11	18	830	180	0.24	0.035	11	16	320	77
(iii)	I = 600 $\mu E/m^2/s$, $D_s = 0.58$				**56**	(iv)	I = 100 $\mu E/m^2/s$, $D_s = 0.58$				**28**
1.4	0.39	23	6.4	59		1.1	0.68	28	6.4	40	
0.90	0.20	12	6.7	59	53	0.88	0.37	13	6.2	36	31
0.71	0.11	11	9.2	91	65	0.70	0.24	11	7.3	43	30
0.49	0.072	8.2	9.2	110	56	0.50	0.15	8.0	8.7	53	26
0.36	0.069	9.9	11.1	140	52	0.35	0.12	9.4	11	83	29
0.27	0.051	10	12.2	200	54	0.22	0.070	7.9	12	110	25
(v)	I = 600 $\mu E/m^2/s$, $D_s = 0.25$				**27**	(vi)	I = 100 $\mu E/m^2/s$, $D_s = 0.25$				**16**
0.87	0.51	23	6.4	45		0.61	0.69	28	6.2	42	
0.71	0.34	13	7.6	38	27	0.51	0.34	11	11	33	17
0.48	0.17	11	13	63	30	0.33	0.20	9.6	12	48	16
0.33	0.12	8.9	15	77	25	0.24	0.16	9.7	17	63	15
(vii)	I = 71 $\mu E/m^2/s$, $D_s = 1$				**27**	(viii)	I = 12 $\mu E/m^2/s$, $D_s = 1$				**11**
1.2	0.62	29	6.3	45		0.53	0.92	34	6.2	37	
0.89	0.56	21	7.8	37	33	0.52	0.57	14	7.0	24	13
0.69	0.28	11	9.2	42	29	0.51	0.64	14	6.1	22	11
0.53	0.22	13	9.3	59	31	0.43	0.44	15	9.4	33	14
0.37	0.11	7.5	11	67	25	0.35	0.36	12	7.5	32	11
0.35	0.14	11	13	77	27	0.25	0.28	11	10	40	10
0.19	0.081	7.5	9.9	91	17	0.24	0.19	7.1	9.5	37	9.0
(ix)	I = 41 $\mu E/m^2/s$, $D_s = 0.58$				**11**	(x)	I = 12 $\mu E/m^2/s$, $D_s = 0.58$				**5.8**
0.80	0.76	30	6.3	40		0.38	0.86	37	6.3	43	
0.50	0.45	12	8.0	26	13	0.28	0.74	19	5.3	25	7.0
0.41	0.40	15	8.3	38	16	0.22	0.39	10	7.1	26	5.6
0.37	0.36	9.7	8.1	27	10	0.20	0.48	13	8.1	28	5.6
0.20	0.22	9.0	11	42	8.0	0.11	0.22	14	12.7	63	6.9
0.10	0.12	12	12	100	10	0.10	0.19	7.7	7.7	40	4.0

Table 3.2: Υ and C:N for *Skeletonema*. Reproduced from Sakshaug *et al.* (1989).

that both C:chl*a* and μ increase with increases in the total amount of light per day (by increasing either I or D_s), as made clear by the very large changes in Υ between groups in table 3.2.

Seeing that C:chl*a* and μ inversely and linearly covary with nitrate availability (Υ is independent of nitrate availability), Sakshaug *et al.* (1989) described phytoplankton growth with a mechanistic equation that ignores nutrients. The exclusion of nutrients is a great simplification from previous attempts to mechanistically model primary production (Cullen, 1990). Slightly rearranged, the equation from Sakshaug *et al.* (1989) is:

$$(\mu + \mathrm{r})\,\mathrm{C} : \mathrm{chl}a = \mathrm{D_s}\,\mathrm{a_c}\,\phi_{\max}\,\frac{1 - \mathrm{e}^{\sigma\,\tau\,\mathrm{I}}}{\sigma\,\tau} \tag{3.6}$$

where

- (μ+r) is the gross growth rate (s^{-1}). r is phytoplankton respiration and extracellular excretion rate. Sakshaug *et al.* (1989) use r = 0.12μ so that (μ+r) = 1.12 μ. Dividing equation 3.6 by 1.12 gives Υ as defined in equation 3.5.
- D_s is the fraction of the illuminated period of the day and is dimensionless.
- I is the quantum scalar irradiance of PAR ($mol/m^2/s$).
- a_c is the specific absorption coefficient of chl*a* (m^2/mol chl*a*).
- ϕ_{max} is the maximum quantum yield (mol C/mol photons).
- σ is the mean absorption cross-section of the photosynthetic unit (m^2/mol PSU).
- τ is the minimum turnover time of the rate-limiting photosystem (s).

Sakshaug *et al.* (1989) conceded that a_c, ϕ_{max}, σ and τ cannot be determined independently. However, the products (a_c ϕ_{max}) and (σ τ) were solved for their data and found to behave as constants. They concluded that μ can be determined with knowledge

of daylength, irradiance and C:chl*a*. This analysis shows that, for *Skeletonema costatum*, Υ can be predicted knowing only daylength and light intensity. Both daylength and light intensity changed between January and June in Sechelt Inlet, yet the linear portion of figure 3.14 suggest that Υ was constant during the study period. Three explanations for the predicted consistency of Υ in Sechelt Inlet are:

1. The data set is too small and errors in data analysis too large to see variations in Υ.

2. The light regime during the study period did not change as much as that for the experiments of Sakshaug *et al.* (1989), lessening the expected range in Υ.

3. The physiological adaptations of a_c, ϕ_{max}, σ and τ may vary among classes and even species of phytoplankton in such a way that light dependent changes in Υ predicted for monospecific cultures are dampened by species succession. During the study period, species other than *Skeletonema costatum* and at times classes other than diatoms made up a significant part of the phytoplankton population.

Without doing experiments designed to better understand the nature of Υ for multispecific populations of phytoplankton in field settings, a proper critique of the results from Sechelt Inlet cannot be made. However, of the light regimes of table 3.2, groups (iii) and (iv) with Υ values of 56 and 28/day, respectively, are possibly the most applicable to the conditions in Sechelt Inlet during the study period (see tables 2.2 and 2.3). The solution of $\Upsilon = 48$/day (table 3.1) suggests that the use of the factors D and M have produced reasonable estimates of daily photosynthetic carbon assimilation during the experiment in Sechelt Inlet.

3.5 Chapter summary

A method to predict photosynthetic carbon assimilation from measurements of chl*a* and estimates of Υ has been presented. A relationship between chl*a* and P_n is found only if P_n is corrected for the possibility that sampling occurred on a day that did not provide irradiance typical of that during the growth of *in situ* phytoplankton. An improved correlation is found despite imperfect estimates of both daily integrated irradiance on the days of ^{14}C incubations (the factor D) and the average irradiance during the growth of the phytoplankton population (the factor M), and despite the lack of correspondence between P_n and chl*a* data.

Knowledge of Υ is essential for the predictive model of net primary production developed in this chapter. Evidence has been presented that although Υ does not change with nutrient availability, it does decrease for decreasing amounts of light for monospecific cultures (Sakshaug *et al.*, 1989). Nevertheless, Υ is found to be relatively constant over a five month period in Sechelt Inlet providing that chl*a* concentrations were low enough that light attenuation was not severe.

The method to predict photosynthetic carbon assimilation used in this chapter raises a number of questions and research possibilities. Would more appropriate measures of irradiance during the development of a phytoplankton population improve the determination of Υ? What is the best length of time to consider for a population's growth period? Does the length of the growth period change with ecological variations?

A relatively simple and potentially important experiment would be to study Υ for a number of phytoplankton grown in the laboratory under the conditions in which they commonly dominate in the oceans. Is there a preferable range for Υ in nature or does it vary as light availability changes and species succession proceeds?

Chapter 4

Photosynthetic Oxygen Production

4.1 Introduction

Carbon assimilation can be converted to oxygen production, since the general equation for photosynthesis shows that one mole of oxygen is evolved per mole CO_2 assimilated.

$$nCO_2 + nH_2O + h\nu \longrightarrow nCH_2O + nO_2 \tag{4.1}$$

In this chapter, stoichiometric deviations from equation 4.1 and the effects of phytoplankton respiration on oxygen production are discussed. A rate of oxygen production per carbon assimilation is given and a model profile is provided with which to distribute photosynthetic oxygen production within the euphotic zone. Finally, a two year data set of chl*a* concentrations in Sechelt Inlet is presented. From these data, daily carbon assimilation and oxygen production throughout the year can be estimated.

4.2 Converting photosynthetic carbon assimilation into oxygen production

The 1:1 stoichiometric relationship between CO_2 fixation and O_2 evolution during photosynthesis holds true for carbohydrate formation, but more highly reduced lipids and proteins require extra energy to be produced (Ryther, 1956b). Furthermore, equation 4.1 assumes that the nitrogen substrate for phytoplankton growth is completely reduced. The assimilation of oxidized nitrate and nitrite instead of reduced ammonium again increase the energy required per mole CO_2 fixation (Ryther, 1956b). Nor does equation

4.1 consider algal respiration, yet this process must be described to properly estimate the oxygen released by a phytoplankton population.

4.2.1 The photosynthetic quotient

Gross photosynthetic carbon assimilation is converted to oxygen production with the use of the photosynthetic quotient.

$$^{O_2}P_g = {}^{C}P_g \left(\frac{\Delta O_2}{-\Delta CO_2}\right)_{PQ} \tag{4.2}$$

$^{O_2}P_g$ and $^{C}P_g$ refer to gross photosynthetic oxygen production and gross photosynthetic carbon assimilation, respectively. $(\Delta O_2/\text{-}\Delta CO_2)_{PQ}$ is the photosynthetic quotient (PQ). Equation 4.2 is on a molar basis.

The photosynthetic quotient varies with the form of nitrogen substrate used by a phytoplankton population. For nitrate-grown cells, PQ is 1.3 to 1.4, while the same population grown on ammonium will exhibit a PQ of 1.1 to 1.2 (Laws, 1991). Haigh *et al.* (1992) reported that nitrate in surface waters drops below levels that are considered limiting for diatoms at inner stations of Sechelt Inlet for periods during the late spring, summer and fall. Ammonium is the preferential nitrogen substrate for phytoplankton and although ammonium utilization is likely especially when nitrate concentrations are low, the degree of continual nitrate supply via estuarine entrainment of deeper water into the euphotic zone of Sechelt Inlet has not been estimated. Ryther (1956b) suggested that a PQ of 1.25 be used for natural populations of phytoplankton. This value is mid-way between the range for nitrate- and ammonium-grown cells as reported by Laws (1991) and is the value chosen for use with the Sechelt Inlet data. Potential errors when predicting photosynthetic oxygen production caused by this choice of PQ are of the order of 10%.

4.2.2 The respiratory quotient

Equation 4.2 provides the oxygen production of gross photosynthetic carbon assimilation. To estimate oxygen production for net carbon assimilation, the respiratory quotient for phytoplankton must be considered.

$$^{O_2}R = {}^{C}R \left(\frac{-\Delta O_2}{\Delta CO_2}\right)_{1/RQ} \tag{4.3}$$

Here ^{O_2}R and ^{C}R refer to respiratory oxygen consumption and organic carbon oxidation, respectively. $(-\Delta O_2/\Delta CO_2)_{1/RQ}$ is the inverse of the respiratory quotient (RQ). Equation 4.3 is in terms of moles.

To convert net carbon assimilation into net oxygen production, P_n is first written in terms of oxygen.

$$^{O_2}P_n = {}^{O_2}P_g - {}^{O_2}R \tag{4.4}$$

Next, $^{O_2}P_g$ and ^{O_2}R are substituted using equations 4.2 and 4.3.

$$^{O_2}P_n = {}^{C}P_g\,(PQ) - {}^{C}R\left(\frac{1}{RQ}\right) = {}^{C}P_n\,(PQ) + ({}^{C}P_g - {}^{C}P_n)\,(PQ) - {}^{C}R\left(\frac{1}{RQ}\right) \tag{4.5}$$

$^{C}P_g - {}^{C}P_n$ and ^{C}R are quantitatively the same by definition, but they differ physiologically in that one is photosynthetically assimilated inorganic carbon and the other is respired organic carbon. Equation 4.5 is the proper description of net photosynthetic oxygen production. It is simplified if PQ = 1/RQ, as the last two terms in equation 4.5 cancel each other.

RQ for phytoplankton is roughly 0.8 to 0.9 (Kremer, 1981) and its inverse is 1.1 to 1.25. This is very close to the value of 1.25 chosen for use with the Sechelt Inlet data. Thus, although photosynthesis and respiration are physiologically very different, they counter-balance each other in equation 4.5; the amount of oxygen that is produced during the photosynthetic reduction of a mole of inorganic carbon is consumed as a mole

of reduced carbon is oxidized. Equation 4.5 is simplified.

$$^{O_2}P_n = {}^{C}P_n\,(PQ) \tag{4.6}$$

4.2.3 Respiration at night

Phytoplankton consume some of the energy they produce during photosynthesis through a number of processes generalized under two types of respiration. Photorespiration (R_P) occurs during photosynthesis and reduces oxygen to water during the enzymatic phase of light driven ATP formation. Phytoplankton dark respiration (R_D) is similar to heterotrophic respiration in that it is required for cellular growth, maintenance and motility. Dark respiration is not dependent on photosynthesis, and occurs throughout the 24 hour day (Raven and Beardall, 1981).

Both photo- and dark respiration occurring during the day are accounted for by ^{14}C uptake measurements if in fact ^{14}C incubations are estimates of P_n rather than P_g. However, the temporal integration of carbon assimilation over the period of a day includes the dark hours of night, during which time photorespiration does not occur but dark respiration continues.

Dark respiration consumes 5 to 50% of P_g depending on the class of phytoplankton being considered (Raven and Beardall, 1981). Flagellated species have higher energy requirements and therefore higher dark respiration rates than non-motile classes of phytoplankton (Raven and Beardall, 1981; Parsons et al., 1984b). If it is assumed that dark respiration is constant throughout the 24 hr day, then 2.5 to 25% of photosynthate is consumed by phytoplankton at night for a light/dark day of 12 hrs/12 hrs. Therefore, measurements of daytime photosynthetic carbon assimilation used to represent a 24 hour period might be over-estimates by as much as 25%.

Although this observation is made, quantification of dark respiration at night is not

included in this work for two reasons. First, the time dependent interactions between dark respiration, photosynthesis and nitrogen assimilation are not clearly understood (Turpin and Weger, 1990). Furthermore, a phytoplankter's rate of dark respiration changes dramatically with variations in light and nutrient history, as well as *in situ* light and nutrients (P.J. Harrison, personal communication). Second, non-motile diatoms were the dominant class of phytoplankton for much of the study period in Sechelt Inlet and are expected to have low rates of dark respiration. Flagellated phytoplankton have higher rates of dark respiration, and are dominant in Sechelt Inlet at times in the summer and winter (Haigh *et al.* 1992). However, there are neither ^{14}C uptake measurements nor proper estimates of Υ for those periods. Errors incurred by applying an approximation of Υ to chl*a* data for a period when diatoms are not dominant are likely to be large enough to make adjustments for night-time respiration for flagellated phytoplankton unnecessary.

4.3 A model vertical profile for photosynthetic oxygen production

If net carbon assimilation ($^{C}P_{n}$) is known, then equation 4.6 can be written as:

$$^{O_2}P_{n}\ (g/m^2/day) = {}^{C}P_{n}\ PQ\ \frac{32}{12} = 3.3\ {}^{C}P_{n}\ (g/m^2/day) \tag{4.7}$$

where a photosynthetic quotient of 1.25 is used and the fraction 32/12 converts equation 4.6 from moles to grams.

If $^{C}P_{n}$ is not known, then it can be written in terms of chlorophyll *a*. Equation 3.5 states that $^{C}P_{n} = \Upsilon$ chl*a*, and Υ was found to be 48/day for the study period in Sechelt Inlet. Therefore, equation 4.6 can also be written as:

$$^{O_2}P_{n}\ (g/m^2/day) = \Upsilon\ chla\ PQ\ \frac{32}{12} = (160/day)\ chla\ (g/m^2) \tag{4.8}$$

The formulations of equations 4.8 and 4.7 estimate oxygen production per m^2 of the euphotic zone but do not describe the vertical distribution of oxygen production in

the euphotic zone. The only way to model photosynthetic oxygen production with depth from the results of equations 4.8 and 4.7 is to empirically distribute it throughout the euphotic zone. The profiles of figures 3.1 through 3.6 are used to do so.

In general, the maximum carbon assimilation occurred at the surface over a small depth range during the experiment, and although P_n usually decreased with depth, it did not do so in a predictable way. For an empirical profile of oxygen production, ${}^{O_2}P_n$ is chosen to be constant from the surface to 1 m depth, and then to decrease exponentially with depth to 9 m (figure 4.1).

$$ {}^{O_2}P_n \text{ (g/m}^2\text{/day)} = {}^{O_2}P_{n_0} \left(e^{-k(1\,m)} + \int_{1\,m}^{9\,m} e^{-kz} dz \right) \tag{4.9} $$

This equation describes the profile of figure 4.1. ${}^{O_2}P_{n_0}$ is the multiplicative constant of the exponential function and ${}^{O_2}P_{n_0}\ e^{-k(1\,m)}$ is the maximum photosynthetic oxygen production (${}^{O_2}P_n^{max}$) in g/m^3/day and occurs over the upper 1 m of the water column.

The total depth of 9 m for the integration in equation 4.9 is chosen because that was approximately the average depth of the deepest samples collected for ^{14}C incubations. However, ^{14}C uptake was usually positive and often significant for ^{14}C incubations on the deepest samples (tables 2.2 and 2.3), so the possibility that photosynthetic oxygen production occurred below 9 m must be considered. For the purpose of numerical simulations, the profile of equation 4.9 could be extended to the 1% light level, often considered the base of the euphotic zone (Parsons *et al.*, 1984b). Using the integrated extinction coefficients of light (K_{int}) from figures 3.1 through 3.6, the average 1% light level during the experiment in Sechelt Inlet was at 17 m. It is emphasised that whether or not this extension is made, estimates of ${}^{O_2}P_n$ (g/m^2/day) must be for the depth interval from which ${}^{C}P_n$ has been made.

A value of k must be chosen for equation 4.9. The depth at which $P_n = (P_n^{max}/e)$ is in the range of 3 to 5 m in figures 3.1 through 3.6, so 4 m is chosen. Because the

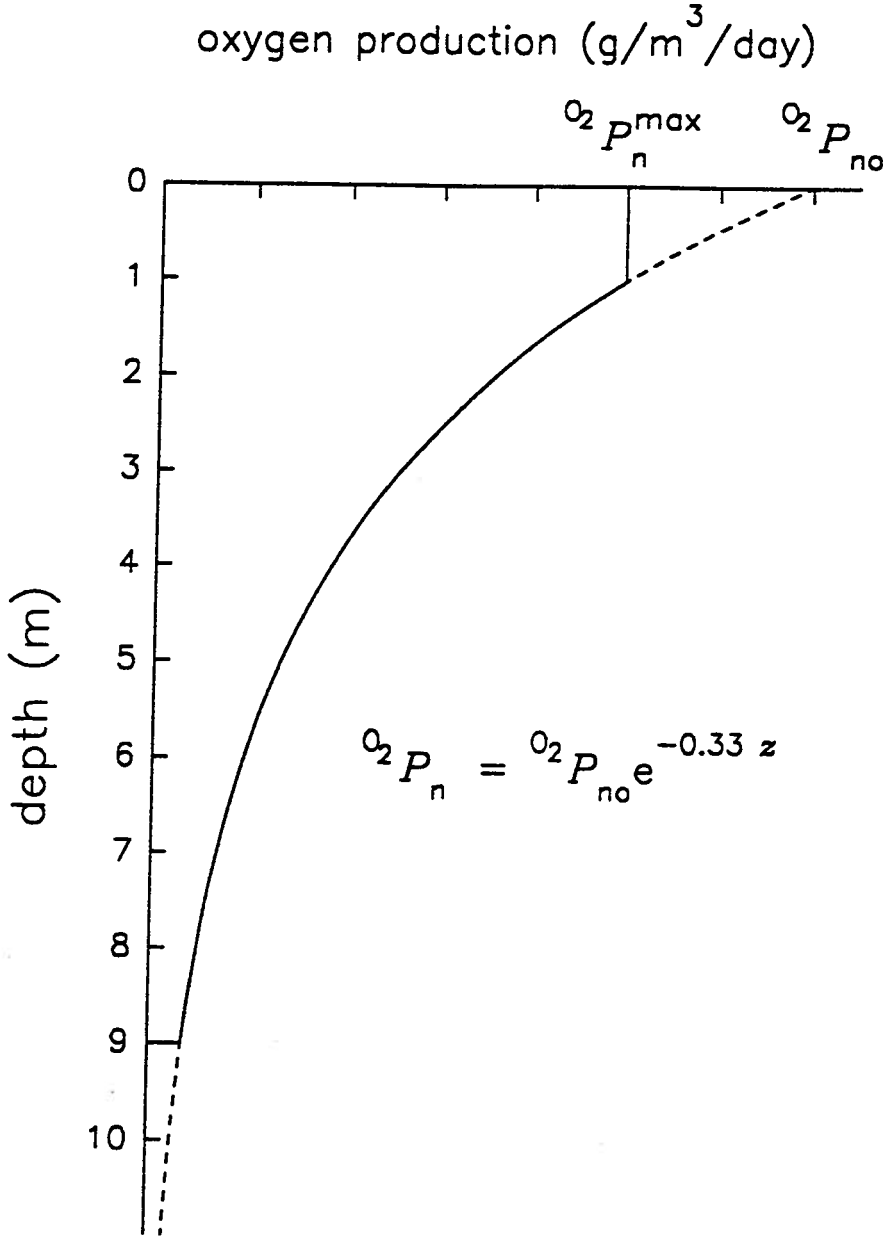

Figure 4.1: Empirical profile for photosynthetic oxygen production. The shape of the profile and the chosen depth to which it extends is explained in the text. $^{O_2}P_{n_0}$ is the multiplicative constant of the exponential function chosen to describe the vertical distribution of photosynthetic oxygen production. $^{O_2}P_n^{max}$ is the maximum realized photosynthetic oxygen production. The possibility that this profile should extend below 9 m for numerical simulations of photosynthetic oxygen production is discussed in the text.

maximum oxygen production in the empirical profile extends to 1 m depth, $1/k$ must be 3 m ($k = 0.33$/m) for ${}^{O_2}P_n$ to be (${}^{O_2}P_n^{max}$/e) at 4 m.

4.4 Two years of chl*a* data from Sechelt Inlet

As part of an ecological survey of Sechelt Inlet, chl*a* data were collected at stations SC-2 through SC-6 on a monthly basis from May 1988 to September 1990 (Haigh *et al.*, 1992). The method of collection was the same as described in chapter 2 of this thesis. These data are presented in figure 4.2 and can be used to estimate daily photosynthetic oxygen production throughout the year in Sechelt Inlet. The solid line in figure 4.2 is determined by taking the average chl*a* concentration for each month and linearly interpolating between months. The discontinuity around March requires explanation.

In chapter 3, it is hypothesized that ${}^{C}P_n$ is limited by the availability of irradiance when chl*a* concentrations exceed 0.11 g chl$a$/m^2 in Sechelt Inlet. This value is considered to be dependent upon meso-scale solar radiation to the region, and so will change from season to season and from year to year. Nonetheless, for the two year data set of figure 4.2, March is the only time when the average chl*a* concentration is greater than 0.11 g/m^2, so March is considered to be the only period when ${}^{C}P_n$ is limited by the availability of irradiance because of light absorption by phytoplankton.

The chl*a* concentration is described as linearly increasing from the average in February to the average for March. However, ${}^{C}P_n$ and therefore oxygen production reaches a maximum at 0.11 g chl$a$/m^2 while chl*a* concentrations continue to rise. From the evidence of chl*a* data taken in March and April, chl*a* concentrations drop precipitously after March. To model the crash of the spring bloom, chl*a* concentrations immediately after March sampling are estimated as a step function and given the value sampled in April. This assumption affects estimates of oxygen production less than estimates of chl*a*

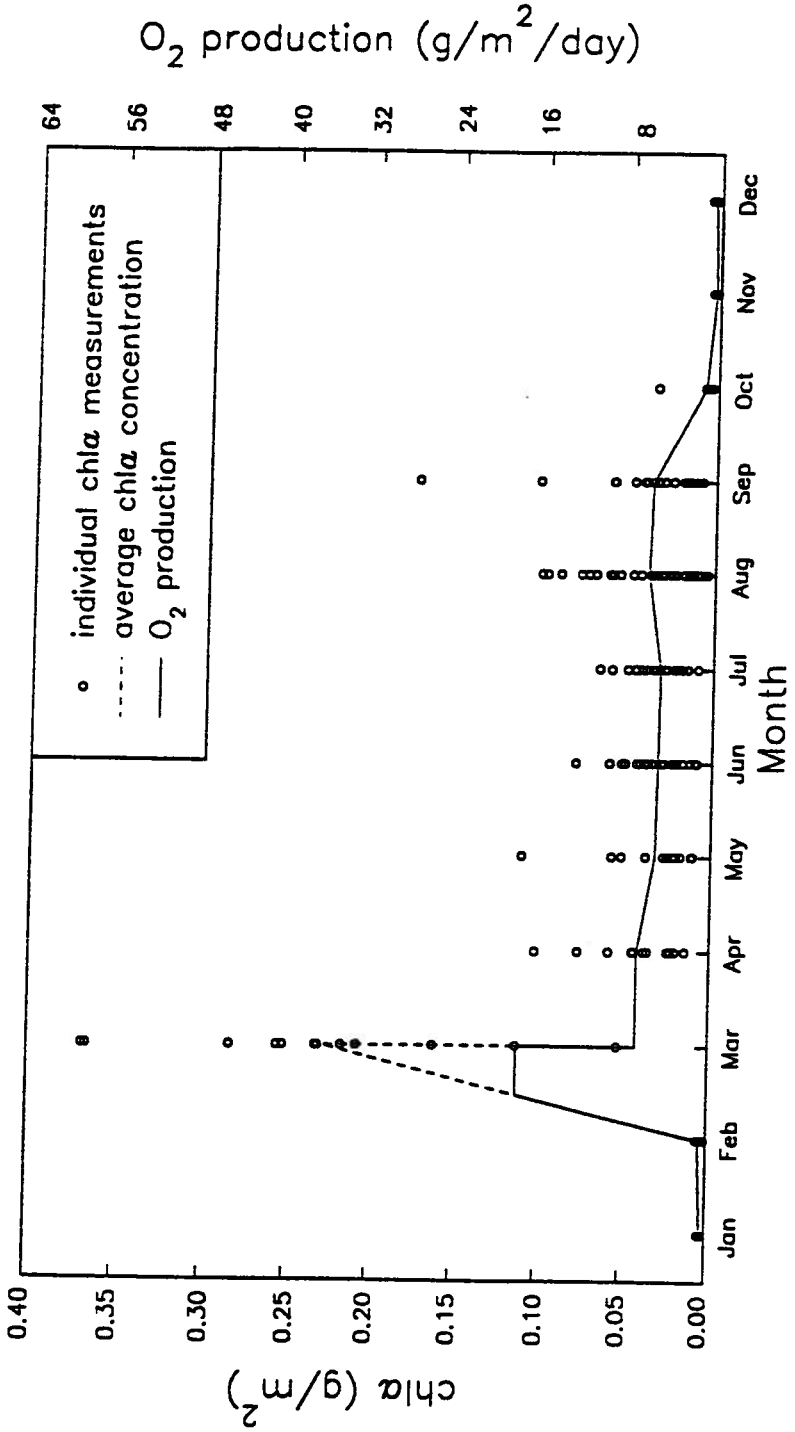

Figure 4.2: Chl*a* and daily photosynthetic oxygen production in Sechelt Inlet. The chl*a* data are from two years of collection where sampling occurred at six stations throughout the inlet. Oxygen production is determined by equation 4.8. Chl*a* and oxygen production diverge only during a brief period preceding maximum chl*a* concentrations of the spring bloom. Chl*a* and oxygen production are described by the same line following the crash of the spring bloom.

concentration because of the cap on P_n at 5.3 g/m^2/day and the corresponding cap on oxygen production at 18 g/m^2/day.

The two year data set of Haigh *et al.* (1992) can be used to estimate differences in oxygen production along channel in Sechelt Inlet if such resolution is needed.

4.5 Chapter summary

By using the photosynthetic quotient, measures of ${}^{C}P_n$ are extended to provide estimates of photosynthetic oxygen production in the euphotic zone of Sechelt Inlet. When necessary, the relationship between chl*a* and net carbon assimilation developed in chapter 3 can be used to approximate oxygen production. Although respiration by phytoplankton in the daytime should not cause large errors in estimates of oxygen production, respiration at night is potentially a sink of oxygen, but left as an unknown in this work. Calculations of oxygen production are per m^2 and are distributed in the water column with an empirical vertical profile for photosynthesis. A two year data set of chl*a* concentrations in Sechelt Inlet can be used to estimate daily oxygen production throughout the year.

The discussion of this chapter has not considered the consumption of organic carbon and oxygen by heterotrophic activity. Chapter 7 shows that heterotrophs may consume much of the organic carbon and oxygen that are produced by photoautotrophs, and therefore can have a large affect on net community production in the euphotic zone.

Chapter 5

Carbon Dynamics Below The Euphotic Zone In Sechelt Inlet

5.1 Introduction

In an effort to quantify the degradation of organic carbon within the pelagic zone using sediment trap data, a set of equations has been developed that quantifies water column decay of any measurable component (ς $\{g/m^2/day\}$) of the total material flux (Γ $\{g/m^2/day\}$). In the text, decay is meant to represent the dissolution of soluble material, the heterotrophic decomposition of organic matter and particle fragmentation.

The total total dry weight (TDW) of any marine sediment-trap sample may be considered as follows:

$$\text{TDW} = \text{organic matter} + \text{biogenic silica} + CaCO_3 + \text{lithogenous matter} \qquad (5.1)$$

Organic matter, or organic 'soft parts', are composed of lipids, proteins and carbohydrates; they may be of terrigenous or marine origin and they often make up a significant portion of the sediment flux in coastal waters. Biogenic silica and $CaCO_3$ are considered organic 'hard parts' because they occur as the result of protective structure formation by phytoplankton and zooplankton. Silica, in the form of diatom frustules, is often a large component of the total flux in Sechelt Inlet, while $CaCO_3$ generally makes up less than 1% of Γ. Organic matter, biogenic silica, and $CaCO_3$ may be expected to decrease in concentration while settling out of the pelagic zone through bacterial oxidation or chemical dissolution, while the lithogenous fraction of Γ is considered non-reactive, or refractory. All particles may fragment and/or aggregate while sinking (McCave, 1984).

The measurements of Γ, organic carbon, silica and $CaCO_3$ for the sediment trap samples from Sechelt Inlet are described in section 2.3. Of the variables in equation 5.1, Γ, silica and $CaCO_3$ are measured directly. Organic matter is determined from direct measurements of organic carbon and by assuming that the ratio of organic matter to organic carbon can be estimated by a constant. With measurements or estimates of all but the lithogenous flux in equation 5.1, the lithogenous flux can be approximated by difference (Γ - silica - organic matter - $CaCO_3$). These estimates of the lithogenous flux have a relatively large uncertainty because the errors in determinations of silica, organic matter and $CaCO_3$ are additive.

This chapter includes solutions for the decay of particulate organic carbon (POC), particulate organic nitrogen (PON), and for biogenic silica. The sediment trap algorithm presented in this chapter is also used on the refractory lithogenous flux in Sechelt Inlet. Because this portion of Γ is not expected to undergo appreciable decay in the water column, testing the algorithm on the lithogenous flux is a measure of the robustness of the algorithm; the decay of the lithogenous fraction of Γ should be negligible. The $CaCO_3$ data are not usable, perhaps because of partial or irregular dissolution in the high NaCl conditions of the sediment trap brine.

5.2 An algorithm to compute water column decay

5.2.1 Characteristic scales of decay

The time-dependent decay of ς may be written as

$$\frac{d\varsigma}{dt} = -k_t\,\varsigma \tag{5.2}$$

where t is time and $1/k_t$ (with units of time) is the characteristic time scale of decay for ς. If ς is sinking in the z direction (defined to be zero at the surface and positive

downward), then equation 5.2 can be written as

$$\frac{d\varsigma}{dz}\frac{dz}{dt} = -k_t\,\varsigma \tag{5.3}$$

where dz/dt is the sinking rate (sr). Then,

$$\frac{d\varsigma}{dz} = -\left(\frac{k_t}{sr}\right)\varsigma = -k_z\,\varsigma \tag{5.4}$$

In equation 5.4, $1/k_z$ (m) is the characteristic length scale of decay for ς. k_z is equal to k_t/sr (Walsh *et al.*, 1988a; Emerson in Banse, 1990) and is more easily measured than k_t from sediment trap studies where the flux of a constituent is estimated at specific depths, but sinking rates are uncertain. Furthermore, for the purpose of understanding the influence of sinking material on the water column, it is useful to know length scales of decay, regardless of k_t or sinking rates. If ς represents a constituent contained in material with a range of sinking rates and k_t for that constituent is or is not constant over a specific depth interval, then k_z is the average of k_t/sr for ς within a specified depth interval.

For the remainder of this chapter, all characteristic scales of decay will be those of length instead of time.

5.2.2 Reactive particle fluxes

If the decay constant of ς, k_ς, is constant between two depths, then integrating equation 5.4 gives

$$\varsigma = \varsigma_0\, e^{-k_\varsigma(z-z_0)} \tag{5.5}$$

z_0 and z are a reference depth and the depth at which ς is being determined, respectively. For two traps at depths z_1 and z_2,

$$\varsigma_1 = \varsigma_0\, e^{-k_\varsigma(z_1-z_0)} \tag{5.6}$$

$$\varsigma_2 = \varsigma_0 \, e^{-k_\varsigma (z_2 - z_0)} \tag{5.7}$$

Eliminating ς_0,

$$\varsigma_2 = \varsigma_1 \, e^{k_\varsigma (z_1 - z_0)} \, e^{-k_\varsigma (z_2 - z_0)} = \varsigma_1 \, e^{-k_\varsigma \Delta z} \tag{5.8}$$

where Δz is $z_2 - z_1$.

The formulation of equation 5.8 was used by Walsh *et al.* (1988a) to solve k_ς for sediment trap data from the North Equatorial Pacific.

5.2.3 The accountable and the unaccountable fluxes

Because of bacterial oxidation of organic matter and particulate dissolution, the flux of each constituent within Γ is expected to either decrease in mass or to remain constant while sinking below the euphotic zone. Equation 5.8 is therefore the basis for all computations of k_ς in the algorithm being developed. However, equation 5.8 ignores a very common complication of sediment trap experiments. It does not consider the apparent increase in material flux with depth recorded by many sediment trap deployments including that in Sechelt Inlet. (Possible causes of this flux increase with depth are discussed in section 5.4.)

Let both Γ and ς at the depth of a lower sediment trap consist of two components.

$$\Gamma_2 = \Gamma_{ac2} + \Gamma_{un2} \tag{5.9}$$

$$\varsigma_2 = \varsigma_{ac2} + \varsigma_{un2} \tag{5.10}$$

Γ_{ac} and ς_{ac} are accountable fluxes because they are representatively caught in a lower as well as an upper trap. It is the behavior of the accountable material flux of ς that is described by equation 5.8. Therefore,

$$\varsigma_{ac2} = \varsigma_1 \, e^{-k_\varsigma \Delta z} \tag{5.11}$$

Γ_{un} and ς_{un} in equations 5.10 and 5.11 are unaccountable fluxes. Although unaccountable fluxes are caught by deeper traps, they are not represented by material in upper traps.

If ς_{un} is considered to be introduced into the water column at the depth of the lower trap (and therefore its history of decay need not be described), then equation 5.10 can be rewritten using the relationship of equation 5.11.

$$\varsigma_2 = \varsigma_1 \, e^{-k_\varsigma \Delta z} + \varsigma_{un2} \tag{5.12}$$

Figure 5.1 provides a schematic of the accountable and unaccountable fluxes.

5.2.4 Solution equations for the sediment trap algorithm

k_ς cannot be obtained from equation 5.12 because of the term ς_{un2}. However, equation 5.12 can be solved by introducing Γ_{un} to quantify ς_{un}.

$$\varsigma_{un} = \frac{\varsigma_{un}}{\Gamma_{un}} \Gamma_{un} \tag{5.13}$$

The ratio $\varsigma_{un}/\Gamma_{un}$ is the fraction of ς in Γ_{un} and is dimensionless. Γ_{un} is quantified below, while $\varsigma_{un}/\Gamma_{un}$ is left as an unknown but solved in the sediment trap algorithm. Equations 5.12 and 5.13 are combined.

$$\varsigma_2 = \varsigma_1 \, e^{-k_\varsigma \Delta z} + \frac{\varsigma_{un2}}{\Gamma_{un2}} \Gamma_{un2} \tag{5.14}$$

k_ς can now be determined by solving equation 5.14, or some form of it. Two assumptions must be made: that k_ς is constant and that $\varsigma_{un}/\Gamma_{un}$ is constant. A statistical check of resulting solutions for k_ς and $\varsigma_{un}/\Gamma_{un}$ will reveal the degree to which these assumptions hold.

Estimation of Γ_{un}

Γ_{un} is the total material flux at a lower trap that is not represented at an upper trap. For traps that are vertically close together, Γ_{un} is dominated by the difference in flux between

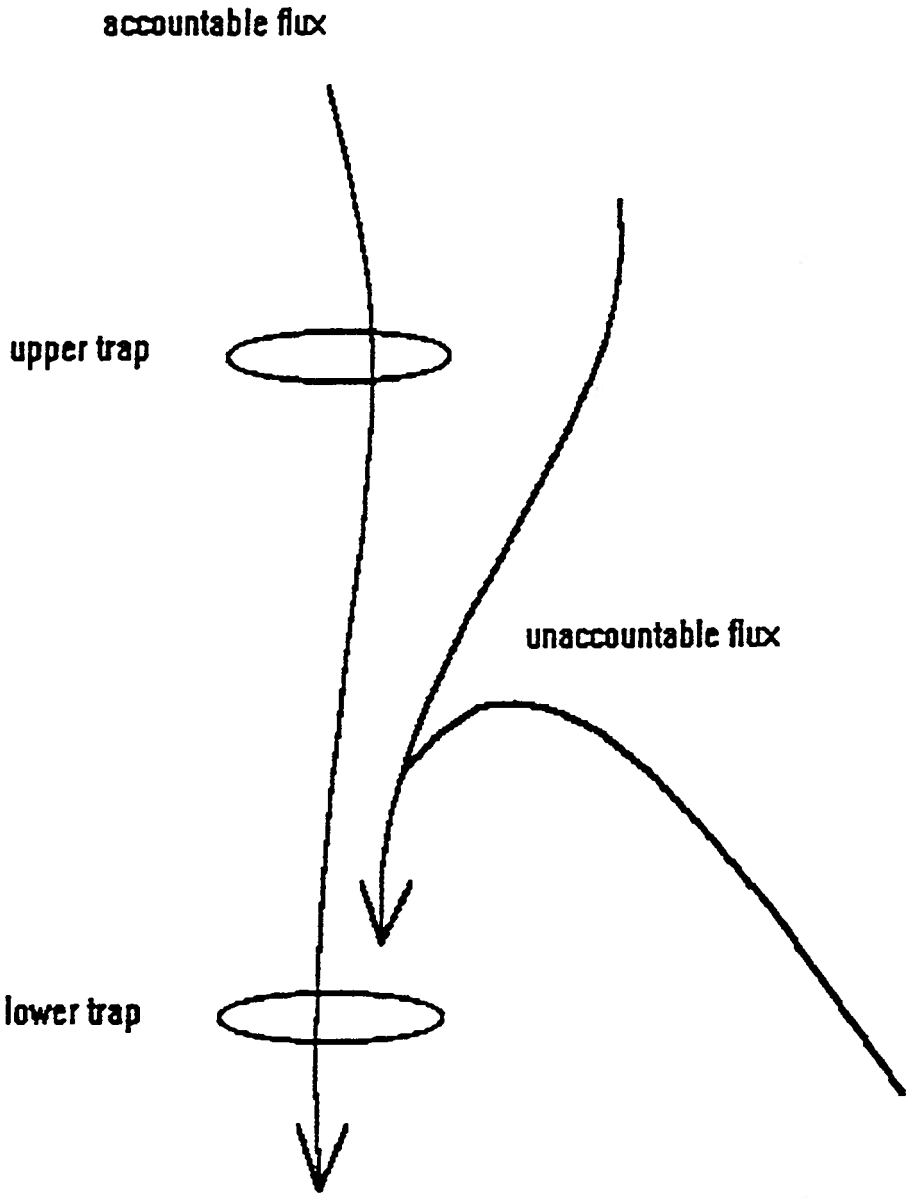

Figure 5.1: A schematic of the accountable and the unaccountable fluxes. The sources of *each* flux can be particles sinking from above, horizontally advected particles or turbulently resuspended material.

the two traps, Γ_2-Γ_1. However, as material passes from an upper trap to a lower one, it will decay somewhat, decreasing the accountable flux and causing the unaccountable flux to be greater than $\Gamma_2 - \Gamma_1$. Allowing for the decay of each constituent within the total flux,

$$\Gamma_{un2} = \Gamma_2 - \Gamma_1 + \sum_{\text{all } \varsigma} \varsigma_1 \left(1 - e^{-k_\varsigma \Delta z}\right) \tag{5.15}$$

The summation in equation 5.15 estimates the total decay of the accountable flux between depths of two sediment traps. Four components of the total material flux are recognized in section 5.1. The lithogenous component is not expected to decay. $CaCO_3$ makes up only about 1% of the total flux, and therefore its dissolution will not have a large effect on the computation of Γ_{un}.

The dissolution of silica and the degradation of organic matter are expected to be large enough so that they might influence equation 5.15. If the ratio of total organic matter to organic carbon is 2.7 by weight (section 2.3.5) and the degradation of organic matter and organic carbon are proportional, then equation 5.15 can be written to account for the degradation of organic matter and the dissolution of silica in the following way.

$$\Gamma_{un2} = \Gamma_2 - \Gamma_1 + 2.7\, C_1 \left(1 - e^{-k_c \Delta z}\right) + S_1 \left(1 - e^{-k_s \Delta z}\right) \tag{5.16}$$

C and S are the fluxes of organic carbon and silica, respectively. $1/k_c$ and $1/k_s$ are the characteristic length scales of decay for organic carbon and silica, respectively.

In a similar manner to equation 5.7, the total accountable flux to a lower sediment trap can be written.

$$\Gamma_{ac2} = \Gamma_1 - 2.7\, C_1 \left(1 - e^{-k_c \Delta z}\right) - S_1 \left(1 - e^{-k_s \Delta z}\right) \tag{5.17}$$

5.3 Application of the algorithm to the Sechelt Inlet data

5.3.1 Data from different depths considered together

Equations 5.14 and 5.16 are algebraically combined and applied to organic matter and to silica fluxes.

$$C_2 = C_1 \left(1 - 2.7\frac{C_{\text{un}}}{\Gamma_{\text{un}}}\right) e^{-k_c \Delta z} + \frac{C_{\text{un}}}{\Gamma_{\text{un}}} \left(\Gamma_2 - \Gamma_1 + 2.7C_1 + S_1 \left\{1 - e^{-k_s \Delta z}\right\}\right) \tag{5.18}$$

$$S_2 = S_1 \left(1 - \frac{S_{\text{un}}}{\Gamma_{\text{un}}}\right) e^{-k_s \Delta z} + \frac{S_{\text{un}}}{\Gamma_{\text{un}}} \left(\Gamma_2 - \Gamma_1 + 2.7C_1 \left\{1 - e^{-k_c \Delta z}\right\} + S_1\right) \tag{5.19}$$

Before equations 5.18 and 5.19 are used on the data from Sechelt Inlet, one more step is taken so that the entire data set can be considered together.

The analysis as described above requires a set of data from two traps, one above the other. In Sechelt Inlet, there are only four or five sets of data from each pair of traps. However, there are three moorings, each with three traps corresponding to three sediment trap pairs at each station: upper to middle, upper to lower and middle to lower. Overall, there are 39 sediment trap pairs from Sechelt Inlet. As a first approximation, it will be assumed that $1/k_\varsigma$ is large relative to Δz so that $e^{-k_c \Delta z}$ can be approximated by $(1 - k_\varsigma \Delta z)$. This assumption allows data from pairs of traps with different depth intervals to be combined in the same analysis. However, consolidating all of the data from Sechelt Inlet into the same analysis also requires the assumption that k_ς and $\varsigma_{\text{un}}/\Gamma_{\text{un}}$ are horizontally and vertically similar. Again, these assumptions can be evaluated once a solution is found.

The approximation that $e^{-k_c \Delta z}$ equals $(1 - k_\varsigma \Delta z)$ is made and equations 5.18 and 5.19 are rearranged.

$$C_2 - C_1 = -C_1 \, \Delta z \left(1 - 2.7\frac{C_{\text{un}}}{\Gamma_{\text{un}}}\right) k_c + \frac{C_{\text{un}}}{\Gamma_{\text{un}}} \left(\Gamma_2 - \Gamma_1 + S_1 \left\{1 - e^{-k_s \Delta z}\right\}\right) \tag{5.20}$$

$$S_2 - S_1 = -S_1 \, \Delta z \left(1 - \frac{S_{\text{un}}}{\Gamma_{\text{un}}}\right) k_s + \frac{S_{\text{un}}}{\Gamma_{\text{un}}} \left(\Gamma_2 - \Gamma_1 + 2.7C_1 \left\{1 - e^{-k_c \Delta z}\right\}\right) \tag{5.21}$$

Equations 5.20 and 5.21 linear equations with the form $y = ax_1 + bx_2$ and are solved using the multivariate linear hypothesis software of SYSTAT (Wilkinson, 1990). For equation 5.20 (and correspondingly 5.21), the dependent variable is $C_2 - C_1$ (correspondingly $S_2 - S_1$). The two independent variables are $-C_1\Delta z$ and $\Gamma_2 - \Gamma_1 + S_1\{1 - e^{-k_s\Delta z}\}$ (correspondingly $-S_1\Delta z$ and $\Gamma_2 - \Gamma_1 + 2.7C_1\{1 - e^{-k_c\Delta z}\}$). The coefficients that are solved are $(1 - 2.7C_{un}/\Gamma_{un})k_c$ and C_{un}/Γ_{un} (correspondingly $1 - S_{un}/\Gamma_{un}k_s$ and S_{un}/Γ_{un}). SYSTAT also finds an error term for equations 5.20 and 5.21; the amount by which the origin (0, 0, 0) is missed by the plane representing the solution to each equation. The error term for this algorithm is a flux of ς with units of $g/m^2/day$.

Equations 5.20 and 5.21 cannot be solved independently, as k_s is required to find k_c, and vice versa. However, equations 5.20 and 5.21 can be solved in an iterative manner as follows.

1. solve equation 5.20 assuming k_s is zero; obtain a k_c.
2. solve equation 5.21 using k_c from (1); obtain a k_s. Use this k_s in equation 5.20.
3. continue until k_s and k_c as inputed converge to the k_c and k_s values of the output of equations 5.20 and 5.21.

Because the correction for decay in the total unaccountable flux is small, the iteration converges quickly.

The solutions of equations 5.20 and 5.21 and their statistics are given in table 5.1. The first four columns of table 5.1 refer to the particular model equation used. The last three columns refer to the solutions of the variables within each model equation. r^2 is a measure of the scatter in data fit to a model equation (r^2 ranges between 0 and 1, and a high r^2 is a good fit), while the P value is an indicator of the positioning of the data scatter. If the data are scattered around the origin, then P approaches one, but if the

scatter of the data is significantly away from the origin, then P approaches zero. Thus, if there is a lot of scatter in the data but the scatter is far from the origin, both r^2 and the P value will be relatively low. P_{m} applies to the scatter of the entire solution equation, while P_{v} refers to the solution of independent variables.

The data from Sechelt Inlet fit equations 5.20 and 5.21 reasonably well ($r^2 > 0.75$) and the model equation is a very good descriptor of the data ($P_{\mathrm{m}} < 0.001$). The very low P_{m} values of table 5.1 are due to the simple way in which equation 5.12 describes 100% of the flux of ς at the depth of a lower sediment trap. Table 5.1 shows that the standard errors of k_c and of k_s are 16 to 17% and the standard errors of $C_{\mathrm{un}}/\Gamma_{\mathrm{un}}$ and of $S_{\mathrm{un}}/\Gamma_{\mathrm{un}}$ are about 10% using equations 5.20 and 5.21. All of these variables are significantly different from zero ($P_{\mathrm{v}} \leq 0.001$). The error terms for the solutions to equations 5.20 and 5.21 are very small, only 2 to 3% of the average total flux of organic carbon and of silica into the middle and deepest sediment traps in Sechelt Inlet (compare the errors to table 5.2 below). Moreover, the errors in the solutions to equations 5.20 and 5.21 are not significantly different from zero, as signified by their relatively large standard errors and very large P_{v} values.

This discussion of the statistics to the solutions of equations 5.20 and 5.21 shows that the primary assumptions of the algorithm, that both k_ς and $\varsigma_{\mathrm{un}}/\Gamma_{\mathrm{un}}$ are constant over depth and time in Sechelt Inlet, are good and that errors caused by treating the whole data set together are not large. Another potential error not addressed in table 5.1 is the assumption that $e^{-k_\varsigma \Delta z}$ can be approximated by $(1 - k_\varsigma \Delta z)$. The average Δz for the sediment trap data set from Sechelt Inlet is 94 m and the maximum is 180 m. From equation 5.20, k for organic carbon is 0.0027/m. Thus, the approximation made for $e^{-k_\varsigma \Delta z}$ produces a 4% error for the average Δz and an error of 18% for the greatest sediment trap Δz in Sechelt Inlet. Equations 5.20 and 5.21 have been run without the upper to lower depth interval at stations SC-3 and SC-7, thus leaving the largest Δz to

equation	n	r^2	P_m	variable	solution	P_v
5.20				k_c	0.0027 ± 0.00045	< 0.001
organic	37	0.77	< 0.001	C_{un}/Γ_{un}	0.081 ± 0.0087	< 0.001
carbon				error	0.0050 ± 0.011	0.625
5.21				k_s	0.0019 ± 0.00031	0.001
biogenic	37	0.80	< 0.001	S_{un}/Γ_{un}	0.42 ± 0.042	< 0.001
silica				error	0.020 ± 0.045	0.662
5.22				k_N	0.0024 ± 0.00035	< 0.001
particulate	39	0.82	< 0.001	N_{un}/Γ_{un}	0.0096 ± 0.00085	< 0.001
nitrogen				error	0.000 ± 0.001	0.730
5.22				k_L	0.00042 ± 0.00040	0.301
lithogenous	39	0.70	< 0.001	L_{un}/Γ_{un}	0.40 ± 0.044	< 0.001
material				error	0.020 ± 0.050	0.684
5.24				k_c	0.0027 ± 0.00067	< 0.001
organic	37	0.49	< 0.001	C_{un}/L_{un}	0.12 ± 0.028	< 0.001
carbon				error	0.030 ± 0.016	0.067
5.25				k_s	0.0020 ± 0.00053	0.001
biogenic	37	0.40	< 0.001	S_{un}/L_{un}	0.50 ± 0.16	0.003
silica				error	0.19 ± 0.069	0.009

Table 5.1: Solutions for the sediment trap algorithm applied to Sechelt Inlet. The equation number from which solutions are derived is given. n is the number of observations for each model equation; biogenic silica was not run on two of the samples so some of the equations have 37 instead of 39 observations. r^2 is a measure of the fit of the data to its model equation, while P_m is the degree to which the data applied to the over-all model diverges from the origin, or the model's significance. Solutions to the variables of each model are given ± their standard errors and P_v is the significance in the difference from zero for the solution of each variable. The solutions for k_c and k_s in this table are very similar to corresponding k values computed from North Equatorial Pacific data by Walsh *et al.* (1988a). Their sediment traps, however, were substantially deeper than the ones in Sechelt Inlet.

be 90 m. The solutions for k_ς and $\varsigma_{un}/\Gamma_{un}$ were different by only 2% and less than 1%, respectively, than the solutions for equations 5.20 and 5.21 of table 5.1.

Equations 5.20 and 5.21 can be rearranged into equations of straight lines by dividing each term by $\varsigma_1 \Delta z$. Figure 5.2 is a graphic presentation of the solution to 5.20 and 5.21, where the y-intercept is $-k_\varsigma$ and the slope is $\varsigma_{un}/\Gamma_{un}$. The line drawn through the data is that determined from the multiple regression and presented in table 5.1. It is not the regression line of the data as plotted, because dividing all terms by $\varsigma_1 \Delta z$ may artificially change the correlation.

5.3.2 Computation of k_N and k_L

With estimates of k_c and k_s, the characteristic length scale of decay for nitrogen ($1/k_N$) and for the lithogenous fraction of the total flux ($1/k_L$) can be computed from equation 5.14. k_N should be similar to k_c and k_L should be zero.

Using the approximation that $e^{-k_\varsigma \Delta z} = (1 - k_\varsigma \Delta z)$ and the use of equation 5.16, equation 5.14 may be expressed as

$$\varsigma_2 - \varsigma_1 = -\varsigma_1 \, \Delta z \, k_\varsigma + \frac{\varsigma_{un}}{\Gamma_{un}} (\Gamma_2 - \Gamma_1 + 2.7 C_1 \{1 - e^{-0.0027 \Delta z}\} + S_1 \{1 - e^{-0.0019 \Delta z}\}) \quad (5.22)$$

where ς is either particulate nitrogen or the lithogenous fraction of the total flux.

Table 5.1 presents the solutions for equation 5.22 and their statistics. k_N (0.0024/m) is within the standard error of the solution for k_c and it is significantly different from zero ($P_v < 0.001$). As well, N_{un}/Γ_{un} is statistically significant. The solution for the lithogenous fraction of Γ shows that k_L is not significantly different from zero ($P_v > 0.3$; there is no decay of the lithogenous flux) but that L_{un}/Γ_{un} is significant. The errors for both nitrogen and the lithogenous flux solved with equation 5.22 are small.

Figure 5.3 is a graphical representation of the algorithm applied to the nitrogen and the lithogenous fluxes.

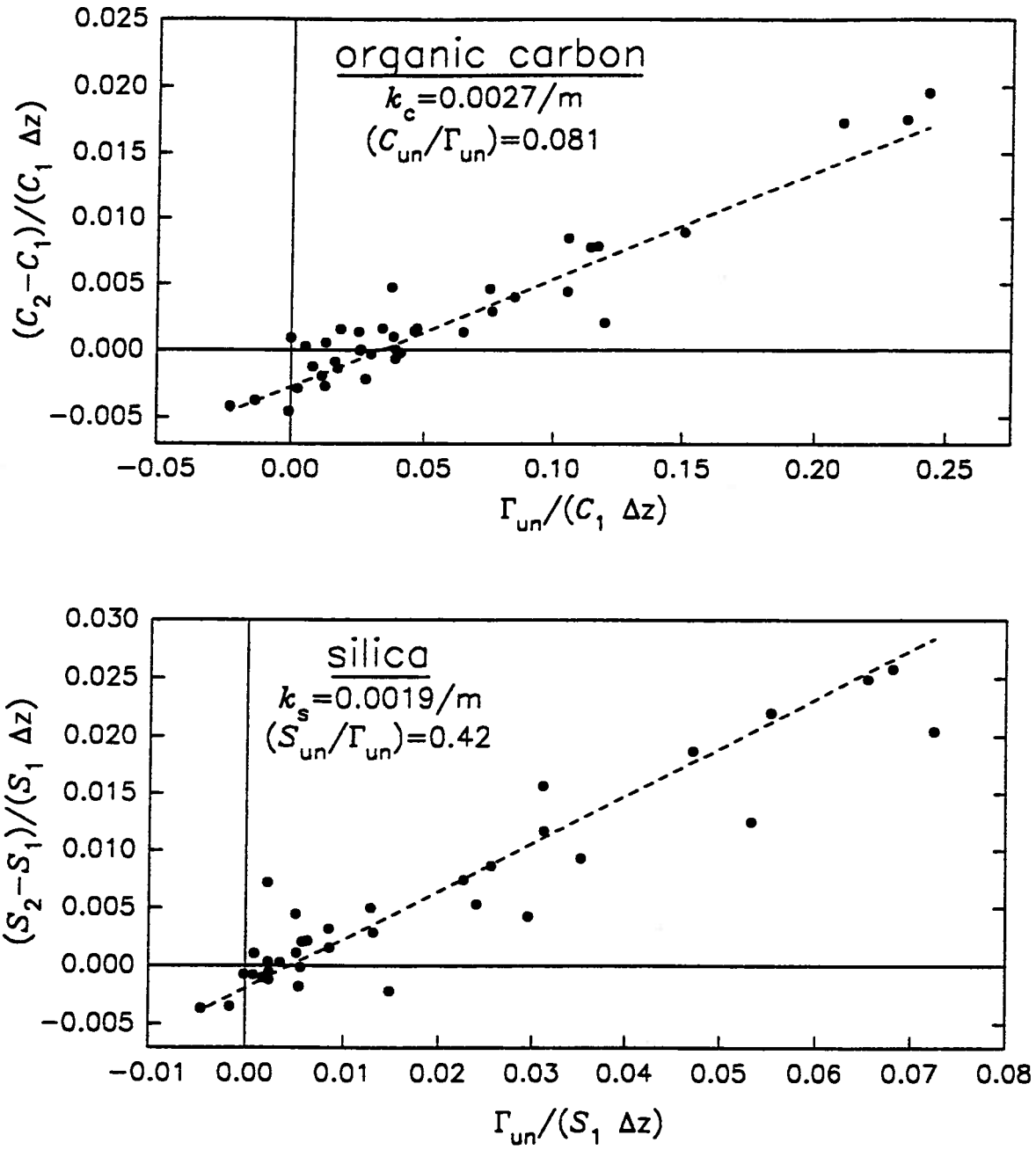

Figure 5.2: Graphic representation of algorithm solutions for organic carbon and for silica from equations 5.20 and 5.21. These plots are created by rearranging equations 5.20 and 5.21 into the equation of a straight line, where the slope is $\varsigma_{un}/\Gamma_{un}$ and the y-intercept is $-k_\varsigma$. The hatched line through each plot is determined by multivariate linear regression on equations 5.20 and 5.21. It is not a regression line of the data as they are plotted in this figure.

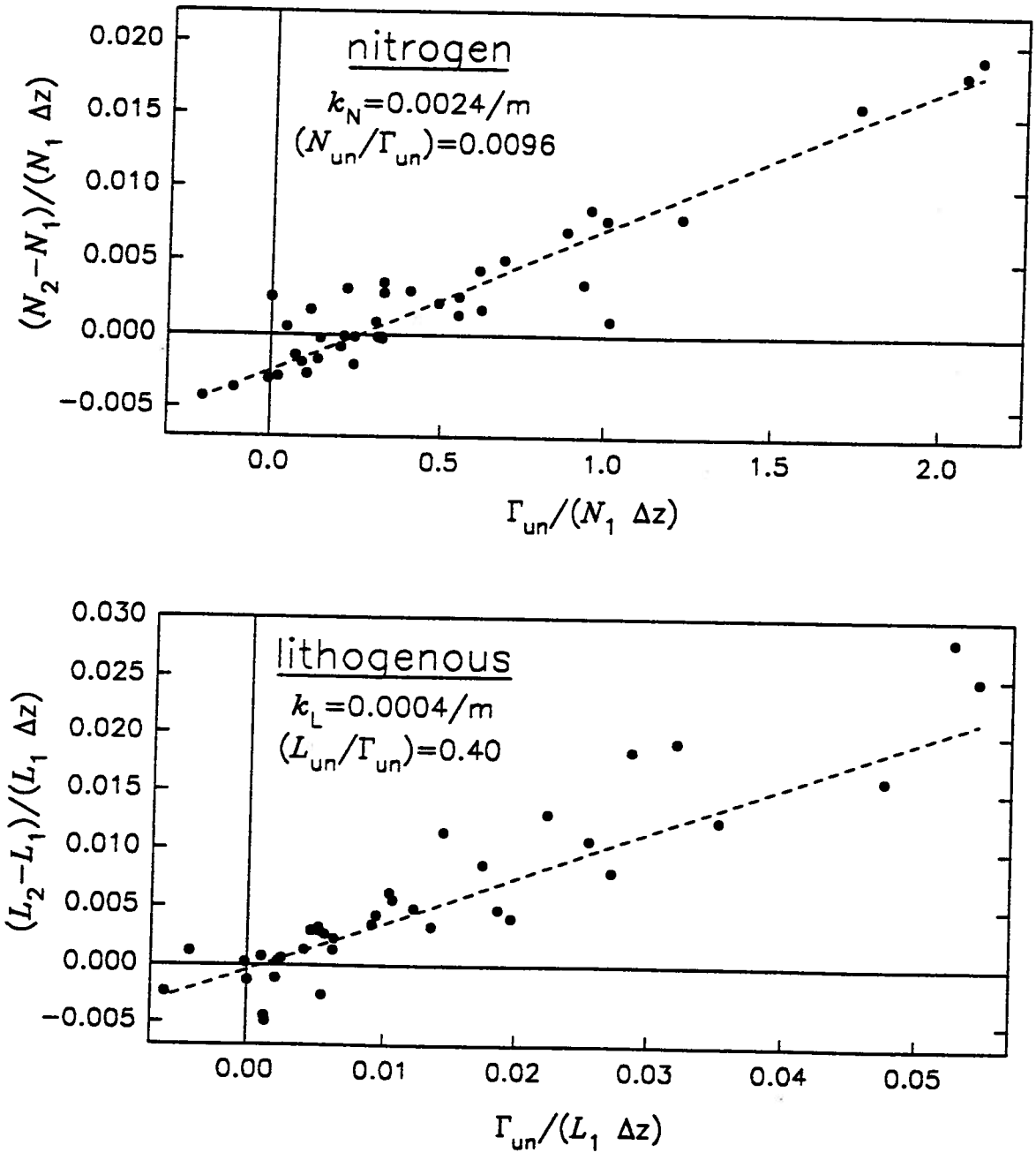

Figure 5.3: Graphic representation of the algorithm solutions for nitrogen and for lithogenous matter from equation 5.22. These plots are created in the same way as those of figure 5.2.

5.3.3 The use of a refractory material to solve the algorithm

The substitution of Γ_{un} into the sediment trap algorithm (equation 5.13) allows the solution of k_ς and of $\varsigma_{un}/\Gamma_{un}$. However, Equations 5.20, 5.21 and 5.22 are complicated by the need to quantify the total decay of the accountable flux in order to estimate Γ_{un} of equation 5.14.

It is postulated that the complication derived from the need to express the total decay of Γ_{ac} can be avoided if a refractory flux is used instead of Γ to solve the sediment trap algorithm. The only measure of a refractory flux in Sechelt Inlet is that of the lithogenous flux; the uncertainty of its estimation was noted in section 2.3.5. Nonetheless, the lithogenous flux is used in place of Γ_{un}. Equation 5.13 first must be rewritten.

$$\varsigma_{un} = \frac{\varsigma_{un}}{L_{un}} L_{un} \tag{5.23}$$

L (g/m^2/day) is the lithogenous flux, ς_{un}/L_{un} (dimensionless) is the amount of ς relative to the unaccountable flux of lithogenous material and L_{un} is simply $L_2 - L_1$. Combining equations 5.23 and 5.12 and applying the result to organic carbon and to silica gives:

$$C_2 - C_1 = -C_1 \, \Delta z \, k_c + \frac{C_{un}}{L_{un}} (L_2 - L_1) \tag{5.24}$$

$$S_2 - S_1 = -S_1 \, \Delta z \, k_s + \frac{S_{un}}{L_{un}} (L_2 - L_1) \tag{5.25}$$

As in equation 5.14, the assumption that both k_ς and ς_{un}/L_{un} are constant must be made.

The results of equations 5.24 and 5.25 applied to the Sechelt data and solved using the multivariate linear hypothesis of SYSTAT are presented in table 5.1 and should be compared to the solutions of equations 5.20 and 5.21 in the same table. Whether the total flux or the lithogenous flux is used to quantify the unaccountable flux, the solutions to k_c and k_s are very similar. ς_{un}/L_{un} is greater than $\varsigma_{un}/\Gamma_{un}$ because the unaccountable

lithogenous flux will always be less than or equal to the unaccountable total flux. Because of errors in the estimation of the lithogenous flux, the data from Sechelt Inlet do not fit equations 5.24 and 5.25 well (low r^2), and the errors of the solutions to those equations are large and significant.

5.4 Probable causes of an increase in flux with depth

Before further discussion of the results of the sediment trap algorithm applied to Sechelt Inlet, it is helpful to consider possible biases in sediment trap experiments and some possible sources of material that cause increases in flux with depth. Average fluxes and material composition for the study period in Sechelt Inlet are given in table 5.2. The data are first averaged globally for the entire study period at all stations and depths. Then they are averaged for each depth at all stations, for each station at all depths and for each month at all stations and depths. For nearly all recorded fluxes and depth intervals in table 5.2, fluxes increases with depth. Figure 5.4 shows that the unaccountable flux is least between the middle and the lower sediment traps.

There are many things that may cause sediment trap records of flux to be different from the real flux at a specific depth. Among these are trapping efficiency as a function of trap Reynolds number, particle sinking rate and trap design (Butman, 1986; Butman *et al.*, 1986; Gardner, 1980a, 1980b), trapping efficiency as a function of trap tilt (Gardner, 1985), *in situ* degradation of trapped organic matter and the choice of a preservative environment during trap deployment (Hedges et al., 1993; Wakeman *et al.*, 1993) and the death of swimmers attracted to the high concentration of organic matter in sediment traps (Michaels *et al.*, 1990). Furthermore, particles can be introduced to or removed from the water column at depth through a number of processes. These include horizontal advection (Walsh *et al.*, 1988a), horizontal diffusion (Siegel *et al.*, 1990), turbulent resuspension of

avg. flux or % total	global	Feb	Mar	Apr	May	Jun
total flux	2.4	2.4	1.3	3.1	2.3	3.1
C **flux**	0.20	0.20	0.12	0.23	0.19	0.25
% *C*	8.6	8.3	9.8	7.6	8.6	8.3
N **flux**	0.023	0.018	0.015	0.027	0.022	0.031
% *N*	0.99	0.73	1.17	0.91	0.99	1.03
S **flux**	0.97	0.22	0.52	1.33	0.96	1.60
% *S*	37	8.0	31	44	41	52
L **flux**	0.99	1.66	0.66	1.15	0.86	0.82
% *L*	41	70	45	37	37	26
C:N ratio	8.7	11	8.4	8.3	8.7	8.1

avg. flux or % total	upper	middle	lower	SC-3	SC-5.5	SC-7
total flux	2.0	2.5	2.7	2.9	2.6	1.8
C **flux**	0.18	0.21	0.20	0.24	0.21	0.15
% *C*	9.5	8.8	7.6	8.2	8.6	9.0
N **flux**	0.021	0.023	0.024	0.027	0.025	0.017
% *N*	1.09	0.99	0.88	0.95	1.00	1.01
S **flux**	0.88	1.01	1.02	1.14	1.19	0.66
% *S*	37	37	37	37	40	35
L **flux**	0.83	0.98	1.14	1.16	1.03	0.80
% *L*	38	41	44	41	39	42
C:N ratio	8.7	8.9	8.6	8.7	8.5	8.9

Table 5.2: Average total and constituent fluxes ($g/m^2/day$) and percent of total flux in Sechelt Inlet. Total flux is the total dry weight, *C* is organic carbon, *N* is nitrogen, *S* is biogenic silica and *L* is lithogenous material. The C:N ratio of the flux is also given by weight. The upper table provides global averages for the entire data set from Sechelt Inlet and averages over all stations for each month. The averages of the lower table are over the five month study period for particular trap positions in the water column and for each station.

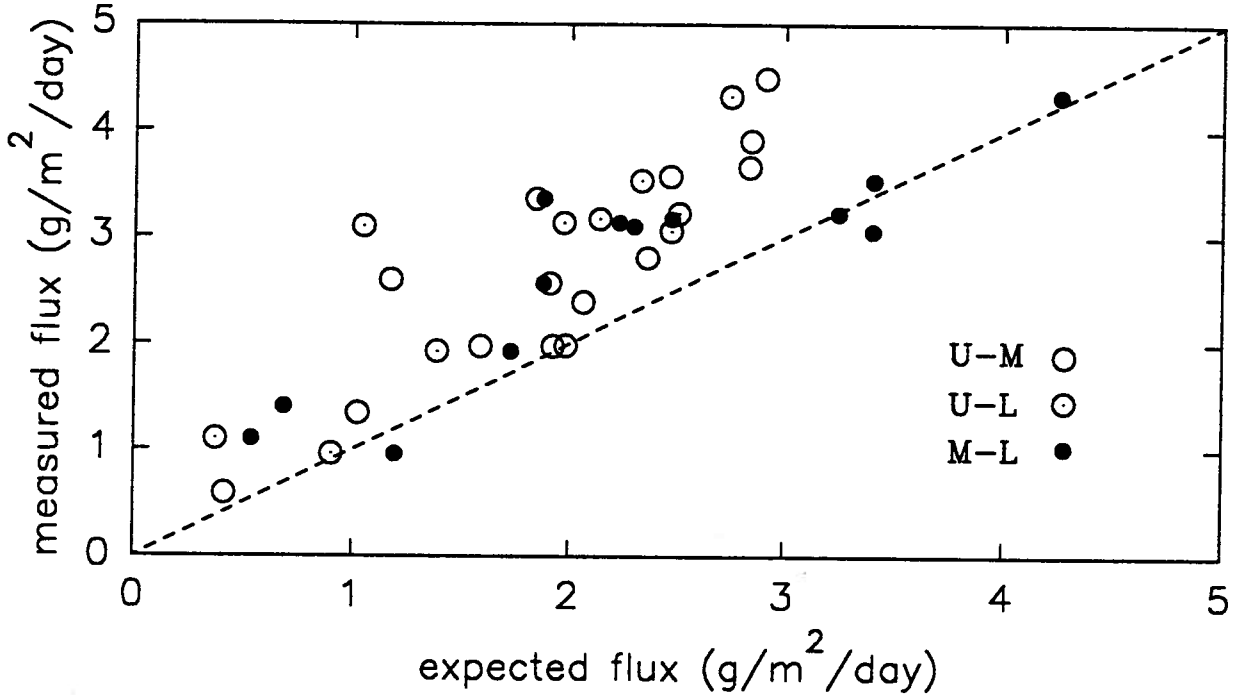

Figure 5.4: Measured vs. expected fluxes at the middle and lower traps. The expected flux is that at an upper trap corrected for the decay of silica and organic matter as it reaches a lower trap. The solid line describes $y = x$, and any deviation from it represents (+) and (-) Γ_{un}. U-M = upper to middle traps; U-L = upper to lower traps; M-L = middle to lower traps. This plot contains data from all stations and months. In general, the least amount of unaccountable flux occurred between the middle and the lower sediment traps during the study period in Sechelt Inlet. The cluster of points from the M-L subset at about 2 g/m^2/day on the x-axis representing (+) unaccountable fluxes is not unique to any month or station.

bottom sediments (Bloesch, 1982; Wassmann, 1983), and migrating zooplankton (Angel, 1984). Because of their nature, these experimental and phenomenal complications are difficult or impossible to quantify.

In an effort to understand the apparent increase in flux with depth in Sechelt Inlet, some of the above physical factors and possible errors in the measurement of particle flux are considered.

5.4.1 Preservative biases

The effects of two preservative environments on the sediment trap samples were discussed in section 2.3.2. In general, it was shown that little difference exists between NaCl and (NaCl+NaN_3) preserved samples for total dry weight, organic carbon, nitrogen and biogenic silica. However, similar changes due to factors such as *in situ* degradation and swimmers in both preservative environments would be undetected in this analysis. As well, there are unexplained differences in the $CaCO_3$ preservation of the two environments. These differences are quantitatively ignored because the $CaCO_3$ flux only comprises about 1% of the total in Sechelt.

5.4.2 Zooplankton migration

Fecal pellets are recognized to be a important flux of material into sediment traps (Dunbar and Berger, 1981; Pilskaln, 1987). However, the characteristics of fecal pellet flux can be complicated by aggregation and disaggregation and are not fully understood (Lampitt *et al.*, 1990; Pilskaln, 1987). In February, 1990, Goldblatt (personal communication) found abundances of *Metridia pacifica* and *Calanus pacificus* as high as $100/m^3$ at the mouth of Sechelt Inlet and of less than $20/m^3$ at the head. Both species of copepod perform diel migrations from surface waters at night to depths below 50 m in the day-time (Dagg

et al., 1989). Fecal pellet excretion below 50 m is a potential source of an increased flux of material in deeper waters.

Dagg *et al.* (1989) studied the daily cycle of pigment transport to the deep waters of Dabob Bay, Washington by *Calanus pacificus* and *Metridia luciens.* They found that 2.3 - 2.9 mg of pigment/m^2 were defecated out of the surface waters during the night. In comparison, 0.01 - 0.02 mg of pigment/m^2 were carried into deeper waters by active transport. Laboratory experiments further showed that gut passage time was very short, approximately an hour or less, leading to the conclusion that copepods consume microplankton and produce fecal pellets in the same vicinity.

Phytoplankton maxima during the study period in Sechelt inlet were found to be within the top 10 m of the water column and chl*a* concentrations decreased between 10 and 20 m (tables 2.6 through 2.9), while the shallowest sediment traps were placed at 50 m depth at all three stations. Regardless of the importance of fecal pellets to the total material flux during the study period in Sechelt Inlet, the excretion of digested material below the upper trap is an unlikely source of the increased material flux in the deeper sediment traps.

5.4.3 Horizontal advection of particles

Changes in the total flux of material (Γ) with depth can be written as $d\Gamma/dz$. An estimate of $d\Gamma/dz$ in Sechelt Inlet during the study period considers the average change in flux between the upper and lower sediment traps. 145 m is the average distance between upper and lower traps at the three stations in Sechelt Inlet. The average increase in Γ between those depths is 0.7 g/m^2/day (table 5.2) and therefore an estimate of $d\Gamma/dz$ in Sechelt Inlet is 0.005 g/m^2/day/m. To test whether or not horizontally advected particles sinking out of surface waters could create this degree of flux increase with depth, a scale

analysis for $d\Gamma/dz$ is performed.

$$\frac{d\Gamma}{dz} = \frac{d\Gamma}{dx}\frac{dx}{dt}\frac{dt}{dz} = \frac{H\,u}{sr} \tag{5.26}$$

H is the horizontal gradient in the flux of Γ, u is the horizontal current velocity and sr is the sinking rate of a particle.

- $H = 7\text{x}10^{-5}$ g/m^2/day/m
- $u = 864 \rightarrow 1728$ m/day
- $sr = 10 \rightarrow 100$ m/day

H is estimated by noting that 0.7 g/m^2/day was a common difference between upper traps at different stations in Sechelt for the same time period and that the stations are approximately 10 km apart. u is estimated knowing that surface currents at SC-3 averaged over monthly intervals (therefore removing the effects of tides) were approximately 1 to 2 cm/s. The choice of a sinking rate is from the discussion of section 5.4.4.

Using $u = 1000$ m/day, $d\Gamma/dz$ is 0.0007 g/m^2/day/m if all particles have a sinking rate of 100 m/day. This is almost an order of magnitude less than the observed $d\Gamma/dz$ in Sechelt Inlet. If all settling material sinks at a rate of 10 m/day, then $d\Gamma/dz$ is 0.007 g/m^2/day/m. This is greater than the observed $d\Gamma/dz$ during the study period in Sechelt Inlet.

Horizontally advected and quickly sinking particles could make up a small fraction of the increase in flux with depth in Sechelt Inlet, and slowly sinking advected material may be the source of all of it. Although accurate estimates of sinking rates do not exist for the material caught in Sechelt Inlet, it is likely that the particles containing silica had sinking rates greater than 10 m/day (section 6.2.2). Furthermore, gradients in the flux of material out of surface waters should create regions with negative as well as positive

changes in flux with depth. It is unlikely that all three moorings in Sechelt Inlet were located at positions where increases but never decreases in flux were received by deeper traps.

5.4.4 Trapping efficiency

For a given sediment trap in an environment with a constant fluid viscosity, two factors control trapping efficiency. They are the current regime at the opening of the sediment trap and the sinking rate of the particles expected to fall into the trap (Gardner, 1980a; Butman *et al.*, 1986). Gardner's work (1980a) recognized that the residence time of an eddy within a sedment trap contributes to overall trapping efficiency. Thus, sediment trap geometry and the Reynolds number at the mouth of the trap (*Re*, defined below) are very important in sediment trap experiments.

The sediment trap Reynolds number is used in this work to compare the collection efficiency at SC-3 during the study period with results from Butman (1986).

$$Re = \frac{u\,D}{\nu} \tag{5.27}$$

u is the instantaneous horizontal current speed, D is the outer diameter of the trap mouth (14 cm for the traps used in Sechelt Inlet) and ν is the kinematic fluid viscosity (1.18 x 10^{-2} cm^2/s at 15^0C and salinity of 30 on the Practical Salinity Scale).

Butman (1986) was not able to describe the absolute efficiency of a sediment trap at a specific *Re* and a defined range of particle sinking rates because of the difficulty measuring the real flux of particles at the mouth of a sediment trap. Nonetheless, her laboratory work evaluated trapping efficiency relative to a 'standard' cylindrical trap with a specific aspect ratio (height:diameter) for particles with approximate sinking rates of 10 to 100 m/day over an order of magnitude change in *Re*. She found the following:

$\underline{Re \simeq 2 \times 10^3 \rightarrow 5 \times 10^3}$: collection efficiency decreases by about a factor of two.

$\underline{Re \simeq 5 \times 10^3 \rightarrow 2 \times 10^4}$: collection efficiency remains constant at about 1/2 maximal.

For these results to be used for evaluating trapping efficiency in field experiments, Butman (1986) made a number of stipulations.

1. Traps must be straight-sided cylinders without threads at the mouth, unbaffled and have an aspect ratio of about 3.

2. Trap moorings must be rigid so there are no high-frequency oscillations and no tilt of the trap with respect to the mean flow (Gardner, 1985).

3. The current field must be steady (i.e. away from surface waves), flow speeds must change gradually and trap collections must be separable into different flow-speed intervals.

4. The true flux must consist of particles sinking at rates of about 10 to 100 m/day.

5. Current speeds near the trap mouth must be available for calculations of *Re*.

At SC-3, conditions 2 and 5 were met. Condition 3 was only partially met, as the trap collections represent material from all flow speeds during each deployment. Condition 4 may not have been met as sinking rates are unknown.

Although the sediment traps used in Sechelt Inlet were straight-sided cylinders without threads and with an aspect ratio of 3.4, they were baffled. Therefore, Condition 1 was not directly met. However, Butman (1986) stipulated that unbaffled cylinders should be used for sediment trap experiments because she found that any obstruction to flow through the mouth of a sediment trap increases between-replicate variability in collection but does not significantly change mean trapping efficiency. Thus, the conclusions of Butman (1986) can be applied to the sediment traps used in Sechelt Inlet, while

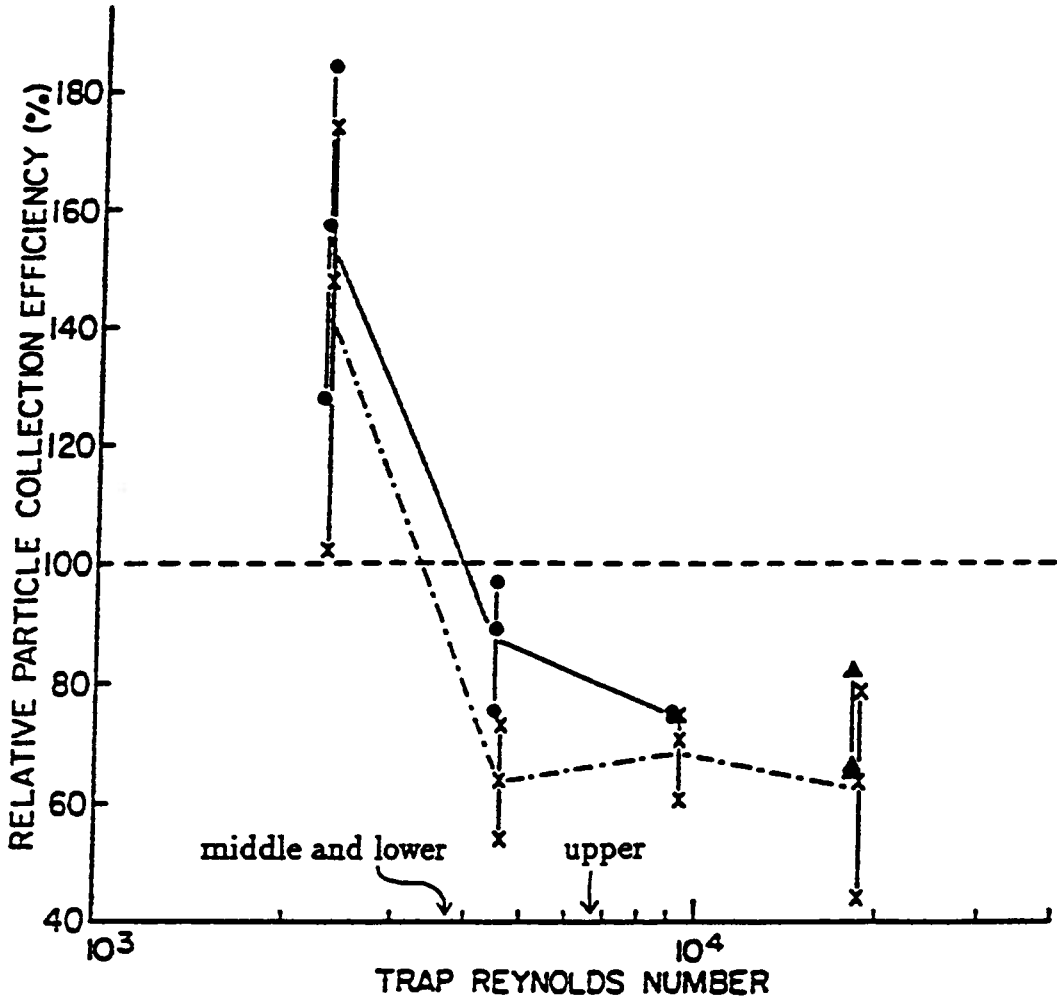

Figure 5.5: Relative particle collection efficiency vs. *Re* for straight-sided cylinders with a height:diameter ratio of about 3. This figure is reproduced from Butman (1986). The circles, crosses and triangles represent experiments run at three different times and vertical bars connect replicate values. The solid and the dot-and-dashed lines connect mean values for the experiments represented by circles and by crosses, respectively. *Re* at SC-3 for the upper, middle and lower sediment traps is indicated.

depth	$\bar{u}$ (cm/s)	SD of u (cm/s)	*Re* at $\bar{u}$	*Re* at $\bar{u}$ + 1SD	*Re* at $\bar{u}$ + 2SD
50 m	5.6	4.0	6.6×10^3	1.1×10^4	1.6×10^4
140 m	3.0	2.4	3.6×10^3	6.4×10^3	9.3×10^3
238 m	3.1	2.0	3.7×10^3	6.1×10^3	8.4×10^3

Table 5.3: Sediment trap Reynolds number at SC-3. u is current speed and $\bar{u}$ is the average current speed. *Re* is calculated for sediment traps with an outer diameter of 14 cm. Current speeds were measured every 3 hrs at 50 and 140 m by cyclesonde, and every 1 hr at 238 m by Aanderaa. There was little variation in $\bar{u}$ throughout the study period; this table represents the mean of the current data collected between February and June.

recognizing that there is a degree of variability in the Sechelt Inlet data that would be less had unbaffled traps been used.

Currents in Sechelt Inlet

As part of the interdisciplinary work to study Sechelt Inlet, a cyclesonde and Aanderaa current meters were in operation at station SC-3 during the study period. Baker (1992) described how the cyclesonde and Aanderaa data are processed. From these instruments, records of horizontal current velocities at 50, 140 and 238 m have been used to calculate *Re* at the upper, the middle and the lower traps of SC-3. Table 5.3 provides current speeds, their standard deviations and the range of *Re* that was experienced by the sediment traps at SC-3.

If current speeds (u) are assumed to be normally distributed, then 50% of current observations are less than $\bar{u}$, 84% are less then $\bar{u}$ + one standard deviation, and 98% are less than $\bar{u}$ + two standard deviations. Comparing table 5.3 with figure 5.5, it is clear that the sediment traps at SC-3 saw a range of current speeds that affected trapping efficiency for particles sinking at rates of about 10 to 100 m/day. At 50 m the mean, the 84% and the 98% occurrence trapping efficiencies were all within the range of *Re* having

a trapping efficiency of 40 to 80%. At both 140 and 238 m, the mean *Re* should have produced trapping efficiencies better than 40 to 80%, while both the 84% and the 98% occurrence trapping efficiencies are expected to have been 40 to 80%. Thus, trapping efficiency of particles sinking at about 10 to 100 m/day probably increased between the upper and the middle traps at SC-3.

Trapping efficiency was similar for the middle and the lower traps if sinking rates remained unchanged between these depths. The average flux increase with depth was greater between the upper and the middle traps than between the middle and the lower sediment traps during the study period in Sechelt Inlet in general (table 5.2), and especially so at station SC-3 (table 5.4).

Accelerated sinking in Sechelt Inlet

If a particle accelerates as it sinks, then its trapping efficiency should increase with depth provided *Re* remains constant. Particle acceleration is not unexpected in the marine environment (McCave, 1984; Alldredge and Silver, 1988; Alldredge and Gotschalk, 1988). However, mechanisms of particle acceleration are difficult to quantify and occur simultaneous with the processes of decay and disaggregation, both tending to decrease settling speeds. The goal of this section is to describe factors that may change sinking rates and therefore contribute to overall trapping efficiency.

The study period in Sechelt Inlet encompassed the growth and 'crash' of the spring bloom, which was dominated primarily by *Skeletonema costatum* and secondarily by *Thalassiosira nordenskioldii* and other small centric diatoms (Appendix A). Figures 3.3 and 3.4 and the species identifications of Appendix A show that the phytoplankton biomass in the euphotic zone decreased dramatically between March and April. Table 5.2 of this chapter shows that high rates of primary production were manifest in the sediment trap samples of April, May and June as large silica fluxes. The silica flux

in Sechelt Inlet is expected to be in two forms: that of fecal pellets and of individual or aggregated senescent diatom cells. Both particle forms may accelerate with depth through aggregation (Alldredge and Gotschalk, 1988), while diatoms will also accelerate for physiological reasons.

Diatoms can physiologically increase their buoyancy if they have sufficient supplies of nutrients and light (Smayda, 1970). Metabolic restraints against sinking require reserves of respiratory carbon, and therefore a diatom will lose buoyancy with the onset of darkness when respiratory carbon becomes depleted, which is on the order of several days (Waite *et al.*, 1992). Appendix I of Smayda (1970) shows that without buoyancy control, the maximum sinking rate of diatoms ranges between about 1 m/day to as high as 500 m/day depending on cell size, cell morphology and chain formation (Smayda, 1970), and for the diatoms most common to Sechelt Inlet it appears that the sinking rate is between 1 and 10 m/day (from Appendix I of Smayda, 1970). In the presence of adequate light and nutrients, these same cells can maintain buoyancy to such a degree that their sinking rates are 0.1 m/day and less (Waite, 1992).

The longer a particle spends in the water column, the more likely are its chances of colliding (McCave, 1984) and bonding (Alldredge and Silver, 1988) with another particle. Alldredge and Silver (1988) described two factors that may increases the probability of particles of biological origin to bond after they have collided. These factors are (1) the production of extracellular mucuses and the 'sticky' products of cell lysis, both created by bacteria and phytoplankton and (2) the non-spherical shapes common to biological organisms. Although not always the case (Asper, 1987), sinking rates tend to increase with the size of particle aggregations (Alldredge and Gotschalk, 1988). Thus, the sinking rate of a diatom out of the euphotic zone will increase through the loss of physiological viability as well as by the increased probability of becoming associated with fast sinking aggregates. Furthermore, resting spores can be a large portion of sediment trap material

(Pitcher, 1986) and their formation at depth would be another mechanism of accelerated sinking for diatom cells.

Despite a possible trend for the sinking rate of diatoms to increase with depth, determining a range of diatom sinking rates for *Skeletonema costatum* is complex. To reduce its requirement for silicate and therefore gain an ecological advantage over other diatoms, *S. costatum* can continue to grow despite a relatively thin and under-developed frustule, raising the question of the susceptibility of *S. costatum* to water column silica dissolution and remineralization of subsequently exposed cytoplasm (Waite, 1992). The sediment trap algorithm applied to Sechelt Inlet shows that both the dissolution of silica and the degradation of organic matter in the water column were significant during the experiment in Sechelt Inlet. Therefore, although the sinking rate of some phytoplankton cells may increase with depth because of physiological deterioration and particle aggregation, the sinking rate of other cells may decrease with depth if they disintegrate and do not become associated with quickly sinking aggregates.

Both a decrease in sediment trap Reynolds number and an increase in particle sinking rate will cause trapping efficiency to increase. *Re* decreases with depth at SC-3 to such a degree that trapping efficiency is expected to increase between the upper and the middle traps, although *Re* for the middle and bottom traps appears to have been quite similar. If sinking rates increased, then the trapping efficiency would have increased between the middle and the lower traps in Sechelt Inlet.

5.4.5 Resuspension and particle diffusion

Resuspension and lateral transport of material from the sediment-water interface may cause the flux of particles to deeper sediment traps to be greater than the flux to shallower traps. This phenomenon has been described in both coastal and oceanic waters (Ansell, 1974; Bloesch, 1982; Wassmann, 1983; Dymond, 1984; Walsh *et al.*, 1988b). In Sechelt

Inlet, bottom scouring may be induced by turbulence along boundary topography more or less continually. It may also occur during episodic events such as deep-water renewals, tidally-driven deep-water turbulence, or turbidity currents flowing down the steep side-walls of the fjord. Because bottom sediments are generally re-worked by heterotrophic bacteria and benthic invertebrates (Hinga *et al.*, 1979), resuspended sediment typically has low organic matter content (Bloesch, 1982; Hedges *et al.*, 1988a). Biogenic silica is expected to be low in concentration for resuspensions as well, as its dissolution generally continues with time until the siliceous material is buried to a depth of centimeters below the benthic interface (Hurd, 1973).

Although resuspended material is often low in organic matter and silica, it is possible that aggregates of organic-rich material sinking quickly through the water column can reach the sediments and then become resuspended (Billett *et al.*, 1983; Lampitt, 1985; Walsh *et al.*, 1988b). Such aggregates are called marine snow when in the water column, and fluff when resting upon the sediments. Walsh *et al.* (1988b) further distinguished between fluff that eventually mixes into sediments and rebound particles that are deposited onto sediments but quickly return to the nepheloid layer. Alldredge and Silver (1988) reported that marine snow has a sinking rate of 1 to 368 m/day, and Lampitt (1985) observed that fluff is easily resuspended from bottom sediments by current speeds greater than 7 cm/s. Combined, these conditions of swift transport and resuspension may result in laterally-focused material that is compositionally very similar to particles sinking through the water column for the first time. Thus, in coastal inlets such as Sechelt, sediments washed off the steep side-walls must be considered a possible source of resuspended material.

If particles sinking at the sides of an inlet are transported towards its center, then the inlet's change in width with depth may be an important influence on increases in flux with depth. With this in mind, channel width at the depths of the sediment traps

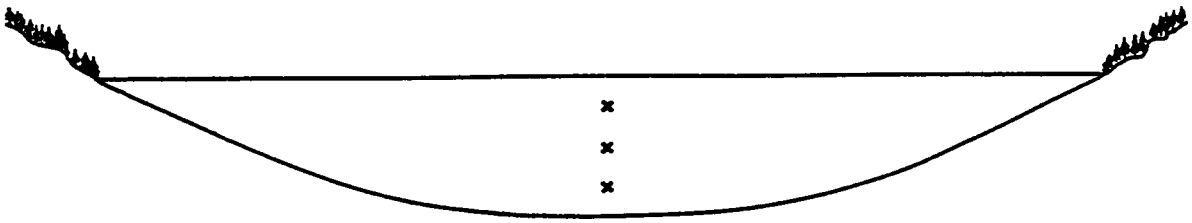

Figure 5.6: Representative cross-section of the sediment trap stations in Sechelt Inlet. The width to depth ratio for this cross-section is 1800 m/240 m = 7.4 (the width to depth ratio at SC-3, SC-5.5 and SC-8 is 7.5, 6.5 and 8.3, respectively). At all three stations, the slope of the side-walls is roughly constant at 23^0 from the surface to the depth of 50 m from the bottom, and the width of the inlet 50 m from the bottom is approximately 0.6 times the width 50 m from the surface. The sediment traps are placed as they would be in a 240 m water column; at 50, 120 and 190 m.

was determined for stations SC-3, SC-5.5 and SC-7. Proportional change of width with depth is similar at all three stations and it is quite constant with depth. The widths at mid-depth and 50 m from the bottom are about 80 and 60%, respectively, of the width 50 m from the surface at stations SC-3, SC-5.5 and SC-7 (figure 5.6).

If particle resuspension occurs, but only within a shallow nepheloid layer along the side-walls, then it will not have been recorded at the middle or lower sediment traps in Sechelt Inlet. However, if resuspension and horizontal transport is felt throughout the width of Sechelt Inlet, then the true flux of material at the depth of the middle and deepest traps may be as much as 1.3 and 1.7 times that at the upper traps. Sediment

DEPTH	SC-7	SC-3	SC-5.5
upper	1.62	2.51	2.05
middle	1.74	3.13	2.69
lower	1.94	3.13	3.16
m/u	1.07	1.25	1.31
l/m	1.11	1.0	1.17

Table 5.4: Fluxes of total dry weight at the upper, middle and lower sediment traps averaged for the study period in $g/m^2/day$. Ratios of fluxes (m/u and l/m) are given in the last two rows.

trap-measured fluxes may even be greater if resuspension causes particles to pass through a depth more than once. The true fluxes of 1.3 and 1.7 times fluxes at an upper trap represent a maximum for particle focusing and it is unlikely that it would be reached because it assumes that no sediments accumulate or remineralize on the side-walls of the inlet.

Because the width change with depth is relatively constant at stations SC-3, SC-5.5 and SC-7 and because of the added influence of resuspension off the bottom of the inlet, resuspension and horizontal advection of particles is expected to be felt more strongly from the middle to the lower sediment traps than from the upper to the middle sediment traps. Although this was not the case during the study period (figure 5.4 and table 5.4), the complexities of resuspension and horizontal transport of material require that they be considered a possible cause of the increase in flux with depth in Sechelt Inlet.

5.5 Discussion

5.5.1 Composition of resuspended and of differentially trapped material

Zooplankton migrations and the horizontal advection of material sinking out of surface waters have been discounted as significant contributors to the increase in flux with depth

in Sechelt Inlet during the study period. The depth-distributed pattern of the unaccountable flux (figure 5.4 and table 5.4) shows that in general the greatest increase in flux with depth occurred between the upper and the middle sediment traps. Changes in the sediment trap Reynolds number at SC-3 and subsequently possible changes in trapping efficiency (figure 5.5 and table 5.3) agree with the observed pattern in the increase in flux with depth better than with the hypothesis that resuspension and particle diffusion were active during the study period.

By calculating the fraction of particular constituents within the unaccountable flux, the algorithm presented in this chapter has the potential to provide further insight into the source of the unaccountable flux in Sechelt Inlet. Although the material composition of neither resuspended nor differentially trapped material can be definitively predicted, the extreme composition of each and the reasons for that composition are discussed.

Resuspended material

Particles can be easily removed from benthic surfaces (Lampitt, 1985) where current shear greatly enhances suspension. However, to be caught by the sediment traps in Sechelt Inlet, resuspended particles must be carried into the center of the inlet where boundary layer turbulent shear will no longer aid particle suspension. Without turbulent shear, a particle will sink downward and be carried in the direction of currents which are predominantly along-channel in Sechelt Inlet. Such currents will not transport resuspended particles from the side walls and bottom to the locations of deeper sediment traps. Any event that does provide such transport must be high in kinetic energy (i.e. turbidity currents and deep water renewals) and will likely scour into and remove refractory sediment components as well as fluff and rebound particles. Therefore, the extreme composition of resuspended material would be high in refractory material and relatively low in organic matter and silica.

Although along-channel currents generally will not bring resuspensions from the benthic boundary to the center of the inlet, they can carry particles away from topographic features such as sills and inlet corners to the locations of the sediment traps. In this way, continually scouring currents may result in the exposure of bedrock, and therefore be able to transport only freshly fallen material. If any sediment has accumulated where along-channel currents move over topography, then again resuspensions may be high in refractory material.

Another factor that may influence the composition of resuspended material is the possibility of particle winnowing. As sinking particles interact with the bottom, the lighter fraction of the total flux may separate from heavier material and thus resuspended matter could be enriched in the low density components of the material flux.

Material differentially caught by sediment traps

If improved trapping efficiency causes deeper sediment traps to catch more material than upper ones, then the accountable and the unaccountable fluxes may be indistinguishable. However, a scenario for compositional differences between these two fluxes exists. Quickly sinking particles will be preferentially caught in high Re environments. As Re decreases, a larger fraction of slowly sinking particles may be caught. In this way, slowly sinking and/or accelerating particles may be better represented in the unaccountable flux than in the accountable flux.

5.5.2 Material composition of Γ_{ac} and Γ_{un}

Having determined k for the three primary constituents of the total flux caught in the sediment traps in Sechelt Inlet (organic matter, silica and lithogenous material), accountable fluxes can be quantified. Two methods are used to determine the amount of accountable flux specific to each trap-pair deployment.

constituent	Γ_{un} table 5.1	Γ_{ac} (a) $\varsigma_{ac2} = \varsigma_1 e^{-kz}$	Γ_{ac} (b) $\varsigma_{ac2} = \varsigma_{total2} - \varsigma_{un2}$
organic carbon	8.1 ± 0.87	8.1 ± 0.23	8.0 ± 0.26
nitrogen	0.96 ± 0.085	0.96 ± 0.037	0.91 ± 0.032
silica	42 ± 4.2	34 ± 2.5	32 ± 3.3
lithogenous matter	40 ± 4.4	44 ± 2.9	46 ± 3.1
C:N ratio	8.4 ± 1.2	8.4 ± 0.40	8.8 ± 0.42

Table 5.5: Composition of Γ_{un} and of Γ_{ac} in Sechelt Inlet. Values and their standard errors are in percent, except for C:N ratios which are presented as weight ratios. Solutions for the constituents of the unaccountable flux are from table 5.1. Solutions for the constituents of the accountable flux are determined using two methods described in the text. The values for the accountable fluxes come from middle and lower traps; upper traps are not included. Because the sediment trap algorithm applied to Sechelt Inlet double-weights the flux to the lower trap by considering the depth intervals U-M, U-L and M-L, values for the accountable flux have been similarly double-weighted so that they can be compared to the unaccountable flux.

(a) Using equation 5.11 and solutions of k_ς from table 5.1, the mass of ς_{ac} expected to have reached the lower sediment trap of each trap-pair deployment has been calculated.

(b) ς_{ac} can also be estimated by subtracting ς_{un} from measured fluxes of ς (equation 5.10). This method requires an estimate of the total amount of ς_{un} reaching each lower sediment trap. Solving for Γ_{un2} specific to each trap-pair deployment using equation 5.16 and multiplying by $\varsigma_{un}/\Gamma_{un}$ from table 5.1 estimates ς_{un} for the lower sediment trap of each pair.

Whether (a) or (b) is used to estimate ς_{ac}, equation 5.17 is used to calculate Γ_{ac}. In this way, $\varsigma_{ac}/\Gamma_{ac}$ is estimated for the lower trap of each pair. The averages (presented in percentage instead of fractions) of $\varsigma_{ac}/\Gamma_{ac}$ for all of the pairs during the study period and for ς = organic carbon, nitrogen, silica and lithogenous matter are given in table 5.5.

The comparative compositional trends of the accountable and the unaccountable fluxes in Sechelt Inlet suggest that there was little difference in the organic content of

the two fluxes and that the lithogenous portion of each flux was statistically similar, although the mean of the lithogenous fraction in the accountable flux was greater than the mean in the unaccountable flux. Only the fractions of silica for the accountable and the unaccountable fluxes were statistically different, with the unaccountable flux containing more silica than the accountable flux.

Thus, the material that caused the increase in flux with depth in Sechelt Inlet during the study period appears to have been similar to the accountable flux, except that it was enriched in silica. It is possible that the source of the unaccountable flux was diatoms missed by upper sediment traps and caught by deeper ones because of improved trapping efficiency. If the remains of diatoms were a part of the lighter fraction of the total material flux, then it is also possible that winnowed and resuspended material was a significant source of the unaccountable flux. If such winnowing and resuspension were important, then the similarity in the decay rate for silica and organic matter would explain the seemingly high percentage of organic carbon in the unaccountable flux: after diatom remains 'rebound' from the benthic interface, silica and organic matter decay while their proportions remain constant.

Two possible causes for the unaccountable flux based on material composition are presented. However, if winnowing and resuspension were the cause of the increase in flux with depth in Sechelt Inlet, then it is expected that the proportional increase in flux would be greater between the middle and the lower traps than between the upper and middle traps. This was not the case during the study period (table 5.4). On the other hand, the change in flux with depth at station SC-3 agrees with predictions made from considerations of trapping efficiency based on the sediment trap Reynolds number (figure 5.5). It is suggested that trapping efficiency affected the quantity of material caught during each sediment trap deployment and that improved trapping efficiency with depth was mostly responsible for the observed increase in flux with depth in Sechelt

Inlet.

5.5.3 Results from a sediment trap experiment in the Baltic Sea

The conclusion that trapping efficiency significantly influenced measured fluxes for a sediment trap experiment is not unique for coastal marine settings. Smetacek *et al.* (1978) described the analysis and results of a sediment trap experiment carried out during the spring bloom in the Bornholm Basin of the Baltic Sea. Two moorings were set in waters of depths 64 and 70 m, and the deepest trap at both stations was only 5 m off the bottom. Samples were measured for total dry weight (DW), for PON and POC by CHN analyzer, for chl*a* and pheopigments and for phytoplankton carbon (PPC) using microscopy. Hydrographic data were taken during the study.

Smetacek *et al.* (1978) found that total flux increased with depth. As well, they showed that much of the material in all the traps, including those 5 m off the bottom, were the remains of fresh *Skeletonema costatum*, the dominant phytoplankton during the study period. Furthermore, the C:N ratio was lowest and PPC:POC highest in the deeper traps. They explicitly discounted locally resuspended sediment as a possible source of the increase in flux with depth, because of its significantly different composition from the sediment trap material. The possibility that phytoplankton were swept laterally underneath upper traps and left to sink into lower traps was also discounted because of hydrographic conditions. Their conclusion as to the cause of the flux increase with depth for that study was that trapping efficiency increased with depth because current speeds decreased and the sinking rates of phytodetritus increased with depth.

Both this study and that of Smetacek *et al.* (1978) were carried out during a spring bloom dominated by *S. costatum*. The findings of these works do not discount other possible causes for increases in flux with depth in regimes where the hydrodynamics and the sediment inputs are different.

5.6 Chapter summary

Sediment trap data collected from late winter to early summer record an increase in particle flux with depth in Sechelt Inlet. An algorithm has been designed for use with these data to calculated the decay of sinking material. The foundation of the algorithm is that the increase in flux with depth can be quantified as the difference in flux between an upper and a lower trap, with a correction for the decay of the material represented in the upper trap. Conceptually similar models have been used with other sediment trap data where fluxes are recorded to increase with depth (Bloesch, 1982; Walsh *et al.*, 1988b). However, these other models assume that the increase in flux with depth is caused by the resuspension of refractory sediments. The algorithm presented here differs from Bloesch (1982) and from Walsh *et al.* (1988b) because it simultaneously determines k_ς and $\varsigma_{un}/\Gamma_{un}$ without making assumptions about $\varsigma_{un}/\Gamma_{un}$. Combined with a discussion of possible causes of an increase in flux with depth, the solutions to the algorithm allow a qualitative consideration of the source of the the accountable and the unaccountable fluxes. In Sechelt Inlet, it appears that the increase in flux with depth was primarily caused by improved trapping efficiency for deeper sediment traps.

Chapter 6

Oxygen Demand from Organic Carbon Degradation

6.1 Introduction

Changes in oxygen content of aphotic waters are driven largely by heterotrophic oxidation of organic material *in situ* and in the sediments. If it is assumed that organic matter in the marine environment occurs at the C:N:P ratio of 106:16:1 (Redfield *et al.*, 1963; Fleming, 1940), then the general equations of aerobic respiration (Richards, 1965) can be written as:

$$(CH_2O)_{106}(NH_3)_{16}(H_3PO_4) + 106O_2 \longrightarrow$$
$$106CO_2 + 16NH_3 + H_3PO_4 + 106H_2O \tag{6.1}$$

Nitrifying bacteria facilitate the oxidation of ammonia (Smethie, 1987):

$$16NH_3 + 32O_2 \longrightarrow 16HNO_3 + 16H_2O \tag{6.2}$$

These equations combine to form the relationship:

$$(CH_2O)_{106}(NH_3)_{16}(H_3PO_4) + 138O_2 \longrightarrow$$
$$106CO_2 + 16HNO_3 + H_3PO_4 + 122H_2O \tag{6.3}$$

From chemical equations such as 6.3, measurements of organic carbon degradation can be stoichiometrically converted to estimates of heterotrophic oxygen consumption (Richards, 1965; Suess, 1980).

In chapter 5, an algorithm to estimate water column decay of organic carbon was developed; the loss of particulate organic carbon can be described by $k_c = 0.0027/\text{m}$ over the study period in Sechelt Inlet. This rate of decay means that about 1/3 of sinking organic carbon is lost to the water column over a 150 m decent. However, C:N values do not increase with depth in the trap samples from Sechelt Inlet, as would be expected for this degree of remineralization (discussed below). C:N ratios and gross estimates of sinking rate in Sechelt Inlet are used to consider whether fecal pellets or phytodetritus comprised the majority of the organic material flux into the sediment traps during the study period. The mechanism of particle fragmentation presented by Karl *et al.* (1988) and Cho and Azam (1988) is then proposed to explain the dichotomy of organic decay concurrent with invariant C:N ratios.

The conclusion that the increase in flux with depth in Sechelt Inlet is primarily caused by changes in trapping efficiency made in chapter 5 has important implications for describing the total flux of organic carbon throughout the water column. In this chapter, total organic carbon flux throughout the water column is estimated by back-calculating fluxes from the deepest traps to the depth of interest. A best estimate of total organic carbon decay is then converted into water column oxygen demand. Finally, an estimate of benthic oxygen demand is made by applying the results of work in Dabob Bay, WA and Saanich Inlet, B.C. (Cowie and Hedges, 1992) to the particle flux regime of Sechelt Inlet.

6.2 Were fecal pellets or phytodetritus the dominant flux of organic material into the sediment traps during the study period?

6.2.1 C:N ratios in Sechelt Inlet

(All C:N ratios in this section are by weight.)

Because the cleavage of C-C and C-H bonds requires more energy than the cleavage of C-N bonds, heterotrophic organisms tend to remove nitrogen faster than carbon from organic matter (Toth and Lerman, 1977). Thus, changes in the C:N ratio are a proxy for the degree of organic degradation (Fowler and Knauer, 1986). The average C:N ratio of the matter caught in the upper, middle and lower sediment traps in Sechelt Inlet ranges between 8.6 and 8.9 (table 5.2). The C:N ratio of the accountable (about 8.6) and the unaccountable (8.4) fluxes is similar to this range, and figure 6.1 shows that the C:N ratio of the organic matter settling into the sediment traps, excluding February data, is 8.5. It appears, therefore, that little heterotrophic degradation of the particles caught by the sediment traps in Sechelt Inlet was occurring during the study period. Here, the possibility of using the C:N ratios found in Sechelt Inlet to determine the form of the sinking organic material is addressed.

The C:N ratio of phytoplankton varies considerably and is dependent upon many factors including nutrient availability and species composition (Redfield *et al.*, 1963). The atomic ratio of 106:16:1 for organic carbon, nitrogen and phosphorus (corresponding to a C:N ratio of 6.6 by atom and 5.7 by weight) in living phytoplankton is only a broad average applicable to large bodies of water (Redfield *et al.*, 1963).

C:N ratios of 6 and less are recorded for *Skeletonema costatum* under nutrient-replete conditions (Sakshaug, 1977; Sakshaug *et al.*, 1983), but as the availability of nitrogen decreases, The C:N ratio of phytoplankton can increase dramatically (Sakshaug *et al.*, 1983). The C:N ratio of *S. costatum* growing in natural populations and in the laboratory

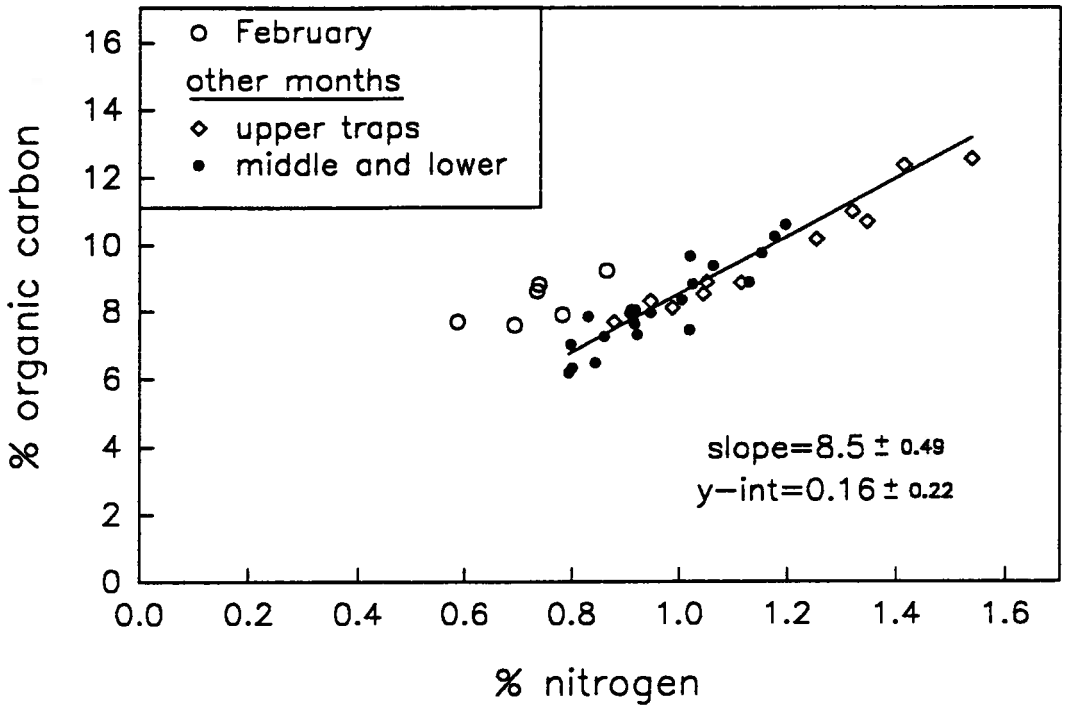

Figure 6.1: % carbon vs. % nitrogen for the sediment trap samples from all depths and months of the study period in Sechelt Inlet. The slope and the y-intercept of the geometric mean regression line (Sokal and Rohlf, 1981; Ricker, 1984) for all data excluding February are given ± their standard errors. The y-intercept of the regression line is not significantly different from zero, so the slope is the average C:N ratio (by weight) of the source material into the sediment traps for months after February.

commonly exceeds 9 (Sakshaug *et al.*, 1983) and has been recorded to be greater than 30 in Narragansett Bay (Sakshaug, 1977). For natural populations sampled from the North Sea in May, 1981 and dominated by diatoms and nanoflagellates, the C:N ratio ranged between 6.3 and 20, with only one value less than 9.1 for a sample size of 11 (Sakshaug *et al.*, 1983). Table 3.6 shows that the C:N ratio for *S. costatum* grown in laboratory conditions increases as nitrogen availability decreases (Sakshaug *et al.*, 1989). The range in the C:N ratio in that table is 6.2 to 18. Similar increases in the C:N ratio with decreases in nitrogen availability for three diatoms and a dinoflagellate were reported by Levasseur *et al.* (1993).

Nutrient stress generally leads to an increase in sinking rate for phytoplankton (section 5.4.4). Because nitrogen stress will tend to increase the C:N ratio and the sinking rates of phytoplankton, cells settling out of the euphotic zone and caught by sediment traps may have C:N ratios greater than phytoplankton grown under optimal conditions of nutrient availability. An example of a sediment trap experiment where trapped phytodetritus was found to have a relatively high C:N ratio is given in Smetacek (1978). He reported the C:N ratios of sediment trap samples collected during a spring bloom of *S. costatum* in the Bornholm Basin. At one station, the organic carbon content of the deepest trap was strongly dominated by phytodetritus and its range in the C:N ratio was 7 to 10. This value is comparable to the average C:N ratio of the sediment trap material from Sechelt Inlet of between 8 and 9.

Pilskiln and Honjo (1987) found the C:N ratio for fecal pellets in oceanic settings to range between 9 and 14, and to be higher than both bulk sediment trap material and local surface sedments. However, in the coastal regime of the Santa Barbara Basin where terrigenous mineral material was a large fraction of total suspended matter, the average C:N ratio of 7.1 for fecal pellets reflected that of total suspended material during a sediment trap experiment (Dunbar and Berger, 1981). These reports show that although

the C:N ratio for fecal material is typically greater than 6, it may or may not vary from the C:N ratio of *in situ* bulk organic material. Therefore, it is concluded that the ratio of C:N cannot be used to distinguish whether fecal matter or phytodetritus dominates the organic material of sediment trap samples. Not only does the range of C:N for each class of material overlap, but the C:N ratio of fecal pellets is not always greater than the source of material on which grazers are feeding.

6.2.2 Sinking rates in Sechelt Inlet

During the month of February the flux of silica was low in Sechelt Inlet (average of 0.22 g silica/m^2/day for all depths and stations; table 5.2). During March and April, the average silica flux increased to 0.52 g and 1.3 g silica/m^2/day, respectively. Phytoplankton analyses of the surface waters of Sechelt Inlet (Appendix A) show that the population of diatoms increased dramatically between February 20 and March 26. If diatom growth is considered the source of the increase in silica flux from February to April, then silica formed in the euphotic zone after February 20 can be considered a particle tracer and used to estimate sinking rates in Sechelt Inlet.

Silica flux vs. time to the upper and lower sediment traps is plotted in figure 6.2. Simultaneous increases and decreases in flux for the upper and the lower sediment traps imply that the time required for the silica-containing particles to sink between those traps was at most the deployment time of the traps. Because the minimum distance between upper and lower traps was 80 m, the maximum distance was 180 m and the sediment trap deployment times were about 30 days, the sinking rate of silica must have been at least 3-6 m/day. This sinking rate assumes that all of the silica-containing particles sank past the upper sediment trap at the beginning of each deployment. Therefore, it is likely that the sinking rate of particles containing silica was much greater than 6 m/day. Fecal pellet transport can account for silica with such high sinking rates (Fowler and Knauer,

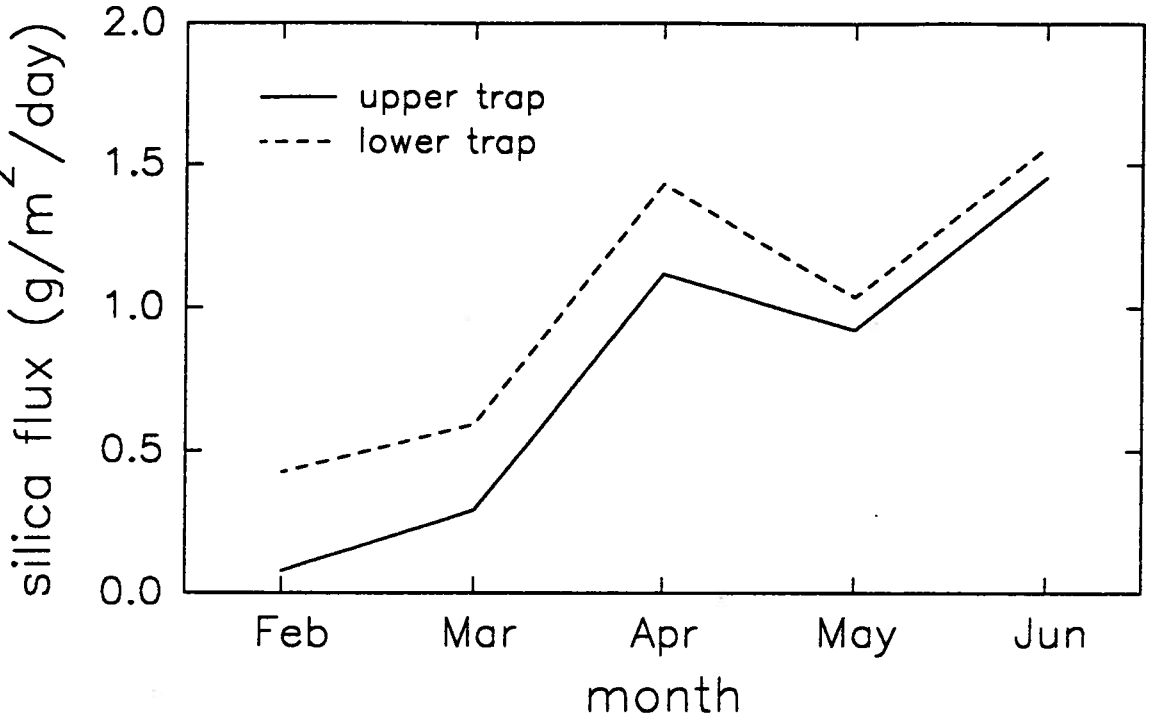

Figure 6.2: Silica flux at the upper and lower sediment traps vs. time in Sechelt Inlet. The lack of evidence of a time lag in silica flux between the upper and the lower traps implies a fast sinking rate for silica relative to the depth between the traps divided by the sediment trap deployment time.

1986). However, aggregates of diatom cells may sink considerably faster than 10 m/day (Alldredge and Silver, 1988).

Although the sinking rates of silica-containing particles were relatively high and C:N ratios were greater than 7 in Sechelt Inlet during the study period, there is no certainty that the flux of organic material was predominantly in the form of fecal pellets or phytodetritus. The flux of phytodetritus was probably large during the study period, especially considering the possibility of mass sedimentation of phytoplankton at the end of the spring bloom (Peinert *et al.*, 1982; Billet *et al.*, 1983; Wassmann, 1984; Davies and Payne, 1984). Visual analysis of samples is the only way to definitively know the form of the flux of organic matter for the sediment trap experiment in Sechelt Inlet. Unfortunately, visual analyses are not available.

6.3 A mechanism of particle sinking and decay

The accountable flux of organic carbon decreased with depth in Sechelt Inlet during the study period (chapter 5). Three mechanisms of organic decay (Cho and Azam, 1988; Karl *et al.*, 1988; Banse, 1990) that may have occurred during the study period are presented. Each mechanism may apply to phytodetritus as well as to fecal pellets.

- Bacteria attached to particles actively oxidized organic matter.
- Mesopelagic zooplankton grazed and oxidized a significant fraction of the organic material flux.
- Particles containing organic material fragmented and/or solublized as they sank. These processes may have been facilitated by the activity of attached bacteria and may have occurred to phytoplankton cells upon physiological deterioration and cell lysing.

The value of 0.0027/m for k_c from table 5.1 implies that 1/3 of particulate organic carbon is lost over a 150 m descent. If this amount of decay were the result of oxidation of organic matter by attached bacteria, then the C:N ratio would be expected to increase with depth because bacteria preferentially remove nitrogen from organic matter (Toth and Lerman, 1977; Fowler and Knauer, 1986). Because the C:N ratio was relatively constant with depth during the experiment, the first mechanism is an unlikely explanation for the decrease in flux with depth of accountable organic carbon in Sechelt Inlet.

The consumption of organic matter by mesopelagic zooplankton cannot be discounted because neither mid-depth zooplankton nor their feeding rates have been quantified in Sechelt Inlet. Because the C:N ratio of fecal pellets is not always higher than that of surrounding organic matter (Dunbar and Berger, 1981), zooplankton grazing between the depths of sediment traps does not conflict with observed C:N ratios in Sechelt Inlet. However, the influence of this process on particle flux below the euphotic zone is not well understood (Banse, 1990) and a number of researchers have found that zooplankton rarely account for the greater part of oxygen demand in aphotic oceanic waters (King *et al.*, 1978; Karl *et al.*, 1988; Cho and Azam, 1988). If these results can be applied to coastal settings, then zooplankton grazing should not be considered the primary cause of organic decay below 50 m in Sechelt Inlet, although it may account for some of it.

Particle fragmentation is left to explain the extent of organic material decay in the water column of Sechelt Inlet and has been hypothesised to occur in other marine environments. Karl *et al.* (1988) recognized that particulate organic matter (POM) is inhabited by heterotrophic microorganisms, and that POM decreases substantially with depth. However, they found that sinking POM is not the predominant site of organic oxidation. Instead, suspended and/or dissolved organic matter (S/DOM) represent the most likely sites of bacterial activity in the oceans. Cho and Azam (1988) showed that free-living bacteria constitute more than 95% of the mesopelagic bacterial population

and are responsible for large amounts of water column remineralization and subsequent oxygen demand. Both Karl *et al.* (1988) and Cho and Azam (1988) concluded that particle fragmentation is likely to be occurring during particle sinking. Once in a suspended or dissolved form, organic matter may be oxidized by free-living bacteria. This mechanism of particle fragmentation can be applied to fecal pellets and to phytodetritus and it allows organic aggregates to maintain a relatively constant chemical composition while decreasing in mass during descent through the water.

Free-living bacteria may degrade S/DOM at a rate proportional to or different from the supply of S/DOM to the water column, and therefore the timing of organic carbon oxidation is decoupled from particle fragmentation. However, the assumption of steady-state for long periods of time (eg. months to years) requires that the flux of S/DOM into the water column is matched by the sum of consumption and the flux of S/DOM out of the water column. Export fluxes of S/DOM from Sechelt Inlet are discussed in section 7.5 and are probably minimal. Furthermore, Cho and Azam (1988) suggested that the growth rate of free-living bacteria reflects the local supply of organic material. Therefore, as a first approximation, it can be assumed that organic oxidation occurs concurrent with particle fragmentation. This approximation will be especially good when temporal changes in the flux of S/DOM are small.

6.4 Water column oxygen demand

6.4.1 Estimates of the total flux of organic carbon in Sechelt Inlet

To use the results of chapter 5 and a form of equation 6.3 for estimates of water column oxygen demand, k_c=0.0027/m must be applied to a total flux of organic carbon. Although resuspension and horizontal diffusion of particles may make up some of the unaccountable flux in Sechelt Inlet, evidence from chapters 5 and 7 suggests that improved trapping

C flux ($g/m^2/day$)	**SC-7** Δz=204 m	**SC-5.5** Δz=121 m	**SC-3** Δz=221 m
9 m extrapolation	*0.24*	*0.35*	*0.40*
upper trap	0.15	0.18	0.22
middle trap	0.15	0.21	0.27
lower trap	0.14	0.25	0.22

Table 6.1: Fluxes of organic carbon ($g/m^2/day$) at the three sediment trap stations in Sechelt Inlet. All fluxes are the average flux for the duration of the study period. Δz is the vertical distance between the lower trap and 9 m depth at that station. The 9 m estimate of organic carbon flux is made using equation 6.4 and k_c=0.0027/m. The choice of 9 m as the depth origin of sinking particles is explained in the text.

efficiency for the deeper traps was the primary cause of an increase in flux with depth. Therefore, the best estimate of total organic carbon flux in Sechelt Inlet is the flux into the deepest sediment traps.

The flux of organic carbon at depths shallower than a sediment trap can be approximated by rearranging equation 5.7.

$$C_0 = \frac{C_2}{e^{-k_c(z_2-z_0)}} \tag{6.4}$$

C_2 is the flux of organic carbon at the depth of a sediment trap (z_2) and C_0 is the organic carbon flux at a shallower reference depth (z_0).

Table 5.2 shows that the flux of organic carbon was different from station to station and from month to month. It does not appear that the flux of organic carbon had a specific trend with respect to time during the five month study (see section 7.7), but there was a consistent difference in flux between the stations. SC-7 (the station closest to the head of the inlet) had a smaller flux of organic carbon than the stations farther into the body of the inlet (SC-3 and SC-5.5).

Particle flux is expected to increase with depth from the water's surface to the base of the euphotic zone and to decrease with depth thereafter (Wassmann, 1983). Determining

the base of the euphotic zone during the study period in Sechelt Inlet is complicated. The model profile of section 4.3 chooses to distribute photosynthetic oxygen production over the depth range of 0 to 9 m. This choice is made because ^{14}C incubations typically extended to 9 m, so measurements or estimates of photosynthetic carbon assimilation and of oxygen production cannot be applied below that depth. Using the integrated extinction coefficients of light (K_{int}) from figures 3.1 through 3.6, the average 1% light level, an approximation of the base of the euphotic zone, was at 17 m.

In order to maintain consistency with figure 4.1, the following calculations assume the base of the euphotic zone to have been 9 m during the experiment in Sechelt Inlet; however, it may have been deeper. If the euphotic zone extended to 17 m, then calculations meant to estimate organic carbon flux at the base of the euphotic zone will be over-estimates by about 2%.

6.4.2 Calculation of water column oxygen demand

The 9 m extrapolation of organic carbon flux and $k_c = 0.0027/\text{m}$ can be used to calculate the loss of organic carbon ($\text{g/m}^2/\text{day}$) for any depth interval, $\Delta z = z_2 - z_1$:

$$\Delta C = C_{9\,\text{m}}\, e^{-0.0027(z_1 - 9\,\text{m})} \left(1 - e^{-0.0027(z_2 - z_1)}\right) \tag{6.5}$$

To estimate the overall decay of organic carbon from 9 m to depth z_2, let $z_1 = 9$ m in equation 6.5:

$$\Delta C = C_{9\,\text{m}} \left(1 - e^{-0.0027(z_2 - 9\,\text{m})}\right) \tag{6.6}$$

Differentiation with respect to z_2 gives the decay of organic carbon per unit depth ($\text{g/m}^3/\text{day}$) at any depth z_2.

$$\frac{d(\Delta C)}{d(z_2)} = 0.0027\, C_{9\,\text{m}}\, e^{-0.0027(z_2 - 9\,\text{m})} \tag{6.7}$$

This formulation can be used to determine the depth distribution of organic carbon decay, which in turn can be converted to estimates of oxygen consumption throughout the water column.

Equation 6.3 predicts that 138 moles of oxygen are consumed as 106 moles of organic carbon are oxidized. However, this prediction is based on the average C:N ratio for phytoplankton of 106:16 by atoms as determined by Fleming (1940), whereas the global C:N average for the sediment trap samples from Sechelt Inlet is 106:10 by atoms (section 2.3.5). Therefore, the relevant translation from organic carbon degradation to oxygen consumption is:

$$\Delta O_2 \text{ (g/m}^2\text{/day)} = \Delta C \text{ (g/m}^2\text{/day)} \left(\frac{126}{106}\right) \left(\frac{32}{12}\right) = 3.2\, \Delta C \text{ (g/m}^2\text{/day)} \qquad (6.8)$$

The fraction 126/106 is the carbon to oxygen stoichiometry of equation 6.3 adjusted for the average C:N ratio in Sechelt Inlet. The fraction 32/12 converts the molar ratio of carbon and oxygen in equation 6.3 into a weight ratio. Using k_c=0.0027/m and the extrapolated fluxes of organic carbon at 9 m (table 6.1), equation 6.5 can be used to determine the decay of organic carbon between any two depths, and equation 6.8 can convert that decay into an estimate of oxygen demand. These calculations have been done for the depth interval from 9 m to the bottom at each station. The results are presented in table 6.2 along with estimates of benthic oxygen demand, which is discussed next.

6.5 Benthic oxygen demand

There is no sediment accumulation or remineralization information from Sechelt Inlet. However, Cowie and Hedges (1992) estimated that 65% of the organic carbon reaching the sediment interface in both Dabob Bay and Saanich Inlet is oxidized. Dabob Bay, Saanich Inlet and Sechelt Inlet are geographically close and are similar in size and in phytoplankton ecology (Sancetta and Calvert, 1988; Cowie and Hedges, 1992; Haigh *et*

all values in $g/m^2/day$	**SC-7** Δz=254 m	**SC-5.5** Δz=171 m	**SC-3** Δz=271 m
9 m carbon flux	*0.24*	*0.35*	*0.40*
water column			
carbon remin	0.12	0.13	0.21
oxygen demand	0.38	0.42	0.67
sediments			
carbon remin	0.08	0.14	0.12
oxygen demand	0.26	0.45	0.38

Table 6.2: Water column and sediment oxygen demand at the three sediment trap stations in Sechelt Inlet. All values are losses in $g/m^2/day$. Δz is the vertical distance between the depth of 9 m and the bottom at each station. The 9 m organic carbon flux is from table 6.1. Water column values represent integrated loss over the depth interval Δz. Determination of carbon remineralization in the sediments is discussed in the text.

al., 1992). They differ in that Saanich Inlet is regularly anoxic with occasional deep water renewals in the fall (Cowie and Hedges, 1992), while Dabob Bay and Sechelt Inlet are generally oxic water bodies. (Sechelt Inlet will go sub-oxic and Narrows Inlet sometimes becomes anoxic near the sediments.)

On the basis of a comparison of the flux of organic carbon to the sediments as estimated from sediment trap data with permanent burial of organic carbon in the sediments, Cowie and Hedges (1992) concluded that the rate of burial of organic carbon is similar in two inlets with vastly different deep-water redox potentials. The difference between organic carbon input and permanent burial is presumed to be the result of remineralization at the benthic interface and within the sediments.

For Sechelt Inlet, organic carbon flux to the sediments is estimated as the flux at the deepest sediment trap minus water column decay for the 50 m descent of material to the bottom (which is equivalent to the 9 m flux minus total water column decay as presented in table 6.2). This procedure differs from that of Cowie and Hedges (1992) because

they argued that there is little water column decay and that the increase in particle flux with depth in Dabob Bay is due to resuspension and horizontal advection (Hedges *et al.*, 1988b). Therefore, the best estimate of the primary particle flux to the sediments in Dabob Bay is the flux into sediment traps in the upper water column. Although these two methods of extrapolating flux to the sediments differ, they provide similar sediment deposition rates if applied to the data from Sechelt Inlet because the measured fluxes of organic carbon at the upper sediment traps are close to the fluxes at the lower traps minus water column decay to the bottom.

The sediment oxygen demands of table 6.2 are within the range of other studies (Hargrave, 1978; Dale, 1978; Wassmann, 1984; Hedges *et al.*, 1988b; and a number of reports presented by C. Knock, 1993).

The possibility of particle resuspension off the steep side walls of Sechelt Inlet is discussed in section 5.4.5. Although it has been concluded that resuspended particles were not a major component of the sediment trap material during the study period, it is possible that resuspension was occurring but that particles moved down the sides and below the depth of the deepest sediment traps. Therefore, even if extrapolations of organic carbon flux to sediment surfaces are accurate, there will be uncertainty in predictions of the oxygen demand of fjordal side walls and bottom until the ultimate resting spot of sinking particles in fjords is established.

6.6 Chemical oxygen demand of anoxic regions

Bacterial consumption of organic carbon continues in waters and sediments that are deficient in oxygen (Froelich *et al.*, 1979). Oxidized forms of nitrogen, manganese and iron oxides, and sulfate can act as electron acceptors for the oxidation of organic matter in sub-oxic and anoxic environments. In regions devoid of available oxidants, organic

material can be further degraded through fermentation. The remineralization of organic carbon by oxidants other than O_2 produces reduced chemical species that will be oxidized in the presence of oxygen. Thus, although there is no biological oxygen demand in sub-oxic and anoxic waters, the accumulation of reduced chemical species can create large chemical oxygen demands. Reduced species are printed in bold face in the following bacterially-mediated reductions.

Nitrate reduction:

$$(CH_2O)_{106}(NH_3)_{16}(H_3PO_4) + 84.8HNO_3 \longrightarrow$$
$$106CO_2 + 42.4N_2 + \mathbf{16NH_3} + H_3PO_4 + 148.4H_2O \tag{6.9}$$

Denitrifying bacteria oxidize ammonia to nitrogen gas with nitrate in sub-oxic and anoxic waters and sediments (Smethie, 1987). The complete reaction for nitrate reduction is:

$$(CH_2O)_{106}(NH_3)_{16}(H_3PO_4) + 94.4HNO_3 \longrightarrow$$
$$106CO_2 + 55.2N_2 + H_3PO_4 + 177.2H_2O \tag{6.10}$$

Manganese oxide reduction:

$$(CH_2O)_{106}(NH_3)_{16}(H_3PO_4) + 236MnO_2 + 472H^+ \longrightarrow$$
$$106CO_2 + 8N_2 + H_3PO_4 + \mathbf{236Mn^{2+}} + 366H_2O \tag{6.11}$$

Iron oxide reduction:

$$(CH_2O)_{106}(NH_3)_{16}(H_3PO_4) + 212Fe_2O_3 \text{ (or } 424FeOOH) + 848H^+ \longrightarrow$$
$$106CO_2 + \mathbf{16NH_3} + H_3PO_4 + \mathbf{424Fe^{2+}} + 530H_2O \text{ (or } 742H_2O) \tag{6.12}$$

Sulfate reduction:

$$(CH_2O)_{106}(NH_3)_{16}(H_3PO_4) + 53SO_4^{2-} \longrightarrow$$
$$106CO_2 + \mathbf{16NH_3} + H_3PO_4 + \mathbf{53S^{2-}} + 106H_2O \tag{6.13}$$

Fermentation:

$$(CH_2O)_{106}(NH_3)_{16}(H_3PO_4) \longrightarrow 53CO_2 + 53CH_4 + \mathbf{16NH_3} + H_3PO_4 \qquad (6.14)$$

In general, these reactions are vertically separated by horizontal boundaries. The boundary between each pair of reactions can be in the sediments or in the water column, depending on the relative availability of specific oxidants and the supply of organic matter. Also, there will be a transitional region where the rate of one redox reaction decreases and another increases with depth. As oxygen concentrations go below 10 μM (0.3 mg/l), the reduction of nitrate and of the metal oxides begins (Murray *et al.*, 1978). Sulfate reduction occurs in anoxic environments, and as sulfate becomes depleted, fermentation begins (Froelich *et al.*, 1979). Of the complete oxidation reactions given by equations 6.10 to 6.13, the only reduced species that might be oxidized upon exposure to oxygen are the metal ions, ammonia and sulfide, although nitrite is known to accumulate in and diffuse outward from sub-oxic waters (Richards, 1965). Iron and manganese oxides occur in low concentrations in the marine environment, so the sum of their oxidizing potential is small. However, sulfide and ammonium accumulation in anoxic waters and sediments can be substantial because of the abundance of sulfate in sea water (Richards, 1965; Calvert and Pedersen, 1992).

Determining the potential chemical oxygen demand of accumulated sulfide is a three-step process. First, the rate of organic carbon oxidation in sulfate-reducing environments must be compared to that in oxygen-reducing regions. Second, the oxygen equivalent of accumulated sulfide must be determined. Third, the rate of sulfide oxidation in waters and sediments exposed to oxygen must be estimated. The second and the third processes are both dependent on the degree of re-oxygenation and therefore are treated together.

- **The rate of sulfate reduction.** The burial efficiency and the rate of degradation of organic carbon in oxygen-reducing and sulfate-reducing sediments has been

compared (Calvert and Pedersen, 1992; Calvert *et al.*, 1992; Cowie and Hedges, 1992; Pedersen *et al.*, 1992; Canfield, 1989; Henrichs and Reeburgh, 1987). There is no solid evidence that the rate of sulfate reduction is different from that of oxygen reduction (Calvert and Pedersen, 1992), although Canfield (1989) argued that organic degradation may proceed more slowly in anoxic than in oxygenated sediments. For the purpose of numerical simulation of the rate of sulfate reduction, a first approximation is to assume that it is the same as oxygen reduction.

- **The chemical oxygen demand of accumulated sulfide and the rate of sulfide oxidation.** In the presence of oxygen, a suite of reactions with S^{2-} can occur that will produce a range of sulfur-bearing compounds including elemental sulfur (S_8^0 which will precipitate within the water column), intermediate oxidation states of sulfur, such as thiosulfate ($S_2O_3^{2-}$), and fully oxidized sulfate (SO_4^{2-}). The reaction and its rate will depend on the oxygen content of newly introduced waters and the presence of reduced species other than sulfide. If elemental sulfur is the end product of the reaction between sulfide and oxygen, then the molar ratio of O_2 consumption to sulfide oxidation (O_2:S^{2-}) is 1:8. If sulfate is the end product, O_2:S^{2-} is 2:1. For the intermediately-oxidized compounds, O_2:S^{2-} is between 1:8 and 2.

  Describing the complete reactions between oxygen and sulfide where oxygenated water meets anoxic waters and sediment is complicated. However, Richards (1965) reported that reactions between O_2 and S^{2-} occur within a few days, and that the final O_2:S^{2-} ratio is between 0.7 and 1.6, and increases with the initial concentration of oxygen. It is suggested that numerical simulations modeling the chemical oxygen demand of sulfide-bearing waters and sediments use a ratio of 1:1 for O_2:S^{2-}.

The oxidation of 106 atoms of organic carbon in sulfate-reducing environments yields

53 moles of S^{2-} (equation 6.13), which in turn will consume about 53 moles of O_2 in oxygenated waters. Therefore, the rate in which sulfide-born chemical oxygen demand accumulates in anoxic waters and sediments in Sechelt Inlet is 53/126 times the O_2 consumption rate due to organic carbon remineralization in oxic waters as computed in section 6.4.2, assuming that the rates of organic carbon degradation in oxic and sulfate-reducing waters are the same.

The concentration of sulfate in oxygenated sea water is about 28,000 μM (compare to oxygen concentrations of 8mg/l = 250 μM). Thus, the maximum amount of accumulated oxygen demand for one cubic meter of sea water isolated from the effects of molecular diffusion is 28 mol or 900 mg O_2/l. The maximum accumulated chemical oxygen demand of sediments cannot be as easily determined because it will depend upon the porosity of the sediments and the depth to which sulfate reduction occurs.

Ammonia can accumulate in strongly anoxic environments where nitrate has been entirely reduced by denitrifying bacteria (the step between equations 6.9 and 6.10). However, determining the accumulation of ammonia during organic carbon degradation in anoxic regions is complicated by the downward diffusion of nitrate. Where ammonia does accumulate and then is exposed to oxygen:

$$NH_3 + 2O_2 \longrightarrow HNO_3 + H_2O \tag{6.15}$$

This reaction is facilitated by nitrifying bacteria and is the source of nitrate below the euphotic zone, discussed in chapter 7.

Although not addressed here, this section suggests the possibility of a large chemical oxygen demand on oxygenated waters bordering anoxic waters and sediments through eddy and molecular diffusion of reduced chemical species.

6.7 Chapter summary

Chapter 5 provides an estimate of the rate of decay of the particles caught by the sediment traps in Sechelt Inlet. These decay rates must be applied to a total flux of material to approximate the magnitude of material loss to the water column. One goal of this chapter has been to use the C:N ratios of the sediment trap samples and sinking rates inferred by changes in the flux of silica-containing particles between depths of the sediment traps to determine whether the majority of the material sinking out of the euphotic zone was in the form of phytodetritus or fecal pellets. It is concluded that this distinction cannot be made from the sediment trap data without visual inspection of the samples, but nonetheless a mechanism for particle decay that applies to both phytodetritus and fecal pellets is proposed. This mechanism relies on particle fragmentation instead of degradation, and allows for constancy in the C:N ratio with depth for the ~200 m water column of Sechelt Inlet while decreasing the magnitude of the accountable flux with depth.

Water column oxygen demand is estimated from extrapolations of organic carbon flux and the decay constant from chapter 5. Sediment oxygen demand is estimated by oxidizing 65% of the organic carbon reaching the sediments as extrapolated from the sediment trap data. The estimates of sediment oxygen demand agree with measurements for similar marine settings made in the literature. Periods of anoxia occur in some B.C. fjords, and considerations for modeling the chemical oxygen demand following a deep water renewal into such anoxic regions are presented.

Chapter 7

Coupling water column processes to net community production in the euphotic zone

7.1 Introduction

In chapters 3 and 4 photosynthetic carbon assimilation and photosynthetic oxygen production within the euphotic zone of Sechelt Inlet are estimated. Chapter 5 determines the decay of carbon in the water column below the depth of 50 m. Chapter 6 estimates water column and sediment oxygen demand from extrapolations of total organic carbon flux in the water column. Therefore, estimates of all biological sources and sinks of oxygen have been made except for the heterotrophic oxygen demand in the euphotic zone. Consideration of nitrogen dynamics in the euphotic zone of highly productive coastal waters provides a way to estimate both upper water column oxygen demand and fluxes of organic carbon out of the euphotic zone in Sechelt Inlet.

7.2 The f-ratio and export fluxes of nitrogen

To avoid confusion in this chapter, a brief explanation concerning the terms used to describe nitrogen dynamics within and below the euphotic zone is given. Pools of nitrogen, N, have units of g N/m^2. Pools are distinguished either by their source or by the oxidation state of the nitrogen within the pool. Fluxes of nitrogen into and out of pools are denoted by ϕ, with units g N/m^2/day. The photosynthetic assimilation of nitrogen from a specific pool is denoted by P with the appropriate subscript to describe the pool

from which the assimilated nitrogen originates. The units of nitrogen assimilation are the same as a flux, g N/m^2/day.

The definitions of autotrophic production presented in section 3.2 are based on carbon dynamics in the euphotic zone. Ecological production can also be classified according to the source of nitrogen used for growth by autotrophs (Dugdale and Goering, 1967; Eppley and Peterson, 1979). Under the nitrogen scheme, 'new' production (P_{new}; g N/m^2/day) applies to phytoplankton growth that uses nitrogen that has entered the euphotic zone and has not yet been assimilated by phytoplankton. 'Regenerated' production (P_{r}; g N/m^2/day) refers to autotrophic growth that is mediated by nitrogen that has been recycled within the euphotic zone. The sum of P_{new} and P_{r} is total production (P_{T}). Because phytoplankton seems not to remineralize nitrogen as it respires, $R_{\mathrm{C:N}}P_{\mathrm{T}}$ is synonymous with P_{n} of the carbon scheme for primary production (section 3.2); and because P_{new} describes growth beyond that consumed by heterotrophs if steady state conditions exist, $R_{\mathrm{C:N}}P_{\mathrm{new}}$ is equivalent to P_{c} of the carbon scheme for steady state (Platt *et al.*, 1989). $R_{\mathrm{C:N}}$ is the C:N ratio by weight of the phytoplankton assimilating nitrogen. Based on the theory of Dugdale and Goering (1967), the *f*-ratio, or f (Eppley and Peterson, 1979) has been defined:

$$f = \frac{P_{\mathrm{new}}}{P_{\mathrm{T}}} \tag{7.1}$$

The mass balance equation for nitrogen in the euphotic zone is

$$\phi N_{\mathrm{new}} - \phi N_{\mathrm{ex}} = \frac{\Delta N}{\Delta t} \tag{7.2}$$

ϕN_{new} and ϕN_{ex} are inward and outward fluxes of nitrogen (g/m^2/day), both taken to be positive. The terminology *new* and *export* are chosen to maintain consistency with the literature. ΔN (g/m^2) is the change in total nitrogen within the euphotic zone and can be positive or negative, and Δt is the length of time for an experiment. Because advection and/or diffusion from deeper waters is the primary source of N_{new} to

the euphotic zone, and because nitrate is the predominant form of nitrogen in aphotic waters, N_{new} is primarily nitrate (Dugdale and Goering, 1967).

Equations 7.1 and 7.2 are independent of each other. However, P_{new}, ϕN_{new} and ϕN_{ex} can be equated if the conditions of two stipulations hold.

1. ϕN_{new} **is a net flux:** Downwelling and downward diffusion are mechanisms by which N_{new} can be carried out of the euphotic zone. The advective process of estuarine entrainment ensures that in general there is no downwelling in Sechelt Inlet. When rates of photosynthesis are low, gradients of N_{new} and the diffusive portion of ϕN_{new} are both small. During more productive periods, gradients of N_{new} are such that the diffusive part of ϕN_{new} will be upward.

2. **Steady state is required:** For a time period long enough to represent steady state, ΔN of equation 7.2 is zero so ϕN_{new} must be equivalent to ϕN_{ex}. Given that stipulation (1) holds,

$$\phi N_{\text{new}} = \phi N_{\text{ex}} = P_{\text{new}} = f\, P_{\text{T}} \tag{7.3}$$

Although this relationship holds for steady state, in dynamic conditions P_{new} does not need to balance ϕN_{new} and so ϕN_{ex} cannot be predicted from $f\, P_{\text{T}}$ (Legendre and Gosselin, 1989) using considerations of mass balance for total nitrogen (equation 7.2).

7.3 $f_{NO_3^-}$ and its estimate in Sechelt Inlet

Experiments can be conducted where ^{15}N-labeled nitrogen compounds are provided to populations of phytoplankton and the relative assimilation rate of that compound determined (Dugdale and Goering, 1967).

$$f_{NO_3^-} = \frac{\text{nitrate uptake}}{\text{total nitrogen uptake}} = \frac{P_{NO_3^-}}{P_{\text{T}}} \tag{7.4}$$

Although nitrate is the predominant form of new nitrogen, as much as 25% of N_{new} mixed into the euphotic zone from deeper waters may be in the reduced forms of ammonium, urea and other dissolved organic compounds (P.J. Harrison, personal communication). Also, secondary inputs of N_{new} into Sechelt Inlet (terrestrial, including anthropogenic run-off {Haigh *et al.*, 1992}, and atmospheric {Legendre and Gosselin, 1989}) will contain reduced nitrogen. Therefore, $\phi N_{new} \geq \phi NO_{3(new)}^{-}$.

The source of regenerated or recycled nitrogen in the euphotic zone is *in situ* heterotrophic remineralization. Ammonium is the most common form of regenerated nitrogen (Dugdale and Goering, 1967), while urea, amino acids and other forms of dissolved organics comprise some of the pool of regenerated nitrogen (Eppley and Peterson, 1979). Although most regenerated nitrogen is reduced, nitrifying bacteria can oxidize ammonium and nitrite to nitrate in the euphotic zone. Nitrification is inhibited by light but can occur towards the base of the euphotic zone and possibly throughout its depth at night (Ward, 1989).

$f_{NO_3^-}$ has been equated with f by Dugdale and Goering (1967) and others, and will be less than f by the amount of N_{new} that can be assimilated by phytoplankton that is not nitrate (Legendre and Gosselin, 1989). $f_{NO_3^-}$ will be greater than f by the amount of nitrification that occurs in the euphotic zone, but where rates of nitrate assimilation are high (requiring a large supply of nitrate such as by entrainment), overestimates of f by $f_{NO_3^-}$ are probably small. (Nitrogen fixation by cyanobacteria will cause $f_{NO_3^-}$ to be an under-estimate of f {Dugdale and Goering, 1967}. However, nitrogen-fixing bacteria are not common in Sechelt Inlet {F.J.R. Taylor, personal communication}.)

Eppley and Peterson (1979) showed that $f_{NO_3^-}$ increases with P_n and asymptotes to approximately 0.5 for $P_n > 1$ g C/m^2/day. Platt and Harrison (1985) determined that if ammonium concentrations remain low (< 0.1 μM), then $f_{NO_3^-}$ is directly related to ambient nitrate concentration and asymptotes to approximately 0.8 for nitrate values

FEB 19-20 $P_n = 0.16$				**MAR 26-27** $P_n = 3.5$			
% I_0	NO_3^-	NH_4^+	$f_{NO_3^-}$	% I_0	NO_3^-	NH_4^+	$f_{NO_3^-}$
surface	17	2.3	0.76	surface	0.98	0.56	0.53
56%	16	1.6	0.79	56%	0.97	1.9	0.24
32%	15	1.4	0.80	32%	2.3	0.80	0.63
22%	20	2.0	0.79	22%	3.5	2.5	0.48
13%	24	1.5	0.82	13%	6.2	0.94	0.75
7%	25	0.64	0.86	7%	10	1.6	0.75
APR 23-25 $P_n \approx 1.7$				**MAY 22-23** $P_n = 1.3$			
% I_0	NO_3^-	NH_4^+	$f_{NO_3^-}$	% I_0	NO_3^-	NH_4^+	$f_{NO_3^-}$
surface	2.8	0.78	0.67	surface	0.55	1.0	0.25
56%	3.6	0.93	0.68	56%	0.77	1.5	0.23
32%	5.8	1.5	0.68	32%	1.8	0.72	0.60
22%	7.5	1.4	0.73	22%	3.9	0.77	0.72
13%	10	2.7	0.67	13%	5.9	2.3	0.61
7%	18	2.0	0.78	7%	12	1.6	0.76

JUN 22-23 $P_n = 1.6$			
% I_0	NO_3^-	NH_4^+	$f_{NO_3^-}$
surface	1.0	0.53	0.55
56%	0.97	0.53	0.54
32%	4.3	0.63	0.76
22%	8.7	0.63	0.81
13%	9.6	1.3	0.76
7%	11	0.70	0.82

Table 7.1: NO_3^-, NH_4^+ (μM) and P_n (g C/m^2/day) averaged over SC-3, SC-5.5 and SC-7 from which an estimates of $f_{NO_3^-}$ for Sechelt Inlet can be made. Nutrients were taken with ^{14}C uptake measurements and are given in terms of percent surface irradiance (% I_0) instead of depth. P_n and NO_3^- can be compared to Eppley and Peterson (1979) and Platt and Harrison (1985) as discussed in the text. $f_{NO_3^-}$ is computed using the regression of Harrison *et al.* (1987) presented in the text. Samples used for NH_4^+ measurement were frozen between collection and analysis and may have high variance relative to true concentrations. However, this variance should be centered upon the mean (P.J. Harrison, personal communication), so averaging over the stations should decrease the variance in the ammonium measurements. Because of ^{14}C incubations occurring too near sunset, P_n in April is estimated from average chl*a* concentrations and $\Upsilon = 48$/day (equation 3.5).

greater than about 0.7 to 0.8 μM. Harrison *et al.* (1987) examined data from a number of coastal environments and reiterated the conclusions of Platt and Harrison (1985), while showing that increases in the concentration of ammonium will decrease $f_{NO_3^-}^{max}$ of a phytoplankton population. For the regions they studied, Harrison *et al.* (1987) found that $f_{NO_3^-}^{max}$ ranged between 0.59 and 0.86, and they presented the regression equation: $f_{NO_3^-} = 0.97\ NO_3^-/(NO_3^- + NH_4^+)$ - 0.09.

Table 7.1 shows that during the experiment in Sechelt Inlet, P_n was greater than 1 g $C/m^2/day$ for all months except February, and that nitrate concentrations averaged over stations SC-3, SC-5.5 and SC-7 were always greater than 0.8 μM except in the upper few meters in May. Ammonium and nitrate data are presented in table 7.1 and the regression of Harrison *et al.* (1987) is applied. Regarding table 7.1, a conservatively low estimate of $f_{NO_3^-}$ during the study period in Sechelt Inlet is 0.5.

7.4 Predictions of the export flux in non-steady state conditions

$f_{NO_3^-}$ can replace f in equation 7.3 to make predictions of the export flux of organic nitrogen from the euphotic zone. However, if the euphotic zone is not in steady state then equation 7.3 does not hold. During the experiment in Sechelt Inlet, fluxes of nitrogen were not in steady state, as nitrate decreased and organic nitrogen increased in the euphotic zone from January to June.

Equation 7.3 is based on the mass balance of total nitrogen within the euphotic zone. Instead, a mass balance equation applied to the amount of nitrate that is assimilated by phytoplankton is written. The equation can be used to predict ϕN_{ex} during periods of non-steady state.

$$(f_{NO_3^-})\ P_T = \frac{\Delta N_{red}}{\Delta t} + \phi N_{ex} \tag{7.5}$$

$(f_{NO_3^-})\ P_T$ is the daily rate of nitrate assimilation by phytoplankton. ΔN_{red} is the pool

of reduced nitrogen in the euphotic zone. It includes all oxidation states of nitrogen less than nitrate, which will be dominated by NH_4^+ and organic nitrogen. For a given rate of nitrate assimilation, positive ΔN_{red} will reduce predictions of ϕN_{ex} and negative ΔN_{red} will increase predictions of ϕN_{ex}. For steady state, ΔN_{red} is zero and equation 7.5 becomes equation 7.3.

Equation 7.5 is converted to carbon and rearranged.

$$\phi C_{\text{ex}} = (f_{NO_3^-})\, P_{\text{n}} - \frac{\Delta C}{\Delta t} \tag{7.6}$$

where

$$\frac{\Delta C}{\Delta t} = R_{\text{C:N}}\, \frac{\Delta N_{\text{red}}}{\Delta t} \tag{7.7}$$

ϕC_{ex} is the export flux of organic carbon out of the euphotic zone. ΔC is the change in organic carbon plus the carbon equivalent of the change in remineralized organic nitrogen (measured as $\Delta\ NH_4^+$). The applicable C:N ratio, $R_{\text{C:N}}$, to convert $\Delta N_{\text{organic}}$ into $\Delta C_{\text{organic}}$ is that of the organic matter in the euphotic zone. The C:N ratio required to translate positive values of $\Delta\ NH_4^+$ into a carbon equivalent is that of recently remineralized organic matter. On the other hand, the C:N ratio most appropriate for converting negative values of $\Delta\ NH_4^+$ into an amount of assimilated carbon is the C:N ratio of the phytoplankton in the euphotic zone. Also, ammonium that accumulates through upward diffusion into the euphotic zone has no carbon equivalence and converting it into carbon will result in under-estimates of ϕC_{ex}.

If ΔN_{red} or ΔC can be estimated, then the stipulation of steady state in section 7.2 is not necessary for equations 7.5 and 7.6. Nor does stipulation (1) need be adhered to for the formulation presented here, because equations 7.5 and 7.6 do not rely on the coupling of P_{new} and ϕN_{new} to predict export flux. However, these equations recognize that following assimilation, nitrate becomes organic nitrogen and accumulates or is exported, or it becomes NH_4^+ and accumulates in the pool of N_{red}. Therefore, downward

diffusion of NH_4^+ will cause overestimates in the export flux of organic material using equation 7.5 or equation 7.6. For the application of equation 7.6 to Sechelt Inlet, it is assumed that the rate of downward diffusion of carbon-equivalent NH_4^+ (g C/m^2/day) is negligible compared to $(f_{NO_3^-})\, P_n$.

7.5 Predicted export flux of organic carbon in Sechelt Inlet

Estimated average P_n from January 27 to June 23 is 1.6 g/m^2/day and 0.5 has been chosen to approximate $f_{NO_3^-}$ for the study period in Sechelt Inlet. Therefore, the assimilation of carbon associated with nitrate assimilation during the experiment is estimated to be 0.8 g C/m^2/day. This value would be the expected export flux had the system been in steady state during the experiment.

The carbon equivalent of ΔN_{red} is estimated by first dividing N_{red} into a pool of organic nitrogen and a pool of ammonium. The pool of organic nitrogen has many components, phytoplankton being only one of them. Haigh *et al.* (1992) showed that the difference in phytoplankton biomass between winter months and June was a maximum of 2 g C/m^2 in Sechelt Inlet during 1989 and in 1990. Species enumeration for this study shows that the timing of the spring bloom and crash, and species succession and phytoplankton concentrations after the spring bloom, were similar in 1989, 1990 and 1991. Thus, 2 g C/m^2 or 0.014 g C/m^2/day over the 147 day experiment is an approximation of the phytoplankton accumulation during the study period. There is no way to accurately estimate the accumulation of other pools of organic material in the euphotic zone during the experiment. Considering phytoplankton, microzooplankton, macrozooplankton, bacteria and dissolved/suspended organic carbon, and assigning to each the accumulation rate of phytoplankton, possibly an upper bound for Δ(organic carbon) in the euphotic zone is 0.070 g C/m^2/day.

Table 7.1 shows that there were no appreciable changes in NH_4^+ in the euphotic zone during the experiment. However, uncertainty caused by freezing samples before NH_4^+ measurement justifies an analysis of the magnitude of possible changes in NH_4^+ relative to $(f_{NO_3^-})\ P_n$. 1 μM of ammonium throughout a 10 m euphotic zone equates to 0.14 g N/m^2. If all of this NH_4^+-nitrogen is the result of heterotrophic degradation of organic matter and using a range for the C:N ratio of 5.7 to 8.7 (lower-bound is the 'Redfield' ratio, upper-bound is the average C:N ratio from the sediment trap samples), then 0.14 g NH_4^+-N/m^2 converts to 0.80 $\rightarrow$ 1.2 g C/m^2. This translates to 0.0054 to 0.0082 g C/m^2/day, less than 1% of $(f_{NO_3^-})\ P_n$.

A conservatively high estimate for the term $\Delta C/t$ in equation 7.6 is 0.1 g C/m^2/day. Using this value, the predicted flux of organic carbon from the euphotic zone during the study period is 0.8 - 0.1 = 0.7 g C/m^2/day. However, only about 0.20 g C/m^2/day were caught by the sediment traps deployed over the same period. The treatment of the data in chapters 5 and 6 estimates the flux of organic carbon at the base of the euphotic zone to be about 0.33 g C/m^2/day. In order to compare the flux of organic carbon to the sediment traps with ϕC_{ex} of equation 7.6, the amount of terrigenous organic carbon in the sediment-trap flux must be subtracted from measured fluxes. The vertical flux of terrigenous organic carbon was neither measured nor is it estimated for the study period. However, terrigenous inputs into Sechelt Inlet are not expected to be substantial, as its drainage basin is small (Pickard, 1961) and the primary source of fresh water into the inlet is dammed. For comparison, about 1/3 of the flux of organic carbon into sediment traps in Dabob Bay is terrigenous (Hedges *et al.*, 1988b). Ignoring terrigenous inputs, expected fluxes of organic carbon in Sechelt Inlet are more than a factor of two greater than those measured by sediment traps. From here on, the carbon that comprises the difference between expected and measured fluxes will be called the missing carbon (C_m).

It is possible that the missing organic carbon was horizontally advected out of Sechelt

Inlet as estuarine circulation is a net sink of surface waters for positive estuaries. Current meters deployed during the study period show that net seaward currents were about 2cm/s = 1.7 km/day near the surface. If a volume of the euphotic zone equal to (inlet width x euphotic zone depth x 1.7 km) left Sechelt Inlet each day during the experiment, then only about 5% of the euphotic zone was lost per day because of estuarine circulation.

Tidal currents through Skookumchuck Narrows into and out of Sechelt Inlet are described by Lazier (1963). Because of differences in density between the water leaving and the water entering the inlet, out-going tides tend to remove surface waters and incoming waters move under the upper layer. This process may be a sink of organic material from Sechelt Inlet. The tides in Sechelt Inlet are semi-diurnal with a diurnal inequality and the sum of the two semi-diurnal tidal ranges is about 3 m. If 3 m of depth are removed from the euphotic zone daily while waters entering the inlet with each tide are devoid of organic material, then for a euphotic zone with a depth of 9 m and one with a depth of 17 m (section 4.3), about 33 and 18%, respectively, of the expected export flux of organic material from the euphotic zone may be horizontally removed from the inlet. Combining possible losses due to tides and estuarine circulation, a maximum of 38% of the missing organic carbon may be horizontally exported from Sechelt Inlet. Even considering the possibility of this loss of material, conservatively low predictions of the flux of organic carbon from the euphotic zone remain about 1.3 times greater than extrapolated sediment-trap fluxes and about 2.2 times greater than measured sediment-trap fluxes. Again, the discrepancy increases with the fraction of terrigenous organic carbon that comprises the total flux and with reductions of horizontal export from its maximal value.

It is hypothesized that much of the predicted export flux of organic carbon in Sechelt Inlet sank or diffused out of the euphotic zone and was either remineralized before reaching the sediment traps or was in a form that was not caught by the sediment traps. Mass

sedimentation succeeding diatom blooms such as the one observed during the study in Sechelt Inlet is a common feature in coastal waters (Wassmann, 1989; and references therein). Single cells and chains of diatoms and other phytoplankton will have low sinking rates and are possibly missed by sediment traps. Also, the downward diffusion of dissolved organic matter (DOM; Legendre and Gosselin, 1989) and perhaps suspended organic matter (SOM) will decrease fluxes of particulate organic matter (POM) while maintaining a flux of organic material away from the euphotic zone. Legendre and Gosselin (1989) suggested that export fluxes of organic material be considered equivalent to the downward flux of (DOM + POM), although they acknowledged that quantifying fluxes of DOM is difficult. The possibility that SOM composes a fraction of the export flux should be considered as well.

7.6 Use of the f-ratio for estimates of oxygen dynamics

7.6.1 Photosynthetic oxygen production from fP_n

Estimates of net carbon assimilation (P_n) and of photosynthetic oxygen production ($^{O_2}P_n$) from chapters 3 and 4 do not consider *in situ* heterotrophic consumption of organic carbon and oxygen. The net growth of the biological community in the euphotic zone is quantified by $P_c = P_{new} = f\ P_n$ for steady state (Platt *et al.*, 1989). The non-steady state term of equation 7.5 was found to be less than 10% of $(f_{NO_3^-})\ P_n$ in Sechelt Inlet during the experiment, so $f\ P_n$ may be used to approximate P_c. However, to convert net community production of organic carbon into oxygen production, the respiratory quotient of heterotrophs including zooplankton must be considered. RQ for zooplankton is similar to that for phytoplankton (Parsons *et al.*, 1984b), so multiplication of $f\ P_n$ by the photosynthetic quotient provides an estimate of $^{O_2}P_c$ (see section 4.2.2 and equation 4.6 for more explanation).

7.6.2 Quantification and degradation of the 'missing carbon'

In Sechelt Inlet, C_m can be quantified as:

$$C_m = (f - s)P_n - C_{hor} \tag{7.8}$$

s is the ratio (sediment-trap flux of autochthonous organic carbon)/(P_n) and was less than or equal to 0.2 during the experiment in Sechelt Inlet. C_{hor} is the amount of autochthonous organic carbon that is horizontally exported through Skookumchuck Narrows but is not replaced by incoming tidal currents. An upper estimate for C_{hor} is $0.38P_n$ (section 7.5). To evaluate the ultimate sink for the missing carbon that is not horizontally exported from Sechelt Inlet and assuming that it is either the water column or the sediments, C_m is considered separately as S/DOM and as POM.

S/DOM will not associate with the sediments, so the water column must be the ultimate sink for S/DOM or its concentration will increase with time. Remineralization by motile bacteria is considered the most likely mechanism of S/DOM removal. However, it is possible that bacteria consume S/DOM and are consumed or aggregate and sink, thereby translating S/DOM into POM.

A large fraction of C_m during the experiment might have been POM but was not caught by the sediment traps because its sinking rate was too small and Re was too large. Slowly sinking POM could associate with the sediments. However, if POM did comprise a large fraction of C_m, it probably did not settle into the sediments for two reasons. First, low sinking rates would have ensured that the water column residence time of C_m was long, allowing time for *in situ* remineralization by unattached, motile bacteria. The other reason comes from comparing two different ways of estimating benthic oxygen demand.

The estimates of benthic oxygen demand in chapter 6 come from oxidizing 65% of the flux to the sediments as estimated by sediment traps (Cowie and Hedges, 1992). The values obtained in this way agree with *in vivo* oxygen demand measured on sediment

cores from Norwegian fjords (Dale, 1978; Wassmann, 1984). If in Sechelt Inlet the flux to the sediments were much larger than that measured by sediment traps, then it would either be permanently buried and the ratio of (permanently buried carbon)/(sediment trap flux of carbon) would be much higher than 0.35 as measured in Dabob Bay and Saanich Inlet; or the benthic oxygen demand would be unusually high when compared to measurements in Norwegian fjords. Therefore, if the processes occurring in Sechelt Inlet can be compared to other temperate fjords, then a large fraction of C_m could not have been deposited onto the sediments.

Whether in the form of POM or S/DOM, it is hypothesized that the sink for most of the missing organic carbon in Sechelt Inlet was the water column. For long-term steady state to be maintained (on the order of months or years), this flux of organic material to the water column must be matched by remineralization and the oxidized compounds must be advected or diffused upwards to the euphotic zone where they were originally assimilated into organic material.

7.7 P_n and the sediment trap flux of organic carbon

A curious feature of the Sechelt Inlet data is the lack of correlation between P_n and the flux of organic material below the euphotic zone (figure 7.1a), despite the relatively high sinking rates of the silicate-bearing particles caught in the traps (figure 6.2). Nor can the organic particle flux to the sediment traps be correlated with the flow of fresh water from the Clowhom River (figure 7.1b).

Particles with high sinking rates in Sechelt may be large aggregates of diatoms, fecal pellets and dead zooplankton, and possibly terrigenous material. Fluxes of any two of these classes are not necessarily correlated, so describing the combination of factors that control the magnitude of organic carbon flux may require a complicated relationship

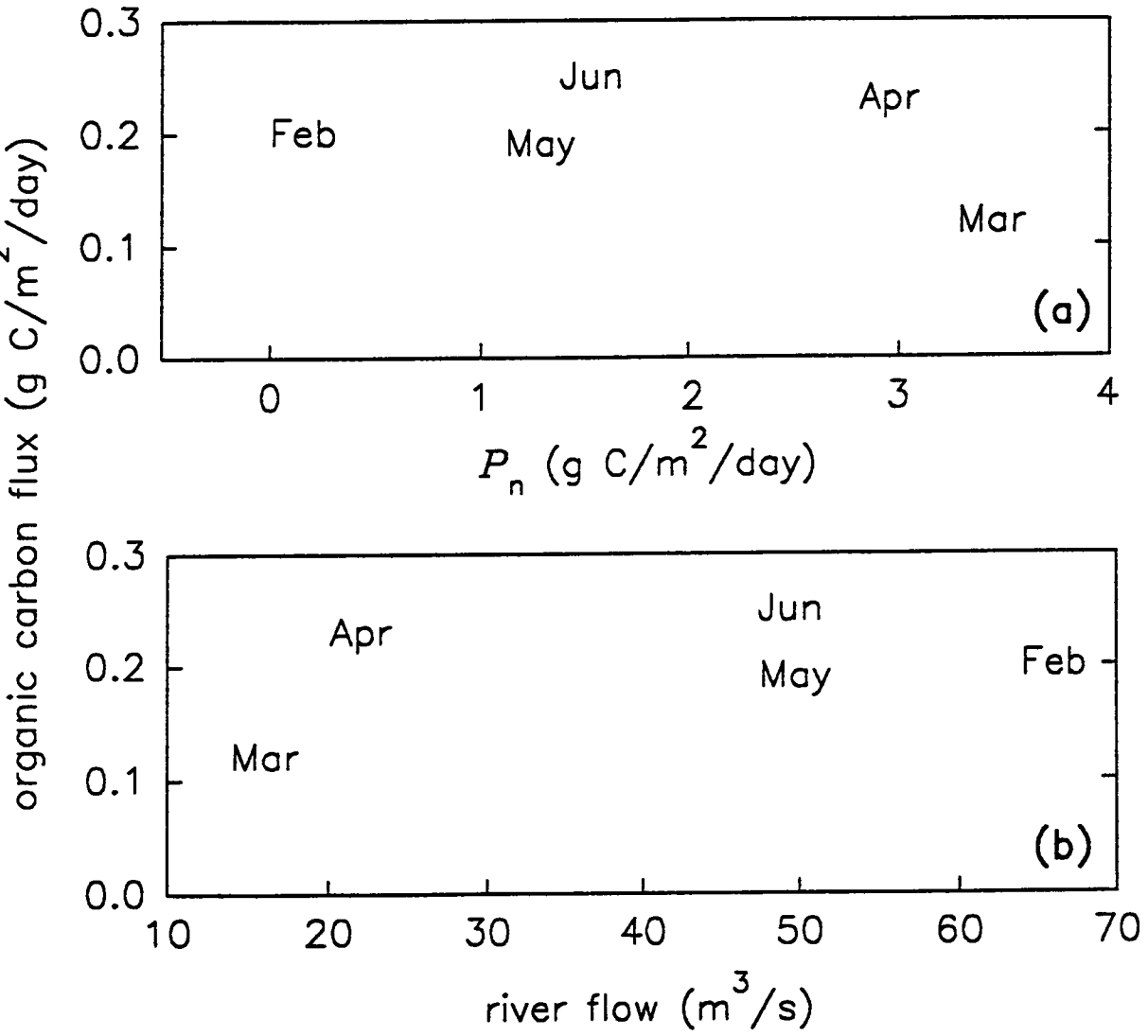

Figure 7.1: Relationship between the trap-measured flux of organic carbon and P_n (a) and the flow of water from the Clowhom River (b). The organic carbon flux (averaged over stations SC-3, SC-5.5 and SC-7 and over all trap depths {table 5.2}) is denoted by the month of the sediment trap deployment and correlated with P_n or river flow for the period of each deployment. Although not shown here, allowing for a one month delay between the forcing variable (P_n or river flow) and measured organic carbon flux gives the same lack of correlation.

between primary production, grazing and run-off. However, in light of the hypothesis that a large amount of organic carbon leaving the euphotic zone was not represented in the sediment traps, the possibility that the amount of material caught in a sediment trap is strongly influenced by one or more factors other than the true flux of (S/DOM + POM) cannot be ignored. Such factors may include conditions that control trapping efficiency. They may also involve poorly-understood physical dynamics of particle formation and disaggregation, perhaps facilitated by bacterial activity.

It is suggested that the organic carbon in the water column of Sechelt Inlet during the experiment be divided into two classes. The first comprises the organic carbon that was representatively caught by the sediment traps. The second includes organic matter passing through the water column but not caught by the sediment traps, the missing organic carbon. The class to which material belonged during the experiment was grossly determined by its sinking rate (which goes to zero for S/DOM), but changes in the sediment trap Reynolds number possibly affected the division between these classes. Furthermore, material may have moved between classes as changes in its sinking rate occurred. Regardless of the subtleties occurring between trapped and untrapped material, the mass of the material leaving the euphotic zone but not caught in the sediment traps may have been large relative to measured fluxes of organic material during the study period in Sechelt Inlet. The suggestion of this possibility is not novel. "(...) two size classes for particles must be considered; i.e. not only the large rapidly sinking particles (...), but also the fine particle size class that sinks slowly (< 1 m/day) if at all" (Martin *et al.*, 1987; and supported by references therein).

7.8 A profile of biologically-mediated oxygen fluxes

In earlier chapters, estimates of oxygen production and consumption have been made without acknowledging the dependence of deep-water processes on euphotic zone dynamics. However, consideration of the f-ratio shows that estimates of water column oxygen production and consumption made in chapters 4 and 6 may require significant modification. The results of this thesis are now summarized in the form of suggestions for determining oxygen production and consumption in Sechelt Inlet.

Organic carbon is assimilated in the euphotic zone at the rate fP_n. Three methods can be used to estimate f, all discussed in the text and summarized in table 7.1. The method of choice is suggested to be the regression equation of Harrison *et al.* (1987). However, the application of their regression equation requires ammonium and nitrate data and ammonium measurements may not be fully reliable because of freezing. Nonetheless, two years of NO_3^- and NH_4^+ measurements were made simultaneous to the chl*a* measurements used to produce figure 4.2. This data base may be used for an approximation of the f-ratio for any month of the year in Sechelt Inlet. P_n can be determined for any time period from ^{14}C uptake measurements, and with less certainty from chl*a* concentration and the relationship of equation 3.5 with an appropriate value for Υ. Photosynthetic oxygen production can then be determined by multiplying fP_n by the photosynthetic quotient and converting from moles to grams (equations 4.7 and 4.8). fP_n is also equivalent to the flux of organic carbon out of the euphotic zone.

The fate of the organic carbon that leaves the euphotic zone may be remineralization in the water column, horizontal export from the inlet, or diagenesis or permanent burial in the sediments. Benthic oxygen demand determined by oxidizing 65% of the trap-estimated flux to the sediments (section 6.5) agrees with other studies in temperate fjords, so the allotment of organic carbon diagenesis in the sediments made in this work

is probably reasonable. Suggesting a flux of material to the sediments for periods other than those represented by these data, however, cannot be done with certainty. The flux of organic carbon to the sediment traps was relatively constant during the experiment, and a correlation with a forcing parameter has not been found. Perhaps the flux of organic carbon to the sediments is best modeled as a constant.

There are two classes of material that will cause a water column oxygen demand; the particles that decay as they sink to the sediments and can be caught by traps, and the S/DOM and the slowly sinking POM that comprise the 'missing organic carbon' in Sechelt Inlet. The oxygen demand of the former is described in section 6.4 and quantified in figure 7.2. The latter, C_{m}, is quantified in equation 7.8 but its degradation is not considered in figure 7.2. It is suggested that C_{m} is remineralized in the water column, but the depth distribution is uncertain. Predicting the temporal relationship between fP_{n} and the remineralization of C_{m} is also problematic and errors may be manifest where temporal changes in fP_{n} are large. Large changes in fP_{n} might occur in the fall and in the spring when P_{n} changes dramatically, but might also occur with changes in f. Haigh *et al.* (1992) reported that nitrate becomes very low in Sechelt during summer months. Low nitrate concentrations will decrease the f-ratio (Harrison *et al.*, 1987) and, therefore, the expected flux of organic carbon from the euphotic zone.

Figure 7.2 is an example of an oxygen production and consumption profile in Sechelt Inlet and represents the conditions of the study period spatially and temporally averaged. It uses an f-ratio of 0.2 and it does not consider the 'missing organic carbon'. Therefore, although the sediment oxygen demand of figure 7.2 is thought to be reasonable, estimates of water column oxygen production and consumption are considered minima because the true f-ratio during the study period in Sechelt Inlet was probably greater than 0.2. If the f-ratio were 0.5 and about 20% of photosynthetically assimilated organic carbon were exported by estuarine circulation and tidal exchange, then water column production and

consumption of oxygen would be almost twice that shown in figure 7.2. The depth distribution of the consumption of S/DOM is not known, but would probably decrease with depth.

This work provides a starting point for numerical simulations of oxygen behavior in Sechelt Inlet and its priciples may be applicable to other British Columbia fjords. Water column oxygen consumption used for numerical simulations can be adjusted until results predict observed concentrations of oxygen. That exercise may help to elucidate the importance of S/DOM and slowly-sinking POM to water column biology and chemistry in coastal seas.

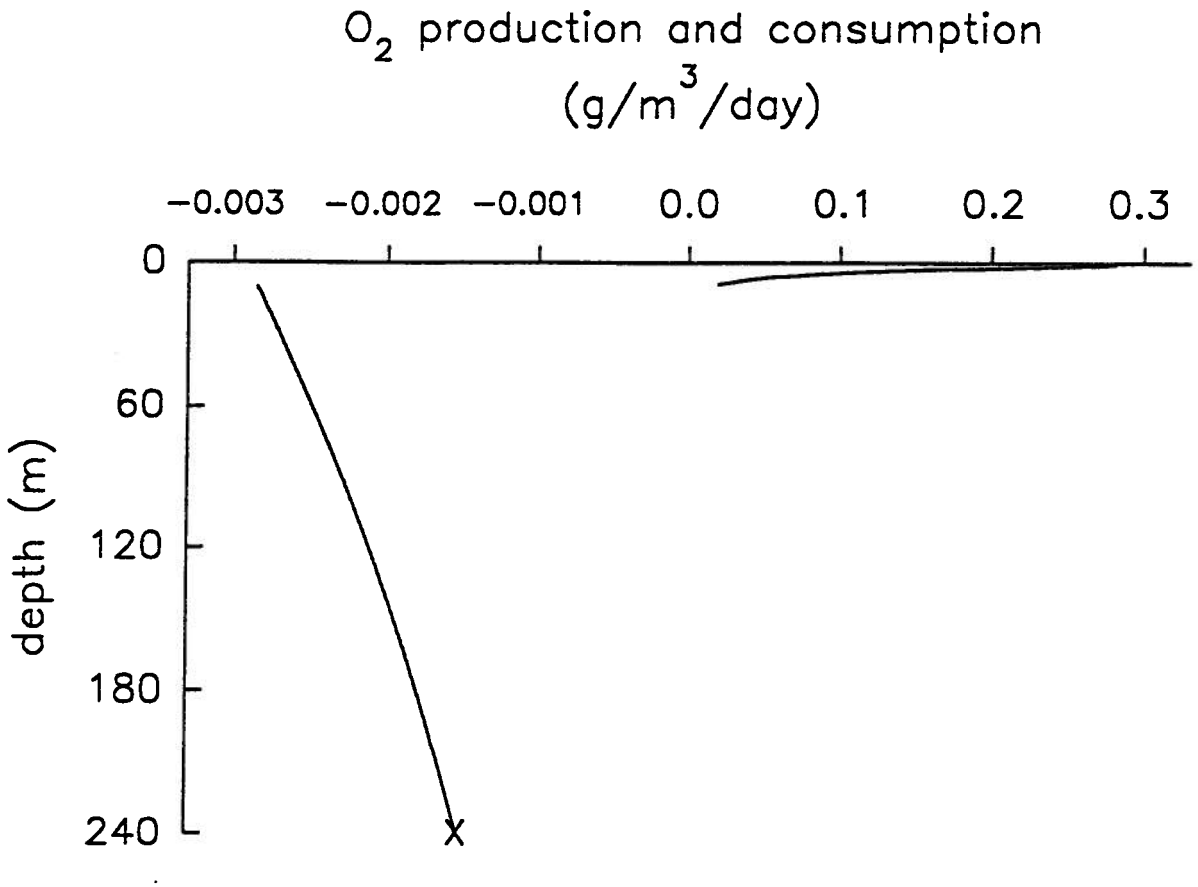

Figure 7.2: A generalized profile of oxygen production and consumption in Sechelt Inlet. Water depth is the average of the three sediment trap stations. Photosynthetic oxygen production is determined using the spatially and temporally averaged estimate for carbon assimilation of 1.6 $g/m^2/day$. $f = 0.2$ is used (section 7.6.1) so that photosynthetic oxygen production is 1.1 $g/m^2/day$ (equations 4.7 and 4.9) and 0.33 g $C/m^2/day$ leave the euphotic zone. The water column oxygen demand decreases exponentially from 0.0029 g $O_2/m^3/day$ at 9 m to 0.0015 g $O_2/m^3/day$ at 240 m (note the change in scale of the x-axis for positive and negative values). The sediment oxygen demand is 0.36 $g/m^2/day$ and is determined by oxidizing 65% of the organic carbon reaching the sediments (chapter 6). So that it has units of g $O_2/m^3/day$, the sediment oxygen demand is divided by the water depth of 240 m and denoted by an '×'. The sum of the water column and sediment oxygen demands, and the oxygen equivalent of the organic carbon that is permanently buried, is about 1.1 g $O_2/m^2/day$. An f-ratio different from 0.2 will have significant consequences for the interpretation of the data from Sechelt Inlet.

Bibliography

Alldredge, A. L. and C. Gotschalk. 1988. *In situ* Settling behavior of marine snow. Limnol. Oceanogr. 33: 339-351.

Alldredge, A. L. and M. W. Silver. 1988. Characteristics, Dynamics and significance of marine snow. Prog. Oceanog. 20: 41-82.

Angel, M. V. 1984. Detrital organic fluxes through pelagic ecosystems. in Flows of energy and materials in marine ecosystems. NATO Conf. Ser. 4, Mar. Sci. V. 13. Plenum Press.

Ansell, A. D. 1974. Sedimentation of organic detritus in lochs Etive and Creran, Argyll, Scottland. Mar. Biol. 27: 263-273.

Asper, V. L. 1987. Measuring the flux and sinking speed of marine snow aggregates. Deep-Sea Res. 34: 1-17.

Baker, P. D. 1992. Low frequency residual circulation in Knight Inlet. Ph.D. U.B.C.

Banse, K. 1990. New views on the degradation and disposition of organic particles as collected by sediment traps in the open sea. Deep-Sea Res. 37: 1177-1195.

Billett, D. S. M., R. S. Lampitt, A. L. Rice and R. F. C. Mantoura. 1983. Seasonal sedimentation of phytoplankton to the deep-sea benthos. Nature 302: 520-522.

Bloesch, J. 1982. Inshore-offshore sedimentation differences resulting from resuspension in the Eastern Basin of Lake Erie. Can. J. Fish. Aquat. Sci. 39: 748-759.

Butman, C. A. 1986. Sediment trap biases in turbulent flows: Results from a laboratory flume study. J. Mar. Res. 44: 645- 693.

Butman, C. A., W. D. Grant and K. D. Stolzenbach. 1986. Predictions of sediment trap biases in turbulent flows: A theoretical analysis based on observations from the literature. J. Mar. Res. 44: 601-644.

Calvert, S. E., R. M. Bustin and T. F. Pedersen. 1992. Lack of evidence for enhanced preservation of sedimentary organic matter in the oxygen minimum of the Gulf of California. Geology 20: 757-760.

Calvert, S. E. and T. F. Pedersen. 1992. Organic carbon accumulation and preservation in marine sediments: how important is anoxia? in Organic Matter: Productivity, Accumulation, and Preservation in Recent and Ancient Sediments, editors J. K. Whelan and J. W. Farrington. 231- 263. Columbia University Press.

Campbell, J. W. and J. E. O'Reilly. 1988. Role of satellites in estimating primary productivity on the northwest Atlantic continental shelf. Continental Shelf Research 8: 179-204.

Canfield, D. E. 1989. Sulfate reduction and oxic respiration in marine sediments: implications for organic carbon preservation in euxinic environments. Deep-Sea Res. 36: 121-138.

Carpenter, E. J. and J. S. Lively. 1980. Review of estimates of algal growth using ^{14}C tracer techniques. in Primary Productivity in the Sea, editor P. G. Falkowski. 161-178. New York: Plenum Press.

Carpenter, J. H. 1965. The Chesapeake Bay Institute technique for the Winkler dissolved oxygen method. Limnol. Oceanogr. 10: 141-143.

Cho, B. C. and F. Azam. 1988. Major role of bacteria in biogeochemical fluxes in the ocean's interior. Nature 332: 441-443.

Clifford, P. J., P. J. Harrison, K. Yin, M. A. St. John and R. H. Goldblatt. 1992. Plankton production and nutrient dynamics in the Fraser River Plume, 1991. Volume 1. Manuscript report no. 59. Dept. of Oceanography, U.B.C.

Cowie, G. L. and J. I. Hedges. 1992. The role of anoxia in organic matter preservation in coastal sediments: relative stabilities of the major biochemicals under oxic and anoxic depositional conditions. Org. Geochim. 19: 229-234.

Cullen, J. J. 1982. The deep chlorophyll maximum: comparing vertical profiles of chlorophyll *a*. Can. J. Fish. Aquat. Sci. 39: 791-803.

Cullen, J. J. 1990. On models of growth and photosynthesis in phytoplankton. Deep-Sea Res. 37: 667-683.

Cullen, J. J., R. J. Geider, J. Ishizaka, D. A. Kiefer, J. Marra, E. Sakshaug and J. A. Raven. 1991. Toward a general description of phytoplankton growth for biogeochemical models. in Proceedings of NATO ARW on Modelling of Marine Biogeochemical Cycles, editors G. T. Evans and M. J. R. Fasham. Springer Press.

Dagg, M. J., B. W. Frost and W. E. Jr. Walser. 1989. Copepod diel migration, feeding, and the vertical flux of pheopigments. Limnol. Oceanogr. 34: 1062-1071.

Dale, T. 1978. Total, chemical and biological oxygen consumption of the sediments in Lindaspollene, Western Norway. Mar. Biol. 49: 333-341.

Davies, J. M. and R. Payne. 1984. Supply of organic matter to the sediment in the northern North Sea during a spring phytoplankton bloom. Mar. Biol. 78: 315-324.

Dugdale, R. C. and J. J. Goering. 1967. Uptake of new and regenerated forms of nitrogen in primary productivity. Limnol. Oceanogr. 12: 196-206.

Dunbar, R. B. and W. H. Berger. 1981. Fecal pellet flux to modern bottom sediment of Santa Barbara Basin (California) based on sediment trapping. Geological Society of America Bulletin part 1(vol. 2): 212-218.

Dymond, J. 1984. Sediment traps, particle fluxes, and benthic boundary layer processes. NAS Global Flux Workshop, Woods Hole, MA.

Eppley, R. W. and B. J. Peterson. 1979. Particulate organic matter flux and planktonic new production in the deep ocean. Nature 282: 677-680.

Eppley, R. W. and P. R. Sloan. 1965. Carbon balance experiments with marine phytoplankton. J. Fish. Res. Bd. Canada 22: 1083-1097.

Eppley, R. W., E. Stewart, M. R. Abbott and U. Heyman. 1985. Estimating ocean primary production from satellite chlorophyll. Introduction to regional differences and statistics for the Southern California Bight. J. Plankton Res. 7: 57-70.

Falkowski, P. G. 1980. Light-shade adaptation in marine phytoplankton. in Primary Productivity in the Sea, editor P. G. Falkowski. 99-119. New York: Plenum Publishing Corp.

Fitzwater, S. E., G. A. Knauer and J. H. Martin. 1982. Metal contamination and its effect on primary production measurements. Limnol. Oceanogr. 27: 544-551.

Fleming, R. H. 1940. Composition of plankton and units for reporting populations and production. in Proceedings of the Sixth Pacific Science Congress of the Pacific Science Association, Stanford University and San Francisco, 1939.

Fowler, S. W. and G. A. Knauer. 1986. Role of large particles in the transport of elements and organic compounds through the oceanic water column. Prog. Oceanog. 16: 147-194.

Francois, R. 1987. Some aspects of the geochemisty of sulphur and iodine in marine humic substances and transition metal enrichment in anoxic sediments. Ph.D. U.B.C.

Froelich, P. N., G. P. Klinkhammer, M. L. Bender, N. A. Luedtke, G. R. Heath, D. Cullen, P. Dauphin, D. Hammond, B. Hartman and V. Maynard. 1979. Early oxidation of organic matter in pelagic sediments of the eastern equatorial Atlantic: suboxic diagenesis. Geochim. Cosmochim. 43: 1075-1090.

Gardner, W. D. 1980a. Sediment trap dynamics and calibration: a laboratory evaluation. J. Mar. Res. 38: 17-39.

Gardner, W. D. 1980b. Field assessment of sediment traps. J. Mar. Res. 38: 41-52.

Gardner, W. D. 1985. The effects of tilt on sediment trap efficiency. Deep-Sea Res. 32: 349-361.

Haigh, R., F. J. R. Taylor and T. F. Sutherland. 1992. Phytoplankton ecology of Sechelt Inlet, a fjord system on the British Columbia coast. I. General features of the nano- and microplankton. Mar. Ecol. Prog. Ser. 89: 117-134.

Hargrave, T. 1978. Seasonal changes in oxygen uptake by settled particulate matter and sediments in a marine bay. J. Fish. Res. Board Can. 35: 1621-1628.

Harrison, W. G., T. Platt and M. R. Lewis. 1987. f-Ratio and its relationship th ambient nitrate concentration in coastal waters. J. Plankton Res. 9: 235-248.

Hasle, G. R. 1978. Using the inverted microscope. in Phytoplankton manual. Monographs on oceanographic methodology 6, editor A. Sournia. 191-196. Paris: UNESCO.

Hedges, J. I., W. A. Clark and G. L. Cowie. 1988. Fluxes and reactivities of organic matter in a coastal marine bay. Limnol. Oceanogr. 33: 1137-1152.

Hedges, J. I., W. A. Clark and G. L. Cowie. 1988. Organic matter sources to the water column and surficial sediments of a marine bay. Limnol. Oceanogr. 33: 1116-1136.

Hedges, J. I., C. Lee, S. G. Wakeman, P. J. Hernes and M. L. Peterson. 1993. Effects of poisons and preservatives on the fluxes and elemental compositions of sediment trap materials. J. Mar. Res. 51: 651-668.

Henrichs, S. M. and W. S. Reeburgh. 1987. Anarerobic mineralization of marine sediment organic matter: rates and the role of anaerobic processes on the oceanic carbon economy. Geomicrobiology Journal 5: 191-237.

Hinga, K. R., J. M. Sieburth and G. R. Heath. 1979. The supply and use of organic material at the deep-sea floor. J. Mar. Res. 37: 557-579.

Huffman, D. W. D., Jr. 1977. Performance of a new automatic carbon dioxide coulometer. Microchem. J. 22: 567-573.

Hurd, D. C. 1973. Interactions of biogenic opal, sediment and seawater in the Central Equatorial Pacific. Geochim. Cosmochim. Acta. 37: 2257-2282.

Iverson, R. L., H. F. Bittaker and V. B. Myers. 1976. Loss of radio carbon in direct use of Aquasol for liquid scintillation counting of solutions containing ^{14}C-$NaHCO_3$. Limnol. Oceanogr. 21: 756-758.

Karl, D. M., G. A. Knauer and J. H. Martin. 1988. Downward flux of particulate organic matter in the ocean: a particle decomposition paradox. Nature 332: 438-441.

Kiefer, D. A. and B. G. Mitchell. 1983. A simple, steady state description of phytoplankton growth based on absorption cross section and quantum efficiency. Limnol. Oceanogr. 28: 770- 776.

Knock, C. 1993. Literature survey of sediment oxygen demand. Manuscript report no. 61. Dept. of Oceanography, U.B.C.

King, F. D., A. H. Devol and T. T. Packard. 1978. Plankton metabolic activity in the eastern tropical North Pacific. Deep-Sea Res. 25: 689-704.

Kremer, B. P. 1981. Dark reactions of photosynthesis. in Physiological Bases of Phytoplankton Ecology, editor T. Platt. 44-54. Can. Bull. Fish. Aquat. Sci.

Lampitt, R. S. 1985. Evidence for the seasonal deposition of detritus to the deep-sea floor and its subsequent resuspension. Deep-Sea Res. 32: 885-897.

Lampitt, R. S., T. Noji and B. von Bodungen. 1990. What happens to zooplankton faecal pellets? Implications for material flux. Mar. Biol. 104: 15-23.

Laws, E. A. 1991. Photosynthetic quotients, new production and net community production in the open ocean. Deep-Sea Res. 38: 143-167.

Laws, E. A. and T. T. Bannister. 1980. Nutrient- and light- limited growth of *Thalassiosira fluviatilis* in continuous culture, with implications for phytoplankton growth in the ocean. Limnol. Oceanogr. 25: 457-473.

Lazier, J. R. N. 1963. Some aspects of the oceanographic structure of the Jervis Inlet system. M.Sc. U.B.C.

Legendre, L. and M. Gosselin. 1989. New production and export of organic matter to the deep ocean: Concequences of some recent discoveries. Limnol. Oceanogr. 34: 1374-1380.

Levasseur, M., P. A. Thompson and P. J. Harrison. 1993. Physiological acclimation of marine phytoplankton to different nitrogen sources. J. Phycol. 29: 587-595.

Martin, J. H., G. A. Knauer, D. M. Karl and W. W. Broenkow. 1987. VERTEX: carbon cycling in the northeast Pacific. Deep-Sea Res. 34: 267-285. p. 281.

McCave, I. N. 1984. Size spectra and aggregation of suspended particles in the deep ocean. Deep-Sea Res. 31: 329-352.

Michaels, A. F., M. W. Silver, M. M. Gowing and G. A. Knauer. 1990. Cryptic zooplankton swimmers in upper ocean sediment traps. Deep-Sea Res. 37: 1285-1296.

Mortlock, R. A. and P. N. Froelich. 1989. A simple method for the rapid determination of biogenic opal in pelagic marine sediments. Deep-Sea Res. 36: 1415-1426.

Murray, J. W., V. Grundmanis and W. M. Jr. Smethie. 1978. Interstitial water chemistry in the sediments of Saanich Inlet. Geochim. Cosmochim. 42: 1011-1026.

Parsons, T. R., Maita, Y. and Lalli, C. M. 1984a. A Manual of Chemical and Biological Methods for Seawater Analysis. Oxford, New York, Seoul, Tokyo: Pergamon press.

Parsons, T. R., Takahashi, M. and Hargrave, B. 1984b. Biological Oceanographic Processes: third edition. New York: Pergamon Press, Inc.

Pedersen, T. F., G. B. Shimmield and N. B. Price. 1992. Lack of enhanced preservation of organic matter in sediments under the oxygen minimum on the Oman Margin. Geochim. Cosmochim. 56: 545-551.

Peinert, R., A. Saure, P. Stegmann, C. Stienen, H. Haardt and V. Smetacek. 1982. Dynamics of primary production and sedimentation in a coastal ecosystem. Netherlands Journal of Sea Research 16: 276-289.

Peterson, B. J. 1980. Aquatic primary productivity and the $^{14}CO2$ method: A history of the productivity problem. Ann. Rev. Ecol. Syst. 11: 359-385.

Pickard, G. L. 1961. Oceanographic features of inlets in the British Columbia mainland coast. J. Fish. Res. Board Can. 18: 907-999.

Pilskan, C. H. and S. Honjo. 1987. The fecal pellet fraction of biogeochemical particle fluxes to the deep sea. Global Biogeochemical Cycles 1: 31-48.

Pitcher, G. C. 1986. Sedimentary flux and the formation of resting spores of selected *Chaetoceros* species at two sites in the southern Benguela system. S. Afr. J. Mar. Sci. 4: 231- 244.

Platt, T. 1986. Primary production of the ocean water column as a function of surface light intensity: algorithms for remote sensing. Deep-Sea Res. 33: 149-163.

Platt, T., K. L. Denman and A. D. Jassby. 1977. Modeling the productivity of phytoplankton. in The Sea, editors E. D. Goldberg, I. N. McCave, J. J. O'Brien and J. H. Steele. 807- 856. New York: John Wiley & Sons.

Platt, T. and W. G. Harrison. 1985. Biogenic fluxes of carbon and oxygen in the ocean. Nature 318: 55-58.

Platt, T., W. G. Harrison, M. R. Lewis, W. K. W. Li, S. Sathyendranath, R. E. Smith and A. F. Vezina. 1989. Biological production of the oceans: the case for a consensus. Mar. Ecol. Prog. Ser. 52: 77-88.

Platt, T., S. Sathyendranath, C. M. Caverhill and M. R. Lewis. 1988. Ocean primary production and available light: further algorithms for remote sensing. Deep-Sea Res. 35: 855-879.

Raven, J. A. and J. Beardall. 1981. Respiration and photorespiration. in Physiological Bases of Phytoplankton Ecology, editor T. Platt. 55-82. Can. Bull. Fish. Aquat. Sci.

Redfield, A. C., B.H. Ketchum and F.A. Richards. 1963. The influence of organisms on the composition of sea-water. in The Sea, editor M.N. Hill. 26-77. New York, London, Sydney: John Wiley & Sons: Interscience Publishers.

Richards, F. A. 1965. Anoxic basins and fjords. in Chemical Oceanography, editors J. P. Riley and G. Skirrow. 611-645. London and New York: Academic Press Inc.

Ricker, W. E. 1984. Computation and uses of central trend lines. Can. J. Zool. 62: 1897-1905.

Ryther, J. H. 1956a. Photosynthesis in the ocean as a function of light intensity. Limnol. Oceanogr. 1: 61-70.

Ryther, J. H. 1956b. The measurement of primary production. Limnol. Oceanogr. 1: 72-84.

Ryther, J. H. and D. W. Menzel. 1965. Comparison of the ^{14}C- technique with direct measurement of photosynthetic carbon fixation. Limnol. Oceanogr. 10: 490-492.

Ryther, J. H. and C. S. Yentsch. 1957. The estimation of phytoplankton production in the ocean from chlorophyll and light data. Limnol. Oceanogr. 2: 281-286.

Sakshaug, E. 1977. Limiting nutrients and maximum growth rates for diatoms in Narragansett Bay. J. Exp. Mar. Biol. Ecol. 28: 109-123.

Sakshaug, E. and K. Andersen. 1986. Effect of light regime upon growth rate and chemical composition of a clone of *Skeletonema costatum* from the Trondheimfjord, Norway. J. Plankton Res. 8: 619-637.

Sakshaug, E., K. Andersen, S. Myklestad and Y. Olsen. 1983. Nutrient status of phytoplankton communities in Norwegian waters (marine, brackish, and fresh) as revealed by their chemical composition. J. Plankton Res. 5: 175-196.

Sakshaug, E., K. Andersen and D. A. Kiefer. 1989. A steady state description of growth and light absorption in the marine planktonic diatom *Skeletonema costatum.* Limnol. Oceanogr. 34: 198-205.

Sancetta, C. and S. E. Calvert. 1988. The annual cycle of sedimentation in Saanich Inlet, British Columbia: implications for the interpretation of diatom fossil assemblages. Deep-Sea Res. 35: 71-90.

Sathyendranath, S., T. Platt, C. M. Caverhill, R. E. Warnock and M. R. Lewis. 1989. Remote sensing of oceanic primary production: computations using a spectral model. Deep-Sea Res. 36: 431-453.

Shuter, B. 1979. A model of physiological adaptation in unicellular algae. J. Theor. Biol. 78: 519-552.

Siegel, D. A., T. C. Granata, A. F. Michaels and T. D. Dickey. 1990. Mesoscale eddy diffusion, particle sinking, and the interpretation of sediment trap data. J. Geophys. Res. 95: 5305-5311.

Smayda, T. J. 1970. The suspension and sinking of phytoplankton in the sea. Oceanogr. Mar. Biol. Ann. Rev. 8: 353-414.

Smetacek, V., K. von Brockel, B. Zeitzschel and W. Zenk. 1978. Sedimentation of particulate matter during a phytoplankton spring bloom in relation to the hydrographical regime. Mar. Biol. 47: 211-226.

Smethie, W. M. Jr. 1987. Nutrient regeneration and denitrification in low oxygen fjords. Deep-Sea Res. 34: 983-1006.

Smethie, W. M. Jr. 1981. Vertical mixing rates in fjords determined using radon and salinity as tracers. Estuarine, Coastal and Shelf Science 12: 131-153.

Sokal, R. R. and Rohlf, F. J. 1981. Biometry. New York: W.H. Freeman and Co.

Strickland, J. D. H. and Parsons, T. R. 1968. A Practical Handbook of Seawater Analysis. Bull. Fish. Res. Bd. Can.

Suess, E. 1980. Particlate organic carbon flux in the oceans - surface productivity and oxygen utilization. Nature 288: 260- 263.

Sutherland, T. 1991. Phytoplankton succession and resting stage occurrence in three regions in Sechelt Inlet, British Columbia. M.Sc. U.B.C.

Sutherland, T. F., C. Leonard and F. J. R. Taylor. 1992. A segmented pipe sampler for integrated profiling of the upper water column. J. Plank. Res. 14: 915-923.

Taylor, F. J. R., R. Haigh and T. F. Sutherland. 1994. Phytoplankton ecology of Sechelt Inlet, a fjord system on the British Columbia coast. II. Potentially harmful species. Mar. Ecol. Prog. Ser. 103: 151-164.

Tinnis, S.W. in progress. The circulation and energetics of the Sechelt Inlet system, British Columbia. Ph.D. U.B.C.

Toth, D. J. and A. Lerman. 1977. Organic matter reactivity and sedimentation rates in the ocean. Am. Jour. Sci. 277: 465- 485.

Turpin, D. H. and H. G. Weger. 1990. Interactions between photosynthesis, respiration and nitrogen assimilation. in Plant Physiology, Biochemistry and Molecular Biology, editors D. T. Dennis and D. H. Turpin. 422-433. Essex, London: Longman Scientific & Technical.

Waite, A. M. 1992. Physiological control of diatom sedimentation. Ph.D. U.B.C.

Waite, A. M., P. A. Thompson and P. J. Harrison. 1992. Does energy control the sinking rates of marine diatoms? Limnol. Oceanogr. 37: 468-477.

Wakeman, S. G., J. I. Hedges, C. Lee and T. K. Pease. 1993. Effects of poisons and preservatives on the composition of organic matter in a sediment trap experiment. J. Mar. Res. 51: 669-696.

Walsh, I., J. Dymond and R. Collier. 1988a. Rates of recycling of biogenic components of settling particles in the ocean derived from sediment trap experiments. Deep-Sea Res. 35: 43-58.

Walsh, I., K. Fischer, D. Murray and J. Dymond. 1988b. Evidence for resuspension of rebound particles from near-bottom sediment traps. Deep-Sea Res. 35: 59-70.

Ward, B. B., K. A. Kilpatrick, E. H. Renger and R. W. Eppley. 1989. Biological nitrogen cycling in the nitracline. Limnol. Oceanogr. 34: 493-513.

Wassmann, P. 1983. Sedimentation of organic and inorganic particulate material in Lindaspollene, a stratified, land- locked fjord in western Norway. Mar. Ecol. Prog. Ser. 13: 237-248.

Wassmann, P. 1984. Sedimentation and benthic mineralization of organic detritus in a Norwegian fjord. Mar. Biol. 83: 83-94.

Wassmann, P. 1989. Sedimentation of organic matter and silicate from the euphotic zone of the Barents Sea. Rapp. P.-v. Reun. Cons. int. Explor. Mer. 188: 108-114.

Wilkinson, L. 1990. SYSTAT: The System for Statistics. Evanston, IL: SYSTAT, Inc.

Appendix A

Species composition

A thorough examination of the spatial and temporal distribution of phytoplankton species in Sechelt Inlet was carried out over a three year period by Haigh et al. (1992), and Taylor et al. (1994). In general, the timing of successional trends and the magnitude of species populations in the winter, spring and early summer of 1991 were similar to those in 1988, 1989 and 1990. A brief chronological description of the phytoplankton dynamics during the study period follows. The discussion is limited to the central region of the inlet where ^{14}C incubations were performed. All cell concentrations represent integration of the top 20 m of the water column (section 2.4.1). This technique may over or under estimate the population concentration at a particular depth by as much as an order of magnitude.

January and February: These months were dominated by nanoflagellates (the chryptophytes *Rhodomonas* and *Plagioselmis* were the only nanoflagellates counted with any certainty) with cell concentrations on the order of 10^4/l to 10^5/l. *Skeletonema costatum* and *Thalassiosira nordenskioeldii* were the dominant diatoms with *S. costatum* reaching concentrations of 10^4/l, but generally found at 10^2/l to 10^3/l. The dinoflagellates *Katodinium rotundatum* and *Gyrodinium* spp. and ciliates were as high as 10^3/l during this period of the study.

March: The diversity and abundance of phytoplankton increased dramatically between the months of February and March. *S. costatum* (10^7/l) and *T. nordenskioeldii* (10^6/l) dominated the system. Other abundant diatoms with concentrations greater than 10^4/l include *Thalassiosira* spp., *Chaetoceros* spp., *Ditylum brightwellii*, *Cylindrotheca closterium* and *Pseudonitzschia delicatissima.* Dinoflagellates (especially photosynthetic

and non-photosynthetic thecates), nanoflagellates, and ciliates all increased in concentration between February and March, but those populations were strongly masked by the diatom bloom.

April and May: For these months, the chl*a* concentrations were an order of magnitude less then they were in March. Nonetheless, species diversity continued to increase. Diatoms still dominated in the central portion of the inlet, but the species composition began to shift to one commonly found in the summer. *S. costatum* dominated at concentrations of 10^6/l, *Thalassiosira nordenskioeldii* was found as high as 10^5/l but was 'patchy' and other *Thalassiosira* spp. were about 10^3/l. *Chaetoceros* spp. became more abundant (10^3 to 10^4 cells l^{-1}) and diverse in April, and reached concentrations of 10^5/l in May. Among diatoms found in concentrations greater than 10^3/l are *Cerataulina pelagica*, *Leptocylindrus* spp., *P. delicatissima*, *Rhizosolenia fragilissima*, *D. brightwellii*, and *C. closterium.* The diversity of diatom species below 10^3/l increased in April and May from that in March.

The number of observed dinoflagellate species in April and May increased from previous months, but were usually below 10^3/l. Dinoflagellates were dominated by *Gyrodinium* spp. and *Gymnodinium* spp., with *Heterocapsa triquetra* and *K. rotundatum* reaching 10^3/l at specific locations. Nanoflagellates remained at 10^4/l to 10^5/l.

Evidence of grazing in April and May include increases in copepods and their fecal pellets, in planktonic larvae, and in tintinnids; as well as an abundant (10^3/l to 10^4/l) and diverse population of ciliates.

June: Species composition changed substantially between sampling dates in May and June. The euphotic zone was dominated by cryptomonads (10^6/l), the prymnesiophyte *Chrysochromulina* spp. (10^5/l), and the raphidophyte *Heterosigma carterie* (10^5/l). Thecate and non-thecate dinoflagellates summed to approximately $2x10^4$/l and were most

abundantly represented by *Gonyiodoma pseudogonyaulax* ($5x10^3$/l). *Scrippsiella trochoidea*, *Micracanthodinium claytonii*, *Alexandrium tamarense*, *Gyrodinium fusiforme*, and *Prorocentrum* sp. all at about 10^3/l.

The diatom population became more patchy in June, but in general was dominated by *Chaetoceros* spp. and *S. costatum*, both at 10^4/l. *T. nordenskioeldii* dropped to less than 10^3/l. Other species that had concentrations at or greater than 10^3/l include *Cylindrotheca longissima*, and *Thalassionema nitzschiodes*. Large diatoms such as *Coscinodiscus* spp., *Pleurosigma* spp., and *Gyrosigma spencerii* may have disproportionately contributed to the chlorophyll biomass relative to their abundance.

The evidence for grazing in June was very similar to that in April and May.

Appendix B.1

Temperature, salinity, dissolved O_2 and nutrients

Presented are tables of temperature, salinity, dissolved oxygen and nutrients collected during the study period in Sechelt Inlet. The methods of collection and analysis for these data are described in chapter 2. For consistency with the text of this work, oxygen concentrations are given in mg/l. Multiplication of mg/l by 0.7 gives oxygen concentration in ml/l. Percent oxygen saturation is also reported, and is relative to equilibrium at one atmosphere of pressure and *in situ* salinity and temperature.

This appendix provides the data of the months December through March.

depth	temp	sal	oxygen		depth	NO_3^-	PO_4^{3-}	NH_4^+
m	°C		mg/l	% sat	m	μM	μM	μM
SC-1: 12 December, 1990								
0	8.1	24.457	-	-	-	-	-	-
2	8.54	25.691	7.71	77.4	-	-	-	-
5	8.71	26.089	7.57	76.4	-	-	-	-
10	9.07	26.924	6.84	70.0	-	-	-	-
20	9.58	29.520	5.21	54.9	-	-	-	-
30	9.66	29.808	5.08	53.8	-	-	-	-
50	9.69	29.948	4.95	52.5	-	-	-	-
60	9.73	30.068	4.83	51.2	-	-	-	-
75	9.75	30.131	4.73	50.2	-	-	-	-
SC-2: 11 December, 1990								
0	6.5	19.606	-	-	0-1.5	16.9	1.0	0.2
2	8.49	23.918	7.62	75.5	1.5-3	11.6	1.3	0.5
5	8.81	24.793	7.20	72.2	3-6	16.8	1.2	0.1
10	8.79	25.289	7.20	72.4	9-12	19.2	1.5	0.1
20	8.94	25.863	6.92	70.2	18-21	19.5	1.6	0.1
30	9.13	26.600	6.44	65.9	30	19.9	0.4	2.6
50	10.46	28.143	4.44	47.3	50	20.2	0.6	0.5
75	9.87	28.358	3.93	41.4	75	18.6	1.1	0.4
100	9.07	28.616	2.50	25.9	100	26.2	1.9	0.9
150	8.66	28.795	1.64	16.9	-	-	-	-
200	8.63	28.819	1.66	17.0	-	-	-	-
250	8.63	28.839	1.2	12.5	-	-	-	-
SC-2.5: 11 December, 1990								
-	-	-	-	-	0-1.5	16.4	-	3.5
-	-	-	-	-	1.5-3	18.3	-	2.4
-	-	-	-	-	3-6	19.1	-	0.8
-	-	-	-	-	9-12	19.9	-	0.1
-	-	-	-	-	18-21	16.4	-	0.0
SC-3: 11 December, 1990								
0	6.3	19.362	-	-	0-1.5	10.7	1.7	0.1
2	8.73	24.968	7.32	73.5	1.5-3	16.2	0.9	0.8
5	8.90	25.688	7.02	71.1	3-6	12.6	1.3	0.3
10	8.95	25.920	6.92	70.3	9-12	19.0	1.6	0.1
20	9.20	26.465	6.55	67.1	18-21	18.8	1.4	0.3
30	9.58	26.792	6.20	64.2	-	-	-	-
50	10.65	28.137	4.18	44.8	-	-	-	-
75	9.96	28.318	4.18	44.1	-	-	-	-
100	9.18	28.589	2.47	25.6	-	-	-	-
150	8.66	28.802	1.54	15.8	-	-	-	-
200	8.62	28.825	1.57	16.1	-	-	-	-
250	8.62	28.829	1.3	13.5	-	-	-	-

Table B.1: Temperature, salinity, dissolved O_2 and nutrients: December.

depth m	temp °C	sal	oxygen mg/l	oxygen % sat	depth m	NO_3^- μM	PO_4^{3-} μM	NH_4^+ μM
SC-4: 12 December, 1990								
0	6.5	21.544	-	-	-	-	-	-
2	7.73	22.698	8.22	79.3	-	-	-	-
5	8.69	24.519	7.31	73.0	-	-	-	-
10	8.82	25.119	7.25	73.0	-	-	-	-
20	9.17	25.951	6.80	69.3	-	-	-	-
30	9.57	26.456	6.32	65.3	30	16.9	0.4	2.2
50	10.76	28.127	3.90	41.8	50	13.5	0.8	0.1
75	10.20	28.341	4.03	42.7	75	22.6	1.4	0.2
100	9.58	28.511	2.64	27.7	100	19.2	1.2	0.3
150	8.66	28.814	1.3	13.8	-	-	-	-
200	8.62	28.831	1.3	13.8	-	-	-	-
225	8.61	28.830	1.50	15.4	-	-	-	-
SC-5: 12 December, 1990								
0	6.5	20.021	-	-	0-1.5	15.3	-	0.2
2	6.71	20.744	8.97	83.3	1.5-3	10.4	1.8	0.2
5	8.70	24.438	7.28	72.7	3-6	18.4	1.6	0.2
10	9.10	25.431	6.97	70.7	9-12	20.1	2.5	0.1
20	9.36	25.988	6.62	67.9	18-21	19.9	2.5	0.5
30	9.83	26.419	6.21	64.5	-	-	-	-
50	10.73	27.818	4.53	48.5	-	-	-	-
75	10.30	28.380	3.53	37.5	-	-	-	-
100	9.55	28.550	1.88	19.7	-	-	-	-
125	8.76	28.776	1.2	12.6	-	-	-	-
150	8.66	28.802	1.3	13.8	-	-	-	-
200	8.62	28.832	1.4	14.5	-	-	-	-
SC-6: 12 December, 1990								
0	5.5	18.054	-	-	0-1.5	15.8	1.4	0.6
2	7.30	20.859	8.82	83.2	1.5-3	10.3	1.0	0.2
5	8.95	24.352	7.20	72.3	3-6	16.9	1.3	0.3
10	9.38	25.410	6.68	68.3	9-12	-	-	-
20	9.91	26.229	6.14	63.8	18-21	15.1	1.6	0.0
30	10.09	26.750	5.62	58.9	30	18.9	1.2	0.2
50	10.75	28.051	3.60	38.6	50	20.7	2.3	0.6
75	10.15	28.398	2.61	27.7	75	21.4	1.8	2.9

Table B.2: December continued.

depth	temp	sal	oxygen		depth	NO_3^-	PO_4^{3-}	NH_4^+
m	°C		mg/l	% sat	m	μM	μM	μM
SC-7: 12 December, 1990								
0	7.4	20.151	-	-	0-1.5	12.6	-	0.1
2	8.54	23.956	7.65	75.9	1.5-3	15.0	-	0.1
5	8.89	24.923	7.11	71.6	3-6	13.4	-	0.1
10	9.18	25.535	6.95	70.8	9-12	15.7	-	0.0
20	9.53	26.126	6.42	66.2	18-21	16.5	-	0.1
30	9.78	26.449	6.30	65.4	-	-	-	-
50	10.61	27.765	4.11	43.9	-	-	-	-
75	10.27	28.377	3.30	35.1	-	-	-	-
100	9.41	28.563	1.4	14.7	-	-	-	-
150	8.63	28.799	1.50	15.4	-	-	-	-
200	8.62	28.817	1.4	14.5	-	-	-	-
250	8.62	28.823	1.50	15.4	-	-	-	-
SC-8: 12 December, 1990								
0	7.5	19.964	-	-	0-1.5	-	1.8	-
2	8.45	23.459	7.69	75.9	1.5-3	-	1.5	-
5	8.98	24.873	7.02	70.8	3-6	-	1.4	-
10	9.38	25.732	6.58	67.4	9-12	-	1.8	-
20	9.81	26.077	6.38	66.1	18-21	-	2.2	-
30	10.06	26.648	6.01	62.9	5	16.9	0.8	0.2
50	10.38	27.890	3.15	33.5	10	15.8	0.7	0.1
75	10.04	28.364	1.88	19.9	20	18.4	0.3	1.4
100	9.15	28.578	0.49	5.0	30	17.4	0.7	0.2
125	8.78	28.752	0.51	5.3	50	21.9	1.6	2.1
150	8.68	28.812	0.90	9.2	75	22.0	1.2	0.3
200	8.64	28.823	0.83	8.5	100	18.4	1.7	4.7
SC-9: 11 December, 1990								
0	5.2	3.180	-	-	0-1.5	-	1.5	-
5	9.22	23.752	6.51	65.6	1.5-3	-	1.1	-
10	9.53	24.638	6.22	63.5	3-6	-	1.3	-
20	9.89	25.540	5.98	61.9	9-12	-	2.0	-
30	11.00	26.386	5.11	54.6	18-21	-	2.3	-
50	11.43	27.428	4.01	43.5	5	16.4	0.3	0.7
60	10.45	27.536	1.66	17.6	10	18.7	0.7	0.7
70	9.66	27.617	0.30	3.1	20	15.7	0.5	0.2
80	9.38	27.655	0.33	3.4	50	13.8	0.5	0.3
-	-	-	-	-	60	14.4	2.6	0.2
-	-	-	-	-	70	4.5	2.8	2.6
-	-	-	-	-	80	3.2	3.0	10.7

Table B.3: December continued.

depth m	temp °C	sal	oxygen mg/l	oxygen % sat	depth m	NO_3^- μM	PO_4^{3-} μM	SiO_4^{4-} μM	NH_4^+ μM
SC-1: 22 January, 1991									
0	7.2	27.075	-	-	-	-	-	-	-
2	7.58	27.335	7.42	73.6	-	-	-	-	-
5	7.58	27.406	7.49	74.3	-	-	-	-	-
10	7.83	27.928	7.14	71.5	-	-	-	-	-
20	8.46	28.728	6.31	64.5	-	-	-	-	-
30	8.96	29.404	5.57	57.8	-	-	-	-	-
50	9.27	29.754	5.13	53.7	-	-	-	-	-
75	9.50	30.085	4.68	49.4	-	-	-	-	-
SC-2: 23 January, 1991									
0	5.9	22.708	-	-	0-1.5	17.71	1.02	10.50	0.09
2	7.93	25.718	7.14	70.6	1.5-3	7.51	0.47	3.60	5.93
5	8.33	26.536	6.68	67.1	3-6	12.13	0.91	7.90	2.64
10	8.37	27.220	6.62	66.9	9-12	7.84	0.87	6.16	3.43
20	8.25	27.343	6.62	66.7	18-21	14.76	1.09	7.74	0.56
30	8.30	27.512	6.62	66.9	30	17.64	1.38	15.44	-
50	8.36	27.699	6.41	64.9	50	18.48	1.86	14.59	5.21
75	8.51	28.015	5.88	59.9	75	23.30	1.93	19.37	2.71
100	8.62	28.320	5.04	51.5	100	22.41	2.05	17.51	7.20
150	8.66	28.802	1.3	14	150	23.27	3.03	24.67	3.12
200	8.64	28.825	1.3	13	200	10.81	1.89	16.42	1.97
250	8.63	28.829	1.1	11	-	-	-	-	-
SC-3: 23 January, 1991									
0	4.5	19.691	-	-	0-1.5	12.37	0.68	6.48	0.06
2	8.13	-	7.49	71.9	1.5-3	21.82	1.68	14.25	4.48
5	8.43	26.864	6.45	65.1	3-6	18.88	1.16	8.98	4.10
10	8.50	27.199	6.37	64.5	9-12	19.15	1.06	8.30	2.99
20	8.35	27.404	6.45	65.2	18-21	7.50	1.08	16.01	3.92
30	8.19	27.552	6.65	67.0	0	18.30	1.90	28.15	0.82
50	8.33	27.781	6.32	64.0	5	21.81	2.25	42.28	0.30
75	8.53	28.019	5.72	58.3	10	27.03	2.47	38.67	0.89
100	8.64	28.334	4.78	48.9	20	26.22	2.37	47.88	0.44
150	8.68	28.793	1.4	14	30	26.79	2.46	37.30	1.07
200	8.64	28.817	1.3	13	50	27.08	2.45	46.37	0.23
250	8.63	28.824	1.2	13	75	26.18	2.49	45.14	0.18
-	-	-	-	-	100	27.42	2.71	44.30	0.36
-	-	-	-	-	150	30.07	3.71	40.67	0.24
-	-	-	-	-	200	31.73	4.11	41.22	0.34
-	-	-	-	-	250	25.91	3.47	38.73	0.37

Table B.4: Temperature, Salinity, dissolved O_2 and nutrients: January.

depth m	temp °C	sal	oxygen mg/l	oxygen % sat	depth m	NO_3^- μM	PO_4^{3-} μM	SiO_4^{4-} μM	NH_4^+ μM
SC-4: 22 January, 1991									
0	4.0	19.685	-	-	-	-	-	-	-
2	7.34	23.876	8.31	80.0	-	-	-	-	-
5	8.61	26.921	6.34	64.2	-	-	-	-	-
10	8.70	27.205	6.07	61.7	-	-	-	-	-
20	8.56	27.438	6.21	63.1	-	-	-	-	-
30	8.79	27.593	5.67	57.9	-	-	-	-	-
50	8.30	27.712	5.81	58.7	-	-	-	-	-
75	8.37	27.911	5.13	52.0	-	-	-	-	-
100	9.51	28.458	2.50	26.1	-	-	-	-	-
150	8.70	28.783	1.3	13	-	-	-	-	-
200	8.64	28.817	1.3	13	-	-	-	-	-
240	8.63	28.823	1.1	12	-	-	-	-	-
SC-5: 22 January, 1991									
0	4.8	19.617	-	-	0-1.5	19.54	0.52	22.28	0.79
2	6.35	22.102	9.29	86.4	1.5-3	4.99	0.47	15.86	0.23
5	8.46	26.612	6.31	63.6	3-6	8.36	0.84	34.08	0.48
10	9.15	27.263	5.72	58.9	9-12	18.91	1.78	30.20	0.19
20	9.14	27.494	5.57	57.3	18-21	18.40	1.67	11.18	1.06
30	8.66	27.572	5.97	60.8	30	8.16	1.38	36.31	3.59
50	9.05	27.842	5.17	53.2	50	16.88	2.00	50.59	0.11
75	8.86	28.051	4.90	50.3	75	27.87	2.74	54.43	-
100	9.56	28.491	2.31	24.2	100	12.15	1.99	72.83	0.94
125	8.89	28.740	1.2	12	125	8.32	1.86	87.67	0.21
150	8.69	28.801	1.3	13	150	12.94	2.65	103.89	0.18
200	8.64	28.817	1.3	13	200	8.74	2.11	107.33	1.02
SC-6: 22 January, 1991									
0	-	16.089	-	-	0-1.5	7.98	0.61	15.30	0.08
2	6.48	21.435	9.52	88.4	1.5-3	12.86	0.80	28.38	0.65
5	9.27	26.858	5.57	57.3	3-6	18.67	1.26	29.16	0.22
10	9.63	27.251	5.21	54.2	9-12	14.33	1.71	17.05	0.36
20	9.72	27.606	5.60	58.5	18-21	12.81	1.27	9.28	0.80
30	9.53	27.727	5.04	52.5	30	24.86	2.41	54.17	2.34
50	9.87	28.059	4.03	42.3	50	6.65	1.24	47.08	0.23
75	10.00	28.262	2.90	30.6	75	21.72	2.46	64.49	0.03

Table B.5: January continued.

depth m	temp °C	sal	oxygen mg/l	oxygen % sat	depth m	NO_3^- μM	PO_4^{3-} μM	SiO_4^{4-} μM	NH_4^+ μM
SC-7: 23 January, 1991									
0	5.0	17.304	-	-	0	15.97	1.33	17.01	0.82
2	7.48	24.573	8.18	79.4	2	24.18	2.15	14.23	3.67
5	8.91	26.822	6.32	64.5	5	25.95	2.38	33.36	1.33
10	9.24	27.277	5.57	57.4	10	24.14	2.30	16.92	5.35
20	9.24	27.532	5.37	55.4	20	27.52	2.56	44.84	0.48
30	9.33	27.721	5.03	52.1	30	28.10	2.72	26.32	2.53
50	8.74	27.806	5.52	56.5	50	28.06	2.61	40.64	0.40
75	9.01	27.993	4.98	51.3	75	28.11	2.74	41.66	0.96
100	9.80	28.451	2.08	21.9	100	32.33	3.44	37.42	1.24
150	8.69	28.782	1.1	12	150	34.24	3.99	38.97	0.37
200	8.64	28.806	1.3	13	200	31.83	3.99	42.48	0.61
250	8.63	28.823	1.3	13	250	32.04	3.63	21.18	5.00
SC-8: 22 January,1991									
0	-	16.178	-	-	0-1.5	5.49	0.48	8.00	0.07
2	8.33	26.673	6.15	61.8	1.5-3	16.29	0.63	11.49	0.77
5	9.02	26.977	5.91	60.5	3-6	3.82	0.43	5.35	1.78
10	10.07	27.499	4.45	46.9	9-12	22.06	1.69	17.25	0.35
20	10.07	27.768	4.01	42.3	18-21	18.32	1.49	12.87	-
30	10.04	27.836	3.91	41.2	30	25.36	2.24	19.57	0.01
50	10.02	28.065	3.93	41.4	50	25.64	2.53	26.08	2.98
75	10.22	28.263	3.40	36.1	75	26.00	2.59	30.38	1.94
100	9.71	28.441	1.1	12	100	25.09	2.43	18.18	0.93
125	8.83	28.739	0.69	7.1	125	29.02	3.45	54.79	2.53
150	8.69	28.795	0.97	10	150	11.66	2.00	48.34	1.13
200	8.64	28.834	0.83	8.5	200	5.83	2.00	8.66	0.27
SC-9: 24 January, 1991									
0	1.7	3.482	-	-	0-1.5	17.62	1.25	11.32	5.13
5	9.65	26.014	5.22	53.9	1.5-3	13.61	0.84	9.10	1.34
10	9.42	26.478	5.17	53.2	3-6	9.97	0.85	5.91	1.84
20	8.71	26.640	6.11	61.9	9-12	21.36	1.83	13.45	0.93
30	8.48	26.645	5.88	59.3	18-21	9.99	1.13	17.17	0.49
50	8.39	26.692	6.30	63.4	30	4.70	0.84	28.24	0.39
60	9.45	27.226	2.56	26.5	50	5.30	1.19	32.17	0.12
70	10.11	27.550	0.24	2.6	60	7.08	0.92	11.22	0.53
80	9.85	27.572	0.00	0.00	70	6.56	2.50	28.23	1.61
-	-	-	-	-	80	0.36	3.46	58.06	2.09

Table B.6: January continued.

depth m	temp ^{0}C	sal	oxygen mg/l	oxygen % sat	depth m	NO_3^- μM	PO_4^{3-} μM	SiO_4^{4-} μM	NH_4^+ μM
SC-1: 19 February, 1991									
0	7.3	25.322	-	-	0-1.5	14.7	1.5	11.1	1.5
2	7.36	25.425	9.24	89.9	1.5-3	15.9	1.6	11.3	1.5
5	7.41	25.539	9.05	88.3	3-6	5.7	0.9	7.1	1.7
10	7.74	25.852	8.37	82.4	9-12	5.0	0.9	5.1	2.1
20	8.20	27.022	7.24	72.7	18-21	18.5	1.9	13.6	1.3
30	8.84	29.215	5.67	58.6	-	-	-	-	-
50	9.05	29.645	5.47	57.0	-	-	-	-	-
75	9.17	29.851	5.31	55.6	-	-	-	-	-
SC-2: 20 February, 1991									
0	7.6	20.593	-	-	0-1.5	16.9	1.6	21.4	0.4
2	7.92	23.942	7.91	77.3	1.5-3	21.9	2.0	21.9	0.4
5	8.14	25.739	7.35	73.1	3-6	21.8	2.0	23.3	0.4
10	8.27	26.844	6.92	69.6	9-12	4.5	1.1	11.5	0.2
20	8.43	27.352	6.61	66.9	18-21	15.2	1.7	20.5	0.2
30	8.69	27.781	5.58	57.0	30	25.4	2.5	35.2	0.2
50	8.48	27.952	5.74	58.4	50	9.0	1.5	19.9	0.4
75	8.46	28.117	5.48	55.8	75	22.6	2.7	33.1	1.0
100	8.49	28.342	4.95	50.5	100	22.4	3.0	28.0	1.2
150	8.69	28.774	1.40	14.4	150	14.8	2.5	21.3	0.3
200	8.66	28.811	1.14	11.7	200	25.2	3.3	29.3	4.6
250	8.64	28.813	1.01	10.4	-	-	-	-	-
SC-3: 20 February, 1991									
0	7.6	19.168	-	-	0-1.5	13.2	1.3	14.7	1.2
2	7.93	24.195	7.85	76.9	1.5-3	16.3	1.6	19.0	1.2
5	8.13	25.422	7.49	74.3	3-6	19.1	1.9	21.3	0.7
10	8.27	26.386	7.20	72.1	9-12	20.1	2.0	16.3	2.0
20	8.36	26.832	6.81	68.5	18-21	16.7	1.9	26.3	0.4
30	8.36	27.436	6.44	65.1	0	14.1	1.3	28.9	3.7
50	8.67	27.875	5.54	56.6	1	12.4	1.4	27.7	1.0
75	8.48	28.120	5.44	55.4	2	23.0	2.1	46.8	0.6
100	8.56	28.349	4.45	45.5	3	15.1	1.6	31.3	4.0
150	8.70	28.780	1.31	13.5	4.5	20.7	1.9	44.1	1.3
200	8.66	28.812	1.21	12.5	5	24.6	2.2	51.8	0.5
250	8.64	28.814	1.20	12.3	5.5	22.2	2.0	45.2	0.4
-	-	-	-	-	10	23.1	2.2	48.0	2.7
-	-	-	-	-	20	26.1	2.4	52.8	0.5
-	-	-	-	-	30	27.5	2.5	45.9	0.9
-	-	-	-	-	50	28.0	2.7	55.4	0.3
-	-	-	-	-	75	28.3	2.8	59.8	0.4
-	-	-	-	-	100	29.6	3.1	66.9	0.2
-	-	-	-	-	150	32.2	4.0	83.1	0.3
-	-	-	-	-	200	32.3	4.1	73.5	0.3
-	-	-	-	-	250	32.2	4.1	76.3	0.2

Table B.7: Temperature, salinity, dissolved O_2 and nutrients: February.

depth m	temp °C	sal	oxygen mg/l	oxygen % sat	depth m	NO_3^- μM	PO_4^{3-} μM	SiO_4^{4-} μM	NH_4^+ μM
SC-4: 19 February, 1991									
0	7.6	17.794	-	-	-	-	-	-	-
2	7.54	20.958	8.77	83.2	-	-	-	-	-
5	8.21	25.357	7.27	72.2	-	-	-	-	-
10	8.30	26.485	6.94	69.6	-	-	-	-	-
20	8.21	27.010	6.87	69.0	-	-	-	-	-
30	8.21	27.302	6.77	68.1	-	-	-	-	-
50	8.71	27.853	5.60	57.2	-	-	-	-	-
75	8.71	28.147	5.10	52.2	-	-	-	-	-
100	8.80	28.373	4.14	42.5	-	-	-	-	-
150	8.72	28.792	1.18	12.2	-	-	-	-	-
200	8.66	28.841	1.11	11.4	-	-	-	-	-
240	8.64	28.826	1.10	11.3	-	-	-	-	-
SC-5: 19 February, 1991									
0	7.7	17.601	-	-	0-1.5	9.3	0.9	21.5	0.7
2	7.77	23.505	7.78	75.5	1.5-3	16.7	1.3	26.3	0.7
5	8.07	25.219	7.44	73.6	9-12	9.1	1.1	14.1	1.3
10	8.21	26.347	6.94	69.4	18-21	19.7	1.9	39.0	0.5
20	8.12	27.015	6.92	69.4	30	20.0	2.0	33.2	0.6
30	8.72	27.502	6.00	61.1	50	9.9	1.3	15.5	0.6
50	9.26	28.045	4.47	46.3	75	8.9	1.3	46.0	0.1
75	8.98	28.222	4.40	45.3	100	27.4	3.0	52.9	0.4
100	9.14	28.382	3.27	33.9	125	22.3	2.9	47.0	0.6
125	9.07	28.637	1.90	19.7	150	19.0	2.9	63.4	0.4
150	8.79	28.797	1.20	12.4	200	19.8	3.0	99.0	0.3
200	8.66	28.873	1.06	10.9	-	-	-	-	-
SC-5.5: 19 February, 1991									
-	-	-	-	-	0	16.9	1.7	41.5	2.7
-	-	-	-	-	0.5	13.2	1.3	32.5	1.0
-	-	-	-	-	1.5	14.9	1.5	37.8	1.8
-	-	-	-	-	2.5	20.4	1.8	44.3	1.3
-	-	-	-	-	4	24.0	2.2	49.1	1.3
-	-	-	-	-	5	25.2	2.4	51.7	0.6
SC-6: 19 February, 1991									
0	7.5	16.406	-	-	0-1.5	16.7	1.7	37.5	1.0
2	7.47	19.206	9.46	88.7	1.5-3	19.8	1.8	28.0	1.2
5	8.05	24.678	7.57	74.5	3-6	9.7	1.2	35.6	0.8
10	8.40	26.519	6.82	68.6	9-12	16.5	1.8	33.9	0.8
20	8.94	27.182	6.04	61.8	18-21	24.7	2.4	29.1	0.7
30	9.18	27.430	5.45	56.2	30	19.0	2.1	52.2	0.2
50	9.51	27.958	4.15	43.3	50	7.9	1.4	42.0	0.2
75	9.51	28.240	3.23	33.7	75	21.9	2.6	57.2	0.3

Table B.8: February continued.

depth m	temp °C	sal	oxygen mg/l	% sat	depth m	NO_3^- μM	PO_4^{3-} μM	SiO_4^{4-} μM	NH_4^+ μM
SC-7: 19 February,1991									
0	7.2	18.037	-	-	0	18.6	1.5	31.5	0.6
2	7.42	20.228	9.09	85.7	1.5	23.1	1.9	35.7	2.8
5	7.99	24.667	7.68	75.6	2	20.0	1.7	30.4	0.9
10	8.00	26.455	7.31	72.8	3	24.2	2.1	41.9	1.5
20	8.10	27.016	6.91	69.2	5	24.4	2.1	42.1	0.6
30	8.45	27.382	6.31	63.9	7	26.3	2.3	46.6	1.8
50	9.62	28.095	4.13	43.1	9	26.6	2.2	48.4	1.0
75	9.43	28.309	3.64	37.9	10	17.2	1.8	33.2	-
100	9.40	28.481	2.36	24.6	20	26.5	2.4	42.7	1.6
150	8.72	28.837	1.01	10.4	30	27.6	2.5	49.2	2.6
200	8.65	28.869	1.03	10.6	50	28.9	2.8	54.3	1.5
250	8.63	28.830	1.08	11.1	75	25.5	2.7	50.1	-
-	-	-	-	-	100	33.4	3.5	57.7	0.4
-	-	-	-	-	150	34.3	4.1	60.0	1.1
-	-	-	-	-	200	33.0	4.1	76.4	0.7
-	-	-	-	-	250	31.6	4.2	62.3	0.8
SC-8: 19 February, 1991									
0	6.6	15.136	-	-	0-1.5	17.2	1.5	42.7	1.2
2	7.44	21.126	8.84	83.8	1.5-3	5.5	0.9	36.6	0.4
5	8.09	25.166	7.51	74.3	3-6	2.6	0.9	29.9	0.2
10	8.40	26.362	7.14	71.7	9-12	6.0	1.2	35.6	0.2
20	8.35	26.901	6.75	68.0	18-21	5.7	1.2	31.1	0.8
30	8.62	27.292	6.20	62.9	30	9.5	1.4	47.8	0.6
50	10.05	27.981	3.28	34.6	50	24.0	2.6	53.2	0.6
75	9.92	28.317	2.93	30.9	75	9.3	1.6	27.6	0.3
100	9.71	28.490	1.46	15.3	100	5.8	1.5	54.4	0.1
125	9.11	28.639	0.63	6.5	125	8.6	1.9	46.6	0.2
150	8.74	28.769	0.73	7.5	150	30.4	3.4	84.0	0.2
200	8.66	28.812	0.76	7.8	200	12.1	2.1	70.7	1.1
SC-9: 20 February, 1991									
0	5.7	2.053	-	-	0-1.5	7.2	0.5	38.4	0.7
5	8.29	24.614	6.35	62.9	1.5-3	7.9	0.6	37.8	0.4
10	8.23	26.097	5.95	59.5	3-6	13.7	1.3	46.3	0.5
20	8.24	26.530	6.37	63.8	9-12	12.7	1.8	44.3	0.7
30	8.77	26.743	5.45	55.4	18-21	24.2	2.3	55.6	0.5
50	8.43	26.802	5.05	50.9	30	19.8	2.1	54.8	0.2
60	8.62	27.008	4.30	43.6	50	22.1	2.4	58.4	0.4
70	9.95	27.498	0.29	3.0	60	12.6	1.9	48.9	1.8
80	9.93	27.546	0.00	0.0	70	4.1	3.7	108.8	1.8
-	-	-	-	-	80	0.3	5.9	113.2	25.3

Table B.9: February continued.

depth m	temp ^{0}C	sal	oxygen mg/l	oxygen % sat	depth m	NO_3^- μM	PO_4^{3-} μM	SiO_4^{4-} μM	NH_4^+ μM
SC-1: 27 March, 1991									
0	8.9	27.771	-	-	-	-	-	-	-
2	8.47	27.919	9.08	92.3	-	-	-	-	-
5	8.46	27.957	9.04	91.8	-	-	-	-	-
10	8.45	28.021	8.98	91.3	-	-	-	-	-
20	8.44	28.069	8.82	89.7	-	-	-	-	-
30	8.43	28.119	8.68	88.3	-	-	-	-	-
40	8.45	28.417	8.54	87.0	-	-	-	-	-
50	8.47	29.079	7.62	78.1	-	-	-	-	-
75	8.47	29.676	6.72	69.1	-	-	-	-	-
SC-2: 26 March, 1991									
0	8.8	26.037	-	-	0-1.5	0.5	0.1	69.4	0.2
2	8.68	26.909	8.38	85.0	1.5-3	0.4	0.1	27.9	0.1
5	8.46	27.184	7.69	77.8	3-6	2.2	0.2	24.3	0.3
10	8.41	27.488	6.85	69.4	9-12	18.2	1.5	52.7	1.0
20	8.20	27.654	7.44	75.0	18-21	19.9	1.7	45.9	1.3
30	8.19	27.729	7.77	78.3	30	21.2	1.9	95.5	1.0
50	8.33	27.966	7.88	79.9	50	10.0	1.1	33.1	0.6
75	8.35	28.022	7.84	79.5	75	17.9	1.7	15.0	1.1
100	8.41	28.178	6.92	70.4	100	8.5	1.2	8.2	0.5
150	8.67	28.740	1.53	15.7	150	19.6	2.7	14.1	1.7
200	8.67	28.815	1.10	11.3	200	18.8	2.7	72.1	1.2
270	8.66	28.799	0.80	8.2	270	13.6	2.3	30.8	3.5
SC-3: 26 March, 1991									
0	9.4	27.063	-	-	0-1.5	0.4	0.0	82.2	0.2
2	9.14	26.175	14.69	150.0	1.5-3	2.3	0.2	81.5	0.2
5	8.65	26.694	10.19	103.2	3-6	0.4	0.0	44.9	0.1
10	8.56	26.033	7.55	76.0	9-12	1.5	0.2	8.4	0.3
20	8.34	27.582	6.51	65.8	18-21	11.0	1.2	11.7	1.6
30	8.27	27.672	6.68	67.5	0	0.9	0.2	2.9	0.3
50	8.30	27.882	6.50	65.7	1	1.1	0.3	6.4	0.4
75	8.36	28.049	7.22	73.3	2	5.4	0.8	18.3	1.1
100	8.40	28.220	6.64	67.5	4	8.7	1.1	22.0	0.6
150	8.69	28.773	1.24	12.8	5	8.2	1.1	22.4	4.0
200	8.67	28.802	1.04	10.7	6	16.8	1.8	38.9	1.2
260	8.65	28.815	1.04	10.7	8	24.9	2.4	49.6	0.6
-	-	-	-	-	10	10.0	1.2	25.2	2.3
-	-	-	-	-	20	24.9	2.3	49.2	1.1
-	-	-	-	-	30	19.6	1.9	43.2	0.8
-	-	-	-	-	50	20.6	2.1	41.5	1.7
-	-	-	-	-	75	18.5	1.7	39.6	-
-	-	-	-	-	100	21.6	2.1	49.0	0.7
-	-	-	-	-	150	24.7	3.5	90.4	1.2
-	-	-	-	-	200	29.8	3.8	98.8	2.2
-	-	-	-	-	260	26.9	3.5	100.8	0.3

Table B.10: Temperature, salinity, dissolved O_2 and nutrients: March.

depth m	temp °C	sal	oxygen mg/l	oxygen % sat	depth m	NO_3^- μM	PO_4^{3-} μM	SiO_4^{4-} μM	NH_4^+ μM
SC-4: 26 March, 1991									
0	8.8	25.952	-	-	-	-	-	-	-
2	8.42	26.650	9.04	91.0	-	-	-	-	-
5	8.40	27.143	7.35	74.2	-	-	-	-	-
10	8.54	27.370	5.91	60.0	-	-	-	-	-
20	8.55	27.660	5.98	60.8	-	-	-	-	-
30	8.34	27.738	6.44	65.2	-	-	-	-	-
50	8.30	27.840	6.42	65.0	-	-	-	-	-
75	8.36	28.013	7.10	72.0	-	-	-	-	-
100	8.58	28.317	4.35	44.5	-	-	-	-	-
150	8.77	28.744	1.28	13.2	-	-	-	-	-
200	8.68	28.811	1.08	11.1	-	-	-	-	-
240	8.65	28.806	0.94	9.7	-	-	-	-	-
SC-5: 26 March, 1991									
0	8.5	25.366	-	-	0-1.5	0.8	0.1	38.4	0.2
2	8.33	25.714	14.88	148.5	1.5-3	0.9	0.1	27.6	0.1
5	8.30	26.188	11.32	113.3	3-6	0.3	0.0	17.1	0.1
10	8.68	27.318	5.68	57.8	9-12	4.1	0.4	29.0	0.5
20	8.66	27.681	5.62	57.3	18-21	12.7	1.3	14.1	1.2
30	8.65	27.794	5.58	56.9	30	22.7	1.9	24.7	2.8
50	8.88	27.972	4.80	49.2	50	15.2	1.4	8.0	1.9
75	8.97	28.154	4.21	43.4	75	21.6	2.2	10.3	3.1
100	8.97	28.333	3.57	36.8	100	17.1	1.8	23.5	2.7
125	8.99	28.617	1.67	17.3	125	6.8	1.7	2.0	5.0
150	8.80	28.739	1.18	12.2	150	14.2	2.3	20.0	3.8
200	8.68	28.803	0.99	10.1	200	28.1	3.3	68.7	3.8
SC-5.5: 26 March, 1991									
-	-	-	-	-	0	0.8	0.2	1.8	0.5
-	-	-	-	-	1	0.8	0.1	1.8	-
-	-	-	-	-	2	0.7	0.1	1.6	0.3
-	-	-	-	-	4	0.8	0.1	1.6	0.5
-	-	-	-	-	6	0.9	0.1	1.9	1.6
-	-	-	-	-	8	4.7	0.7	11.6	1.7
SC-6: 26 March, 1991									
0	9.2	25.559	-	-	0-1.5	1.7	0.1	83.3	0.1
2	8.86	25.503	16.23	163.9	1.5-3	1.1	0.0	38.5	0.1
5	8.45	25.587	16.03	160.4	3-6	0.7	0.1	58.7	0.1
10	8.92	27.245	4.73	48.3	9-12	1.2	0.1	12.9	0.1
20	8.95	27.689	5.01	51.4	18-21	17.1	1.6	42.4	1.2
30	9.09	27.869	4.61	47.5	30	20.0	1.8	93.0	1.0
50	9.14	28.036	4.14	42.8	50	18.3	1.8	63.6	0.9
75	9.21	28.184	3.44	35.6	75	14.6	1.3	66.1	0.7

Table B.11: March continued.

depth m	temp ^{0}C	sal	oxygen mg/l	% sat	depth m	NO_3^- μM	PO_4^{3-} μM	SiO_4^{4-} μM	NH_4^+ μM
SC-7: 27 March, 1991									
0	8.3	26.439	-	-	0	1.3	0.3	6.3	0.9
2	8.51	26.465	13.28	133.8	0.5	1.0	0.4	2.9	0.7
5	8.55	26.648	11.15	112.6	1.5	0.8	0.1	2.0	1.0
10	8.42	27.436	6.78	68.6	2	1.5	0.1	3.6	-
20	8.74	27.674	5.87	59.9	2.5	0.9	0.2	2.0	6.2
30	8.98	27.841	5.08	52.3	3.5	0.9	0.2	2.2	-
50	8.98	28.045	4.81	49.5	5	3.0	0.6	11.2	-
75	8.94	28.201	4.51	46.4	6	1.2	0.2	3.1	2.3
100	9.29	28.407	2.83	29.4	10	17.6	1.7	39.8	-
150	8.75	28.827	1.04	10.7	20	13.8	1.7	33.6	1.8
200	8.67	28.834	0.93	9.5	30	15.0	1.6	37.0	-
250	8.65	28.842	0.91	9.4	50	21.1	2.1	42.6	-
-	-	-	-	-	75	19.1	2.0	34.2	-
-	-	-	-	-	100	15.3	2.4	31.3	-
-	-	-	-	-	150	25.4	3.4	52.5	-
-	-	-	-	-	200	19.9	3.1	51.4	1.8
-	-	-	-	-	250	20.6	3.0	47.8	-
SC-8: 27 March, 1991									
0	7.2	24.378	-	-	0-1.5	1.1	0.1	29.0	0.3
2	8.42	26.448	12.31	123.7	1.5-3	2.3	0.1	62.1	0.5
5	8.75	27.039	8.54	86.8	3-6	0.6	0.1	28.7	0.4
10	8.86	27.334	6.27	64.0	9-12	7.6	0.7	16.8	1.0
20	9.25	27.783	4.45	46.1	18-21	19.8	1.7	54.5	1.8
30	9.48	27.937	4.17	43.4	30	12.9	1.3	38.9	2.0
50	9.66	28.053	3.53	36.9	50	26.0	2.4	51.9	2.8
75	9.61	28.221	3.37	35.2	75	18.7	2.2	28.7	2.8
100	9.54	28.726	1.16	12.1	100	15.0	2.0	30.2	2.4
125	8.86	28.723	0.64	6.6	125	10.5	2.3	22.3	2.2
150	8.72	28.788	0.64	6.6	150	20.2	2.9	15.7	5.6
200	8.66	28.813	0.56	5.7	200	0.3	0.1	1.4	0.0
SC-9: 26 March, 1991									
0	7.6	23.344	-	-	0-1.5	1.6	0.2	40.6	0.5
2	9.23	26.173	8.27	84.6	1.5-3	8.2	0.6	44.4	1.2
5	8.79	26.368	6.91	70.1	3-6	14.8	1.2	46.9	1.7
10	8.51	26.658	5.62	56.8	9-12	19.2	1.6	31.9	2.9
20	8.36	26.744	6.35	63.9	18-21	15.7	1.1	39.5	1.2
30	8.31	26.836	7.01	70.5	30	12.7	1.2	42.8	1.2
50	8.31	26.914	7.05	70.9	50	7.1	3.5	54.1	4.1
75	9.56	27.362	0.36	3.7	75	5.4	2.1	14.6	2.2

Table B.12: March continued.

Appendix B.2

Temperature, salinity, dissolved O_2 and nutrients

Presented are tables of temperature, salinity, dissolved oxygen and nutrients collected during the study period in Sechelt Inlet. The methods of collection and analysis for these data are described in chapter 2. For consistency with the text of this work, oxygen concentrations are given in mg/l. Multiplication of mg/l by 0.7 gives oxygen concentration in ml/l. Percent oxygen saturation is also reported, and is relative to equilibrium at one atmosphere of pressure and *in situ* salinity and temperature.

This appendix provides the data of the months April through June.

depth m	temp °C	sal	oxygen mg/l	oxygen % sat	depth m	NO_3^- μM	PO_4^{3-} μM	SiO_4^{4-} μM	NH_4^+ μM
SC-1: 23 April, 1991									
0	11.5	27.950	-	-	-	-	-	-	-
2	10.25	27.939	9.35	99.1	-	-	-	-	-
5	10.03	27.973	9.21	97.1	-	-	-	-	-
10	9.88	28.032	8.92	93.8	-	-	-	-	-
20	9.84	28.110	8.74	91.8	-	-	-	-	-
30	9.58	28.344	8.41	88.0	-	-	-	-	-
50	9.21	28.906	7.45	77.6	-	-	-	-	-
60	8.79	29.443	6.55	67.8	-	-	-	-	-
70	8.69	29.524	6.44	66.5	-	-	-	-	-
75	8.66	29.431	6.27	64.6	-	-	-	-	-
SC-2: 24 April, 1991									
0	10.2	24.530	-	-	0-1.5	5.7	0.4	7.3	1.2
2	10.49	26.195	9.59	101.1	1.5-3	5.6	0.4	5.1	2.6
5	9.76	27.407	8.61	89.9	3-6	5.5	0.3	7.4	0.9
10	9.57	27.638	8.34	86.8	9-12	-	-	-	-
20	9.35	27.919	8.05	83.6	18-21	10.2	0.8	14.3	1.2
30	9.08	28.079	7.59	78.4	30	11.5	1.0	14.7	1.1
50	8.89	28.209	7.42	76.3	50	15.4	1.2	8.2	2.3
75	8.87	28.323	7.01	72.1	75	14.5	1.2	20.2	1.0
100	8.85	28.450	6.20	63.8	150	5.4	1.4	47.5	0.4
150	8.69	28.781	1.27	13.1	200	17.1	1.9	55.4	0.5
200	8.67	28.793	0.83	8.5	270	18.1	2.1	44.3	2.3
280	8.66	28.814	0.57	5.9	-	-	-	-	-
SC-3: 24 April, 1991									
0	10.7	24.769	-	-	0-1.5	4.3	0.4	12.6	1.9
2	10.50	25.673	10.26	107.8	1.5-3	6.1	0.6	11.9	1.2
5	9.53	26.956	9.68	100.2	3-6	8.0	0.9	13.5	5.8
10	9.58	27.649	8.58	89.4	9-12	6.2	0.7	12.9	3.0
20	9.32	27.811	8.05	83.4	18-21	9.1	1.1	18.5	3.2
30	9.02	27.961	7.41	76.3	0	5.0	0.6	11.0	0.7
50	8.59	28.131	7.08	72.3	2	6.5	0.8	12.2	0.7
75	8.82	28.311	7.15	73.5	4	13.0	1.3	20.3	2.1
100	8.71	28.376	6.34	65.0	5	11.9	1.2	17.9	0.8
150	8.71	28.725	1.46	15.0	6	17.8	1.8	29.0	2.7
200	8.68	28.796	0.77	7.9	8	18.0	1.8	30.0	2.3
270	8.66	28.807	0.47	4.8	10	12.7	1.5	25.2	1.6
-	-	-	-	-	13	19.1	1.9	33.5	2.0
-	-	-	-	-	20	17.1	1.8	31.5	1.6
-	-	-	-	-	30	19.7	2.0	33.4	2.2
-	-	-	-	-	50	20.6	2.1	37.6	2.6
-	-	-	-	-	75	20.0	2.1	37.6	2.4
-	-	-	-	-	100	22.3	2.4	45.2	2.6
-	-	-	-	-	150	31.8	3.9	57.5	1.1

Table B.13: Temperature, salinity, dissolved O_2 and nutrients: April.

depth m	temp °C	sal	oxygen mg/l	% sat	depth m	NO_3^- μM	PO_4^{3-} μM	SiO_4^{4-} μM	NH_4^+ μM
-	-	-	-	-	200	29.3	3.9	58.4	1.9
-	-	-	-	-	250	24.3	4.2	61.7	2.9
SC-4: 24 April, 1991									
0	11.4	22.321	-	-	-	-	-	-	-
2	11.31	22.528	11.32	118.8	-	-	-	-	-
5	10.85	25.033	11.45	120.8	-	-	-	-	-
10	9.09	27.583	7.89	81.2	-	-	-	-	-
20	8.61	27.799	5.74	58.5	-	-	-	-	-
30	8.61	27.946	5.25	53.6	-	-	-	-	-
50	8.51	28.062	6.21	63.2	-	-	-	-	-
75	8.62	28.248	5.44	55.6	-	-	-	-	-
100	8.68	28.340	6.64	68.0	-	-	-	-	-
150	8.76	28.719	1.31	13.5	-	-	-	-	-
200	8.69	28.800	0.84	8.7	-	-	-	-	-
240	8.67	28.803	0.81	8.4	-	-	-	-	-
SC-5: 24 April, 1991									
0	11.3	23.396	-	-	0-1.5	0.8	0.2	3.2	1.8
2	11.30	23.460	11.05	116.6	1.5-3	1.0	0.2	3.3	4.0
5	10.77	25.684	11.26	119.1	3-6	1.0	0.2	7.6	1.6
10	9.30	27.354	9.84	101.6	9-12	3.1	0.5	9.1	4.3
20	8.76	27.697	5.45	55.7	18-21	15.5	1.7	24.3	4.5
30	8.79	27.986	4.57	46.8	30	22.6	2.1	51.3	1.7
50	8.79	28.176	4.47	45.8	50	17.7	2.0	47.9	0.5
75	8.71	28.235	4.77	48.8	75	19.4	2.2	56.8	0.6
100	8.88	28.346	3.28	33.8	100	22.6	2.7	67.2	0.2
125	8.83	28.563	2.61	26.9	125	26.8	3.1	74.9	1.1
150	8.80	28.687	1.38	14.3	150	17.7	2.7	90.2	0.7
200	8.68	28.817	0.74	7.6	200	18.5	3.0	91.4	0.8
SC-5.5: 24 April, 1991									
-	-	-	-	-	0	1.8	0.4	4.6	0.8
-	-	-	-	-	1	3.1	0.6	5.9	1.0
-	-	-	-	-	2.5	3.1	0.6	5.5	1.3
-	-	-	-	-	4	7.0	1.0	10.0	1.6
-	-	-	-	-	6	7.0	0.9	8.8	4.0
-	-	-	-	-	8	13.3	1.6	15.2	2.2
SC-6: 24 April, 1991									
0	9.8	25.756	-	-	0-1.5	1.9	0.5	6.0	4.2
2	9.76	27.051	11.29	117.7	1.5-3	2.2	0.7	5.2	2.2
5	9.08	27.542	8.18	84.1	3-6	2.8	0.6	5.7	1.8
10	8.92	27.691	5.21	53.4	9-12	9.6	1.2	11.0	1.7
20	9.01	27.920	3.73	38.4	18-21	19.3	2.2	47.5	2.9
30	9.05	28.044	3.28	33.9	30	16.9	1.7	13.3	3.4
50	8.96	28.199	3.50	36.0	50	20.1	2.6	59.4	0.9
70	8.91	28.280	3.34	34.4	75	15.5	2.2	10.4	2.9

Table B.14: April continued.

depth	temp	sal	oxygen		depth	NO_3^-	PO_4^{3-}	SiO_4^{4-}	NH_4^+
m	°C		mg/l	% sat	m	μM	μM	μM	μM
SC-7: 23 April, 1991									
0	-	14.334	-	-	0	1.7	0.0	15.8	0.8
2	11.11	26.159	14.02	149.8	2	0.8	0.2	1.9	0.9
5	9.36	27.439	12.49	129.3	4	1.2	0.4	2.2	1.0
10	8.98	27.745	5.07	52.1	5	3.4	0.7	4.1	1.7
20	9.12	27.915	4.21	43.5	6	5.3	0.8	4.3	1.5
30	9.24	28.068	3.87	40.1	8	22.5	2.2	29.3	1.4
50	8.63	28.146	5.52	56.5	13	29.0	2.8	50.6	1.6
75	8.67	28.263	5.10	52.2	20	29.2	2.8	52.6	1.7
100	8.75	28.379	4.07	41.8	30	30.2	2.9	54.2	1.3
150	8.81	28.746	0.90	9.3	50	26.6	2.6	49.8	1.3
200	8.69	28.795	0.83	8.5	75	24.7	2.5	51.8	2.6
250	8.66	28.815	0.53	5.4	100	30.5	3.2	60.7	1.1
-	-	-	-	-	150	35.6	4.1	65.4	0.8
-	-	-	-	-	200	34.1	4.1	68.0	0.4
-	-	-	-	-	250	29.8	4.7	76.6	0.8
SC-8: 23 April, 1991									
0	9.8	11.686	-	-	0-1.5	0.9	0.0	13.5	1.3
2	10.78	27.410	11.45	122.4	1.5-3	2.2	0.1	8.8	4.3
5	9.30	27.732	4.71	48.8	3-6	1.0	0.0	6.5	1.5
10	9.45	27.911	3.30	34.3	9-12	2.1	0.5	2.5	1.8
20	9.50	28.029	3.38	35.3	18-21	17.2	2.1	37.9	3.4
30	9.41	28.169	3.31	34.5	30	18.9	2.4	54.4	0.4
50	9.26	28.239	3.28	34.1	50	8.7	1.7	49.4	0.7
75	9.19	28.336	2.83	29.3	75	29.2	3.2	65.0	0.7
100	9.29	28.438	1.97	20.5	100	13.5	1.9	21.2	2.5
125	9.26	28.553	1.04	10.8	125	27.3	3.4	72.8	0.3
150	8.96	28.692	0.61	6.3	150	7.7	1.9	82.9	0.7
200	8.69	28.790	0.37	3.8	200	21.8	3.4	93.2	0.2
SC-9: 25 April,1991									
0	-	4.354	-	-	0-1.5	2.2	0.2	8.4	1.6
2	10.18	23.400	10.65	109.4	1.5-3	1.6	0.2	5.8	1.6
5	9.49	25.788	10.34	106.1	3-6	2.0	0.3	4.4	1.2
10	8.99	26.604	7.10	72.4	9-12	6.6	0.6	8.0	2.0
20	8.56	27.018	5.71	57.8	18-21	18.6	1.2	20.8	2.1
30	8.48	27.113	6.41	64.8	30	6.8	1.3	25.6	1.6
40	8.55	27.152	6.95	70.4	40	11.5	1.6	35.7	2.0
50	8.62	27.171	7.28	73.9	50	8.0	1.2	24.7	2.4
60	8.64	27.202	7.29	74.1	60	13.7	1.7	35.1	4.3
75	8.66	27.222	7.15	72.7	75	10.8	1.7	27.0	3.7

Table B.15: April continued.

depth m	temp °C	sal	oxygen mg/l	oxygen % sat	depth m	NO_3^- μM	PO_4^{3-} μM	SiO_4^{4-} μM	NH_4^+ μM
SC-1: 22 May, 1991									
0	-	27.406	-	-	-	-	-	-	-
2	10.28	27.401	8.04	84.9	-	-	-	-	-
5	10.19	27.433	8.01	84.5	-	-	-	-	-
10	10.15	27.591	7.87	83.0	-	-	-	-	-
20	9.98	27.938	7.59	80.0	-	-	-	-	-
30	9.84	28.148	7.35	77.3	-	-	-	-	-
40	9.66	28.329	7.22	75.7	-	-	-	-	-
50	9.30	29.068	6.52	68.1	-	-	-	-	-
60	8.67	29.604	5.94	61.3	-	-	-	-	-
70	8.58	29.708	5.84	60.2	-	-	-	-	-
SC-2: 23 May, 1991									
0	13.5	22.719	-	-	0-1.5	0.8	0.2	4.8	0.9
2	12.63	23.517	13.46	146.4	1.5-3	0.6	0.2	3.8	0.8
5	11.71	25.635	12.03	129.9	3-6	0.5	0.1	2.2	0.6
10	10.42	27.014	8.18	86.5	9-12	2.4	0.5	8.8	0.7
20	10.19	27.343	7.71	81.3	18-21	14.1	1.6	21.0	1.4
30	9.94	27.589	7.37	77.3	30	19.8	1.8	26.2	1.4
50	8.94	28.078	5.32	54.8	50	29.9	2.6	45.5	0.6
75	8.87	28.239	5.50	56.5	75	14.6	1.6	23.4	0.9
100	8.86	28.345	5.37	55.2	100	22.5	2.2	33.3	2.0
150	8.70	28.812	0.90	9.2	150	25.7	3.4	91.0	0.4
200	8.69	28.831	0.76	7.8	200	20.1	3.1	93.6	0.3
220	8.68	28.823	0.46	4.7	250	21.9	3.6	98.1	0.8
SC-3: 23 May, 1991									
0	14.3	18.997	-	-	0-1.5	0.7	0.2	8.1	1.2
5	10.73	26.486	11.04	117.2	1.5-3	1.0	0.1	7.4	0.6
10	10.24	27.243	7.98	84.2	3-6	1.3	0.2	5.1	0.6
20	9.78	27.623	7.17	75.0	9-12	15.3	1.5	24.6	2.5
30	9.70	27.900	6.92	72.4	18-21	4.1	1.0	8.8	1.6
50	9.30	28.101	6.30	65.3	0	0.8	0.1	6.3	1.5
75	9.11	28.291	5.94	61.4	1.5	0.7	0.1	6.3	1.3
100	8.79	28.405	4.88	50.2	2	5.7	0.6	10.3	4.5
150	8.73	28.654	2.30	23.6	3	2.9	0.4	9.1	0.5
200	8.69	28.771	0.84	8.7	4.5	5.9	0.7	13.2	0.8
270	8.68	28.791	0.23	2.3	5	15.1	1.5	28.2	2.1
-	-	-	-	-	6	12.0	1.3	22.6	5.4
-	-	-	-	-	7.5	16.8	1.7	31.5	2.0
-	-	-	-	-	10	20.1	1.9	36.5	1.4
-	-	-	-	-	20	20.6	2.0	38.3	1.3
-	-	-	-	-	30	23.9	2.2	44.4	0.8
-	-	-	-	-	50	24.2	2.4	46.9	1.1
-	-	-	-	-	75	27.3	2.8	58.4	0.4
-	-	-	-	-	100	30.1	3.7	88.6	0.4
-	-	-	-	-	150	29.5	3.7	87.8	0.5

Table B.16: Temperature, salinity, dissolved O_2 and nutrients: May.

depth m	temp °C	sal	oxygen mg/l	oxygen % sat	depth m	NO_3^- μM	PO_4^{3-} μM	SiO_4^{4-} μM	NH_4^+ μM
-	-	-	-	-	200	30.7	4.0	106.3	1.7
-	-	-	-	-	270	30.6	4.8	112.1	1.4
SC-4: 22 May,1991									
0	12.3	25.572	-	-	-	-	-	-	-
2	11.92	26.986	8.22	90.0	-	-	-	-	-
5	10.14	27.233	7.69	81.0	-	-	-	-	-
10	9.91	27.359	7.35	77.0	-	-	-	-	-
20	9.67	27.512	7.12	74.3	-	-	-	-	-
30	9.44	27.663	6.82	70.8	-	-	-	-	-
50	9.13	28.031	5.71	59.0	-	-	-	-	-
75	8.64	28.207	4.91	50.2	-	-	-	-	-
100	8.68	28.348	4.87	49.9	-	-	-	-	-
150	8.75	28.713	1.63	16.7	-	-	-	-	-
200	8.70	28.797	0.77	7.9	-	-	-	-	-
240	8.69	28.826	0.71	7.3	-	-	-	-	-
SC-5: 22 May, 1991									
0	13.1	24.666	-	-	0-1.5	0.7	0.3	7.5	2.2
2	11.17	26.626	10.89	116.9	1.5-3	0.8	0.4	6.3	0.7
5	10.69	26.842	8.94	95.0	3-6	2.4	0.5	9.4	1.2
10	10.06	27.190	7.67	80.5	9-12	14.7	1.4	20.6	1.9
20	9.69	27.472	7.11	74.2	18-21	13.6	1.5	19.0	4.0
30	9.28	27.743	6.00	62.0	30	15.2	2.0	21.4	4.3
50	8.92	27.969	4.43	45.5	50	24.9	2.7	43.0	0.6
75	8.80	28.231	3.50	35.9	75	14.0	2.0	41.3	0.7
100	8.77	28.396	3.37	34.6	100	20.4	2.7	53.3	1.3
125	8.77	28.581	2.01	20.7	125	25.0	3.6	64.7	0.8
150	8.73	28.728	1.18	12.2	150	17.0	3.0	64.6	0.1
200	8.69	28.773	0.69	7.0	200	14.6	2.4	38.4	1.1
SC-5.5: 23 May, 1991									
-	-	-	-	-	0.5	0.8	0.2	4.8	0.4
-	-	-	-	-	2	1.7	0.4	8.0	0.7
-	-	-	-	-	3	4.8	0.7	10.9	0.6
-	-	-	-	-	4	5.0	0.7	11.5	0.4
-	-	-	-	-	5	5.8	0.7	12.4	2.0
SC-6: 22 May, 1991									
0	13.5	25.123	-	-	0-1.5	0.5	0.3	6.3	1.5
2	11.13	26.491	12.61	135.1	1.5-3	0.6	0.3	7.3	1.3
5	10.20	27.016	8.02	84.4	3-6	1.3	0.4	4.6	1.1
10	9.90	27.267	7.42	77.7	9-12	10.3	1.6	16.1	2.9
20	9.50	27.511	6.60	68.5	18-21	14.5	2.1	19.6	3.9
30	9.17	27.767	5.28	54.5	30	15.4	2.2	18.6	6.1
50	8.92	28.111	3.27	33.6	50	20.5	2.9	44.1	1.9
75	8.81	28.319	2.94	30.2	75	23.9	3.2	57.0	0.3

Table B.17: May continued.

depth m	temp °C	sal	oxygen mg/l	oxygen % sat	depth m	NO_3^- μM	PO_4^{3-} μM	SiO_4^{4-} μM	NH_4^+ μM
SC-7: 22 May, 1991									
0	-	18.531	-	-	0	0.8	0.1	9.4	1.5
2	14.06	24.742	12.45	140.8	1.5	0.8	0.1	7.6	2.9
5	11.97	25.835	12.89	140.2	long	2	2.8	0.1	4.0
10	10.20	27.192	8.12	85.6	3	0.7	0.1	6.9	1.0
20	9.81	27.455	7.34	76.7	4	0.9	0.2	8.1	0.9
30	9.46	27.781	6.98	72.6	5	0.8	0.3	8.2	0.6
50	9.31	28.003	3.31	34.4	5.5	0.8	0.2	8.3	1.1
75	8.82	28.203	4.33	44.4	8.5	12.1	1.3	24.2	0.8
100	8.91	28.355	3.40	35.0	10	13.6	1.4	25.5	1.9
150	8.81	28.778	1.00	10.3	20	16.7	1.8	31.1	2.3
200	8.72	28.780	0.83	8.5	30	19.2	2.0	31.7	3.0
250	8.68	28.810	0.31	3.2	50	31.3	2.9	51.1	0.7
-	-	-	-	-	75	19.1	2.2	42.1	1.2
-	-	-	-	-	100	29.9	3.0	59.2	1.0
-	-	-	-	-	150	33.9	4.0	91.3	0.5
-	-	-	-	-	200	32.7	4.1	101.4	0.4
-	-	-	-	-	250	22.6	3.9	86.9	0.7
SC-8: 22 May, 1991									
0	13.0	8.985	-	-	0-1.5	1.7	0.8	9.4	2.3
5	12.62	24.856	12.25	134.3	1.5-3	1.0	0.2	6.5	0.7
10	10.39	27.045	8.35	88.3	3-6	0.8	0.1	10.2	0.8
20	9.86	27.318	7.81	81.7	9-12	2.0	0.4	9.7	1.3
30	9.54	27.496	7.28	75.7	18-21	10.1	1.4	16.4	2.4
50	9.41	27.964	3.37	35.0	30	13.1	2.0	23.4	4.3
75	9.24	28.349	2.78	28.9	50	19.9	2.6	16.6	4.9
100	9.25	28.501	1.87	19.4	75	26.0	3.0	46.4	0.9
125	9.14	28.635	0.77	8.0	100	11.8	2.0	51.1	0.3
150	8.88	28.742	0.59	6.0	125	26.7	3.5	74.0	0.4
200	8.73	28.851	0.49	5.0	150	10.4	2.4	60.6	1.3
-	-	-	-	-	200	24.6	3.9	81.2	0.4
SC-9: 23 May, 1991									
0	10.5	1.583	-	-	0-1.5	1.9	0.1	7.0	1.4
2	12.81	16.711	13.25	138.6	1.5-3	2.0	0.2	9.2	0.9
5	10.62	25.407	11.12	117.0	3-6	1.2	0.2	8.4	0.7
10	9.73	26.384	8.02	83.2	9-12	4.7	0.8	7.8	0.9
20	9.41	26.820	7.07	72.9	18-21	11.9	1.4	19.8	2.4
30	9.24	27.009	6.75	69.5	30	13.0	1.8	26.6	3.0
40	8.76	27.050	5.74	58.4	40	12.9	1.8	22.7	1.4
50	8.62	27.129	5.52	56.1	50	16.8	2.3	34.6	0.9
60	8.58	27.157	5.42	55.0	60	12.0	2.1	24.0	4.7
75	8.68	27.222	4.51	45.9	70	7.8	2.7	37.9	8.5

Table B.18: May continued.

depth m	temp °C	sal	oxygen mg/l	oxygen % sat	depth m	NO_3^- μM	PO_4^{3-} μM	SiO_4^{4-} μM	NH_4^+ μM
SC-1: 22 June, 1991									
0	12.0	26.027	-	-	-	-	-	-	-
2	11.70	26.212	7.64	82.8	-	-	-	-	-
5	11.62	26.243	7.68	83.1	-	-	-	-	-
10	11.36	26.350	7.58	81.6	-	-	-	-	-
20	11.15	26.530	7.48	80.2	-	-	-	-	-
30	10.70	27.207	7.02	74.9	-	-	-	-	-
40	10.48	27.698	6.60	70.2	-	-	-	-	-
50	9.55	28.898	5.85	61.4	-	-	-	-	-
60	8.94	29.468	5.48	56.9	-	-	-	-	-
70	8.77	29.617	5.41	56.0	-	-	-	-	-
SC-2: 22 June, 1991									
0	14.8	19.658	-	-	0-1.5	5.4	0.7	17.2	0.8
2	13.67	23.822	10.02	111.8	1.5-3	7.8	0.9	18.1	1.1
5	11.98	25.547	8.48	92.1	3-6	7.8	1.0	13.9	1.3
10	11.81	25.934	8.11	87.9	9-12	11.7	1.4	18.1	0.9
20	11.12	26.631	7.34	78.7	15-18	12.2	1.3	17.7	1.7
30	10.92	26.678	7.31	78.0	30	15.9	1.7	23.9	0.7
50	9.50	27.743	5.41	56.3	50	23.1	1.8	21.3	0.4
75	9.00	28.167	4.37	45.0	75	25.3	2.8	21.7	0.4
100	8.88	28.302	3.98	41.0	100	25.9	2.8	22.1	1.1
150	8.75	28.590	2.28	23.5	150	27.6	3.7	24.1	0.5
200	8.70	28.732	0.84	8.7	200	27.0	3.4	27.1	1.6
275	8.69	28.779	0.29	2.9	270	26.6	4.8	35.8	0.5
SC-3: 22 June, 1991									
0	14.6	22.000	-	-	0-1.5	0.8	0.3	18.4	0.9
2	12.48	25.025	9.04	98.9	1.5-3	1.6	0.4	14.3	1.3
5	11.91	25.518	8.31	90.1	3-6	5.0	0.7	22.7	1.2
10	11.47	26.147	7.87	84.8	9-12	9.9	1.2	22.7	0.9
20	10.96	26.305	7.71	82.2	15-18	12.0	1.4	22.2	1.0
30	10.60	26.869	7.17	76.0	0	1.0	0.3	23.8	0.7
50	9.54	27.454	5.97	62.0	1	0.6	0.1	21.5	0.3
75	9.01	28.133	4.38	45.2	2	7.7	0.8	29.6	0.6
100	8.79	28.347	3.81	39.1	2.5	7.5	0.9	29.0	1.1
150	8.72	28.679	1.26	12.9	4	10.7	1.1	30.5	0.8
200	8.70	28.766	0.60	6.2	5	11.9	1.1	33.1	0.6
270	8.69	28.778	0.29	2.9	6.5	12.9	1.3	33.7	0.7
-	-	-	-	-	10	14.1	1.3	34.7	0.9
-	-	-	-	-	20	15.3	1.5	35.4	0.4
-	-	-	-	-	30	17.3	1.6	29.7	0.3
-	-	-	-	-	50	22.1	2.0	36.0	0.8
-	-	-	-	-	75	28.7	2.7	54.6	0.2
-	-	-	-	-	100	28.9	2.9	63.7	0.6
-	-	-	-	-	150	30.2	3.9	94.3	0.3

Table B.19: Temperature, salinity, dissolved O_2 and nutrients: June.

depth m	temp °C	sal	oxygen mg/l	oxygen % sat	depth m	NO_3^- μM	PO_4^{3-} μM	SiO_4^{4-} μM	NH_4^+ μM
-	-	-	-	-	200	31.5	4.3	108.8	0.3
-	-	-	-	-	270	29.8	4.5	117.6	0.4
SC-4: 22 June, 1991									
0	14.5	23.488	-	-	-	-	-	-	-
2	14.28	23.871	10.16	114.9	-	-	-	-	-
5	12.74	25.193	9.07	99.9	-	-	-	-	-
10	11.41	26.141	8.04	86.5	-	-	-	-	-
20	10.99	26.494	7.52	80.4	-	-	-	-	-
30	10.60	26.947	7.17	76.1	-	-	-	-	-
50	9.34	27.643	5.62	58.3	-	-	-	-	-
75	8.82	28.140	3.54	36.3	-	-	-	-	-
100	8.72	28.293	3.80	38.9	-	-	-	-	-
150	8.73	28.648	1.24	12.8	-	-	-	-	-
200	8.71	28.756	1.31	13.5	-	-	-	-	-
240	8.70	28.767	0.44	4.5	-	-	-	-	-
SC-5: 22 June, 1991									
0	14.1	24.044	-	-	0-1.5	1.0	0.4	18.0	0.7
2	13.72	24.406	9.91	111.0	1.5-3	1.3	0.4	14.7	1.0
5	12.65	24.951	9.41	103.3	3-6	3.3	0.6	15.0	1.5
10	11.97	25.638	8.47	92.0	9-12	9.5	1.1	19.8	1.0
20	11.15	26.413	7.75	83.1	15-18	13.2	1.5	19.1	0.7
30	10.70	26.768	7.25	77.1	30	15.6	1.8	26.6	1.6
50	9.45	27.621	5.01	52.0	50	23.1	2.6	20.0	0.5
75	8.88	28.085	2.98	30.7	75	29.5	3.3	23.5	0.6
100	8.76	28.307	2.56	26.2	100	31.1	3.5	28.4	0.3
125	8.77	28.435	1.93	19.8	125	29.5	3.8	29.6	0.4
150	8.73	28.642	1.01	10.4	150	21.7	3.4	41.4	0.5
200	8.71	28.754	0.64	6.6	200	28.2	4.5	59.2	0.5
SC-5.5: 22 June, 1991									
-	-	-	-	-	0	1.1	0.5	20.6	0.5
-	-	-	-	-	1	1.4	0.5	21.0	0.7
-	-	-	-	-	2.5	4.8	0.7	25.0	0.4
-	-	-	-	-	3.5	7.4	1.0	25.8	0.4
-	-	-	-	-	5	8.6	1.1	27.1	0.8
-	-	-	-	-	7	9.5	1.2	26.8	0.9
SC-6: 22 June, 1991									
0	-	24.598	-	-	0-1.5	1.6	0.5	19.4	1.5
2	13.64	24.788	10.26	115.1	1.5-3	1.9	0.6	20.0	0.6
5	13.14	24.991	9.96	110.6	3-6	2.7	0.6	17.3	0.7
10	12.06	26.013	8.99	98.1	9-12	7.0	0.9	23.6	1.4
20	11.29	26.465	7.97	85.7	15-18	9.3	1.3	20.5	1.4
30	10.94	26.667	7.44	79.4	30	11.5	1.7	21.4	3.4
50	9.81	27.474	4.83	50.5	50	22.6	2.4	24.2	1.8
70	8.97	28.054	2.53	26.0	75	31.3	3.4	28.5	0.4

Table B.20: June continued.

depth	temp	sal	oxygen		depth	NO_3^-	PO_4^{3-}	SiO_4^{4-}	NH_4^+
m	°C		mg/l	% sat	m	μM	μM	μM	μM
SC-7: 23 June, 1991									
0	13.4	8.655	-	-	0	1.0	0.0	18.1	0.3
2	14.41	22.442	10.82	121.6	1.5	0.8	0.2	21.4	0.6
5	12.08	25.578	9.07	98.7	2	0.7	0.1	20.5	0.4
10	11.48	26.138	8.08	87.1	4	7.8	0.8	28.3	0.6
20	11.08	26.486	7.62	81.6	5	8.2	0.7	27.4	1.8
30	10.74	26.782	7.39	78.7	6	10.0	1.0	26.8	0.5
50	9.59	27.516	5.74	59.7	10	12.8	1.2	28.9	0.9
75	8.97	28.144	3.21	33.1	15	14.9	1.4	29.9	0.7
100	9.00	28.356	2.64	27.3	20	15.7	1.4	30.1	0.7
150	8.85	28.653	1.06	10.9	30	16.1	1.4	27.6	0.6
200	8.73	28.753	0.63	6.5	50	20.9	2.1	31.9	3.1
250	8.72	28.780	0.36	3.7	75	31.3	2.9	54.7	0.3
-	-	-	-	-	100	30.2	3.0	55.1	0.9
-	-	-	-	-	150	33.1	3.8	77.4	1.2
-	-	-	-	-	200	31.3	4.2	90.3	0.4
-	-	-	-	-	250	28.5	4.3	98.6	0.4
SC-8: 23 June, 1991									
0	12.4	10.978	-	-	0-1.5	1.4	0.2	10.7	1.2
2	13.17	19.886	11.21	120.6	1.5-3	1.1	0.2	16.2	1.6
5	12.59	25.431	10.48	115.3	3-6	0.9	0.3	17.1	0.7
10	11.76	26.106	9.02	97.8	9-12	4.2	0.8	18.8	1.1
20	11.11	26.498	8.11	86.8	15-18	8.1	1.1	20.1	1.4
30	10.67	26.770	7.74	82.2	30	14.0	1.6	22.8	1.0
50	9.73	27.446	5.64	58.9	50	19.7	2.3	24.3	1.2
75	9.23	28.201	2.48	25.8	75	25.2	2.9	27.3	0.3
100	9.26	28.415	1.63	16.9	100	31.8	3.6	26.3	0.3
125	9.13	28.562	0.99	10.2	125	32.8	3.8	33.7	0.3
150	8.92	28.690	0.61	6.3	150	31.2	4.0	39.8	0.5
200	8.77	28.761	0.41	4.3	200	30.1	4.2	40.9	0.7
SC-9: 22 June, 1991									
0	13.2	2.634	-	-	0-1.5	2.6	0.3	12.8	3.0
2	13.05	23.026	11.86	129.9	1.5-3	1.4	0.3	12.0	1.5
5	11.31	24.767	8.62	91.8	3-6	2.2	0.4	15.3	1.5
10	10.63	25.673	7.52	79.3	9-12	10.3	1.3	18.5	1.4
20	10.20	26.229	6.88	72.0	18-21	12.5	1.5	19.3	1.8
30	9.81	26.568	6.44	66.9	30	17.4	2.0	21.5	2.8
40	9.43	26.757	5.65	58.3	40	19.9	2.2	21.9	3.3
50	8.86	27.027	4.33	44.1	50	22.1	2.4	30.1	0.3
60	8.64	27.125	2.87	29.1	60	23.1	2.8	32.0	1.1
75	8.66	27.171	1.03	10.4	75	9.5	3.7	89.8	10.4

Table B.21: June continued.